OFR 132-85

A mining research contract report
JUNE 1984

A BOREHOLE PROBE FOR IN-SITU NEUTRON ACTIVATION ANAYLSIS

Contract H0262045
Princeton Gamma-Tech, Inc.

BUREAU OF MINES
UNITED STATES DEPARTMENT OF THE INTERIOR

DISCLAIMER NOTICE

The views and conclusions contained in this document are those of the authors and should not be interpreted as necessarily representing the official policies or recommendations of the Interior Department's Bureau of Mines or of the U.S. Government.

50272-101

REPORT DOCUMENTATION PAGE	1. REPORT NO.	2.	3. Recipient's Accession No.
4. Title and Subtitle A BOREHOLE PROBE FOR IN SITU NEUTRON ACTIVATION ANALYSIS			5. Report Date June, 1984 6.
7. Author(s) J. A. Baicker, D. B. Lister, R. E. Marr, III, L. H. Goldman			8. Performing Organization Rept. No.
9. Performing Organization Name and Address Princeton Gamma Tech, Inc. 1200 State Road Princeton, New Jersey 08540			10. Project/Task/Work Unit No. 11. Contract(C) or Grant(G) No. (C) H0262045 (G)
12. Sponsoring Organization Name and Address US DEPARTMENT OF THE INTERIOR, Bureau of Mines, P. O. Box 25086, Building 20, Denver Fedearl Center, Denver, CO 80225			13. Type of Report & Period Covered Final - 9/28/76 - 8/1/80 14.

15. Supplementary Notes

16. Abstract (Limit: 200 words)

A prototype borehole probe for ore grade determinations by means of in-situ neutron activation analysis was designed, built, and tested in a two-phase program. Phase I dealt with the design and fabrication of a borehole logging system for operation in 7.6 cm (3 in.) diameter or larger boreholes. It consisted of a 5.06 cm (2 in.) diameter borehole probe containing an intrinsic germanium detector, a canister-type solid cryogen cooling system, cooled system, cooled FET preamplifier, linear amplifier, high voltage supply, analog-to-digital converter, microprocessor-based multichannel analyzer, buffer memory, bi-directional cable link, power supplies, and a Californium-252 neutron source. A surface support vehicle was designed and outfitted. A minicomputer system was constructed and software developed and tested.

In Phase II the system was field tested at several mine sites. The system was calibrated, tested, improved, and demonstrated in a variety of applications. Tests were performed at sites pertinent to uranium, iron, coal, copper, silver and gold. Technical feasibility was demonstrated for all these applications except gold; the gold results were inconclusive. In-situ neutron activation analysis using high resolution gamma ray spectrometry was found to be a potentially viable logging method for ore grade analysis under certain conditions.

17. Document Analysis a. Descriptors

b. Identifiers/Open-Ended Terms

c. COSATI Field/Group

18. Availability Statement	19. Security Class (This Report)	21. No. of Pages
Release unlimited		119
	20. Security Class (This Page)	22. Price

(See ANSI-Z39.18) See Instructions on Reverse OPTIONAL FORM 272 (4-77)
(Formerly NTIS-35)
Department of Commerce

FOREWORD

This report was prepared by Princeton Gamma-Tech, Inc., 1200 State Road, Princeton, New Jersey 08540, under USBM Contract No. HO262045. The contract was initiated under the Advancing Mining Technology Metal and Nonmetal Program of the Bureau of Mines. It was administered under the technical direction of the Denver Mining Research Center with George Schneider acting as the Technical Project Officer. B.G. Horton was the Contract Administrator for the Bureau of Mines. This report is a summary of work completed during the period September 28, 1976 - August 1, 1980. This report was first submitted on November 11, 1980. It contains no patentable features.

PREFACE

This project could not have been carried out without the generous help, cooperation, and dedication of many individuals and organizations.

The United States Department of the Interior, Bureau of Mines (USBM), conceived and supported the project and actively participated throughout. Special thanks go to Mr. George Schneider, Technical Officer, whose advice and encouragement aided all phases of the work. We are grateful to the staff of the USBM Reno Research Center for extensive analytical work on the gold ore samples.

The cooperation and advice of Frank Senftle and his group at the United States Geological Survey was contributed throughout the project.

We thank the following people and organizations for assistance in the field tests: Jimmy Finley, Research Geologist, Chevron Oil Field Research; D.A. (Don) Porter, Manager, Uranium Exploration, Conoco; Stan Hafenfeld, District Geologist Conoco; Robert Hidalgo, Coal Exploration Manager, United States Steel Corporation; the staff at Ray Mine, Kearny, Arizona; Robert Wilson, Research Engineer, Bendix Corporation; Paul Downs, Mine Superintendent, Texasgulf Golden Cycle Mining Companies; and Henry Schwellenbach, Halecrest Company.

Employees of PGT who participated importantly in this project included: Dr. Juan Ferrer, Robert Macy, Steve Miller, Dr. Neil A. Stein, Gary Schnerr, and Richard Zych.

CONTENTS

A BOREHOLE PROBE FOR IN-SITU NEUTRON ACTIVATION ANALYSIS

ABSTRACT

A prototype borehole probe for ore grade determinations by means of in-situ neutron activation analysis was designed, built, and tested in a two-phase program. Phase I dealt with the design and fabrication of a borehole logging system for operation in 7.6 cm (3 in.) diameter or larger boreholes. It consisted of a 5.06 cm (2 in.) diameter borehole probe containing an intrinsic germanium detector, a canister-type solid cryogen cooling system, cooled FET preamplifier, linear amplifier, high voltage supply, analog-to-digital converter, microprocessor-based multichannel analyzer, buffer memory, bi-directional cable link, power supplies, and a Californium-252 neutron source. A surface support vehicle was designed and outfitted. A minicomputer system was constructed and software developed and tested.

In Phase II the system was field tested at several mine sites. The system was calibrated, tested, improved, and demonstrated in a variety of applications. Tests were performed at sites pertinent to uranium, iron, coal, copper, silver and gold. Technical feasibility was demonstrated for all these applications except gold; the gold results were inconclusive. In-situ neutron activation analysis using high resolution gamma ray spectrometry was found to be a potentially viable logging method for ore grade analysis under certain conditions.

INTRODUCTION

Purpose

A major purpose of this project was to develop and test a field-worthy borehole spectrometer based on high-resolution germanium detector technology, and investigate its applicability in selected in-situ analytical situations. In principle, better resolution ought to reduce interferences among gamma-ray peaks that have nearly the same photon energies (peak overlaps) and would improve peak-to-background (signal-to-noise) ratios. The hoped-for results would be lowered detectability limits of elements, improved accuracy, and increased speed of analysis.

This work was confined to a study of neutron-induced and natural gamma activity. These techniques were judged to have several properties appropriate to the borehole situation (13,28). Fast neutrons penetrate matter to a moderate degree and, after slowing, react with many isotopes. Gamma rays of energy in the range 0.2 MeV to 7 MeV also penetrate centimeters or tens of centimeters of matter. Furthermore, neutron sources of small physical size are available for borehole work.

Background

Nuclear techniques were first applied to the exploration of minerals in the mid-1950's (23). Although neutron and gamma ray logs are now quite familiar to mineral exploration and mine development geologists, most of these logs represent indirect measurements of gross physical or chemical characteristics of the formations penetrated by the drillhole.

It has long been recognized that gamma-ray spectroscopy has the potential to be a powerful technique for in-situ elemental analysis. Ideally, the identification and quantification of elements can be inferred from the intensities of specific gamma-ray energies that are emitted by naturally-occurring and neutron-activated radioisotopes.

The technical literature contains numerous reports on various tools for in-situ gamma-ray spectroscopy. The interested reader is referred to several excellent review articles (28,30). There have been two major problems. The gamma ray sources have (often) low intensities, and the long-standard sodium iodide scintillation detectors have poor energy resolution. As a result the applicability of the method has been severely limited. Improvements in either or both of these problem areas would greatly expand the potential of the method.

At the present time elemental analysis for delineation of ore deposits is accomplished primarily by chemical analysis of samples obtained from holes drilled for that purpose. Drilling-and-assaying methods have the advantages of being

relatively simple to perform and to understand. The chemical analyses are normally performed in an assay laboratory by means of accepted techniques, which may be gravimetric or instrumental. Also, the confidence of field geologists is usually enhanced when they physically see, handle and select the samples that come out of the drillhole.

Nevertheless, the various types of drilling and sampling methods have problems. All samples removed by drilling suffer the disadvantage of having a relatively small volume. Samples may not be representative of the average local ore grade, especially in heterogeneous deposits. The ideal situation occurs if the analytical sample truly represents the average composition of the formation at depth. Departure from the ideal is called "sampling error". Here are brief descriptions of the more common sample-gathering methods:

(1) Rotary or percussive drilling-chips or slimes. Mud, brought out of the drillhole as drilling continues, is sampled at the surface. The main problem here is that the depth of origin of the sample is not accurately known; also, muds from different depths can, to a degree, mix in the drillhole.

(2) Rotary or percussive drilling for a number of feet followed by washing out the hole. The collected drilling chips or slimes come from the differential depth drilled and constitute the mother sample, which represents the average ore grade of the removed material in an accurately known depth interval.

(3) Coring. A hollow drill is used to physically remove, with a minimum of mechanical disturbance, a long cylindrical sample, called a "core", from the penetrated rock. Ideally, the disturbance is nil and the depth pertaining to any portion of the core is accurately known. Core diameters are typically about half those of rotary or percussive drillholes; that is, they range from 5 cm diameter to about 12 cm diameter in surface drilling operations. Smaller sizes are typical of underground drilling and some exploration drilling. Consequently, the part of the sampling error that comes from the size of the sample is increased. Cores from unconsolidated formations can be lost because they can fall out of the core barrel before recovery, resulting in gaps in the data. Cores can be mishandled or mislabeled. Clayey cores can swell. Although core drilling is relatively expensive, it is the preferred drilling method whenever depth accuracy is important and the mineral of interest is relatively evenly distributed in the orebody. Because of the expense and

delays of coring and analysis, exploration companies that use it sometimes make decisions based on insufficient data and possibly carry out exploration programs that are suboptimal. As a result, marginal resources may remain undeveloped or may be inefficiently developed.

IN-SITU NEUTRON ACTIVATION ANALYSIS

The neutron activation procedure for in-situ analysis consists of irradiating the borehole surroundings with energetic neutrons which are slowed by, and react with, nuclei present in the formation and in the borehole. This technology is based on the analysis of gamma rays emitted as a result of the neutron interactions. The two main kinds of neutron interactions of concern here are, 1) inelastic scattering of fast neutrons, and 2) nuclear capture of neutrons that have been slowed to speeds characteristic of the local temperature (thermal neutrons). Of the two, neutron capture is the more prevalent; it occurs to a greater or lesser degree in the vast majority of the natural isotopes. Emitted gamma rays are classified as prompt or delayed depending on how soon they are emitted after the neutron interaction. Prompt gammas are emitted immediately, as the stimulated product isotope de-excites to a stable or metastable state. If the state is metastable, a further transition occurs, usually by means of betta decay. Depopulation of the metastable states by beta decay is a relatively slow process. The activity diminishes exponentially in time with a characteristic half-life that varies from isotope to isotope. Gamma rays emitted following the beta decay constitute the delayed gammas.

Prompt and delayed gammas have energies, or energy "spectra," that are characteristic of the isotopes that are present in the formation. Prompt gammas typically have energies less than 10 MeV. Spectral data for many elements have been tabulated (21,36). Delayed gammas usually have less than 3 MeV energy. Compilations of neutron activation tables and spectra have been published (7,10,14).

Delayed gamma rays are emitted following neutron-induced radioactivity by neutron capture, neutron inelastic scattering or other neutron reaction. The product radioisotope from the reaction has a unique half-life that, to be useful for borehole logging must have a value between several seconds and several hours. There is a delay between the end of the activation period and the start of the counting period. During the delay the prompt radiation and much of the shorter-lived activity die away, reducing some of the unwanted background and interfering peaks in the detected spectrum. However, should the delay be too long, useful activity would be wasted; so a compromise must be struck. Physical constraints put a lower limit on the delay. The optimum periods for irradiation, delay, and counting vary from isotope to isotope.

Prompt gammas are emitted immediately following neutron capture or neutron inelastic scattering. Most of the stable isotopes found in nature will capture neutrons that have been slowed to thermal energies as a result of collisions. Consequently, an in-situ prompt gamma-ray spectrum contains information about many of the elements in the rock surrounding the neutron source.

Ideally, prompt gamma spectroscopy offers a method for simultaneous, multi-elemental analysis, but complicating factors intervene. Many of the gamma rays are of relatively high energy-up to 10 MeV-and there can be many different gamma rays within the recorded spectrum. The pulse-height spectrum of even a simple, monoenergetic gamma-ray emitter is not itself simple. It is complex because of the physics of gamma ray absorption and energy loss processes within the detector. Aside from the full-energy peak, the spectrum contains escape peaks, Compton edges, the Compton continuum.

In a typical gamma ray analysis each individual isotope may emit a number of different-energy gamma rays, with some characteristic relative abundance. There may be any number of different isotopes present. Furthermore, in the process of traversing the formation from emitting nucleus to detector the gammas may be scattered, thus having their energies altered. The end result of all this is an analysis that may be completed with relatively poor detection limits and poor analytical precision.

On the other hand, research on the applicability of prompt gamma-ray spectroscopy in borehole assays has to date been relatively limited. Our work on this project included prompt-gamma analyses of one element, gold, which is of commercial interest in trace amounts, one element, copper, of interest at moderate levels, and a third element, iron, of interest in greater concentrations. In the coal work prompt gammas were used to determine ash content, ash composition, and heat of combustion. The prompt gamma ray from hydrogen was used directly in the coal tests and indirectly in other tests to monitor the health of the sonde and to help compensate for the effect of water on the neutron flux.

Natural gammas from long-lived gamma-emitting radioisotopes and their radio- active daughter products occur in rocks. There are three parent isotopes: Uranium 238, Thorium 232, and Potassium 40. Of these, uranium is commercially valuable.

Traditional "natural gamma" or "gross gamma" logging tools used in uranium mining simply count all gamma rays above a threshold energy. A relatively high gamma count usually comes from the presence of Bismuth-214, which is a distant daughter isotope of U-238; a high gamma count normally signals the presence of uranium in the vicinity. It is often employed as a quantitative in-situ assay. This "gross gamma" assay may be unreliable in certain situations. For example, the presence of relatively high thorium levels will cause errors. A second more subtle problem occurs if, over time, natural water has transported uranium as a result of geochemical processes of dissolution and reprecipitation. If the uranium has been mobile in an area within the past million years, then the Bi-214 may not exist in secular equilibrium with the U-238 and so will not provide a true indication. On the other hand,

Protactinium-234, a close daughter isotope of U-238 achieves equilibrium with U-238 in less than 3 months. It emits a weak, but detectable, gamma ray of 1001 keV energy (17). The present project investigated the practicality of using the Pa-234 gamma ray as a direct indicator of U-238 despite previous pessimistic interpretations (2,4,35).

In-situ neutron activation analysis (NAA) by gamma ray spectroscopy has, for applicable elements, the potential of solving many of the problems associated with drilling-and-assaying. NAA has the following advantages:

1) the depth of the analyzed sample is accurately known

2) the sample volume is relatively large (it depends on the composition of the formation and the gamma ray emissions energies),

3) samples cannot be lost,

4) there is a small chance of human error, and

5) analyses are virtually immediate

Furthermore, total cost per assay can be less than cost of traditional methods, particularly corehole assays. On the other hand, in NAA there is a necessary tradeoff between costs and accuracy, which is element-dependent. Tool development costs and capital equipment costs can be relatively high. Some NAA techniques make use of highly radioactive sources, which typically require specialized equipment and handling, and which must be licensed.

If a logging technique capable of delivering accurate and reliable downhole elemental analysis were available, it could have significant value to the minerals and energy industry. Ore bodies could be located and mapped more precisely than with drilling-and-assaying methods. Site evaluation costs could be reduced, or more information could be obtained for the same outlay of money. In addition, there are potential benefits in conservation and in reduction of environmental disruption, if orebodies can be mapped and mined with improved precision.

In order to place our focus on in-situ, high-resolution NAA in better perspective we note that there are other techniques available for instrumental in-situ assays. These include, but are not limited to, x-ray fluorescence, x-ray diffraction, photoluminescence, and infrared spectroscopy. One report has stated that, "The technology assessment and cost-benefit analysis shows neutron activation analysis in its various forms to have the highest priority for research and development as a borehole logging technique....Of the twelve industries considered in the study, those where the need for advanced borehole logging technology is greatest are uranium, copper, gold, and iron." (13)

Past NAA work with moderate-resolution detectors has met with limited applicability because of actual or potential interferences.

In high resolution gamma ray spectroscopy the key component is the detector. The best "State-of-the-Art" detector for gamma ray spectroscopy in the photon energy range from 0.1 MeV to 10 MeV is the germanium detector. Its resolution is about 30 times better than the thallium-activated sodium iodide scintillator, the most commonly used gamma ray detector. The efficiency of a germanium detector is substantially lower than that of a sodium iodide scintillation counter.

In general, the tradeoff between detector resolution and efficiency, implied by the choice of detector, means that the germanium detector is better in dealing with complex spectra and NaI(Tl) is better with simple spectra. NAA work in rock formations usually results in complex spectra. Cobalt-60 spectra from these two types of detectors are compared in Figure 1.

At the beginning of the present work in 1978 no fieldworthy, integrated, germanium detector logging probe was available, although research probes had been constructed and used in laboratory and shallow borehole studies (28,29).

Technical Concepts

Germanium detector.

The relatively large germanium detectors required for borehole logging are cylinders of single crystal germanium. Because germanium is a semiconductor, it can be prepared as a solid state ionization chamber for gamma ray detection. It is the best semiconductor material currently available for that purpose. The size of a typical detector is 50mm diameter x 50mm long. Such a detector has an efficiency of about 20% relative to that of a 76mm diameter x 76mm NaI(Tl) scintillator (measured at 1.332 MeV energy using a Co-60 source spaced 25cm from the detector). Its computed relative efficiency curve is presented in Figure 2.(15)

The germanium detector works by converting the energy of individual gamma ray photons into a small electronic signals that are amplified and analyzed by the electronics in the sonde. When a gamma ray is absorbed in the detector, electrical charges are freed within the detector as a result of interactions with atoms in the crystal. The charge is collected at the electrodes, forming an electric impulse. The higher the energy of the incident gamma ray, the greater the charge created, and the greater the size of the electrical pulse. The electronic circuits filter, shape, amplify and finally convert the signal into a digital number which is

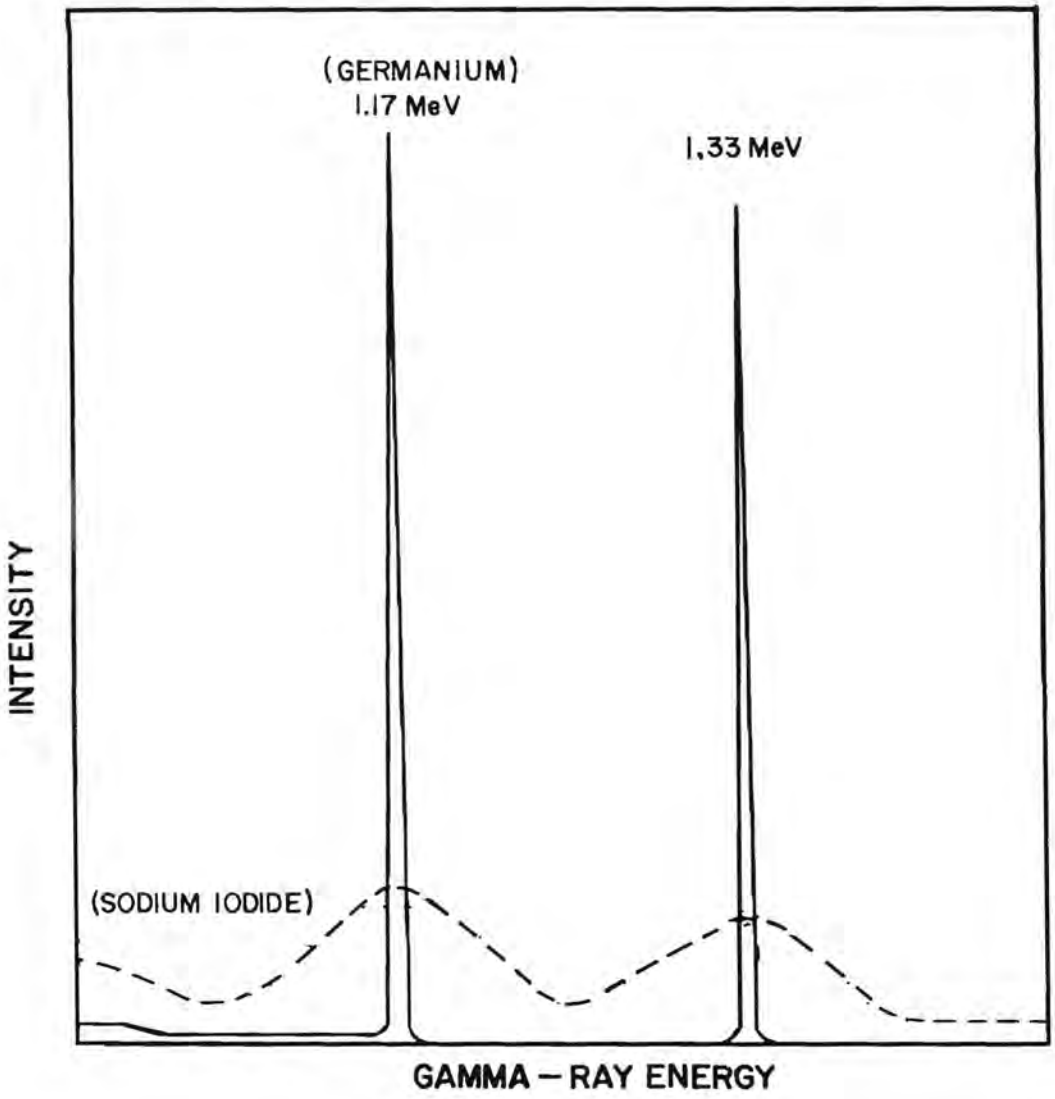

FIGURE 1.

SPECTRA OF A 10% GERMANIUM DETECTOR AND A 3"X3" (7.6cm.X7.6cm) SODIUM IODIDE DETECTOR. THE RESOLUTION OF THE Ge DETECTOR IS 2.3KeV(FWHM); THE SODIUM IODIDE DETECTOR'S RESOLUTION IS ABOUT 80KeV(FWHM).

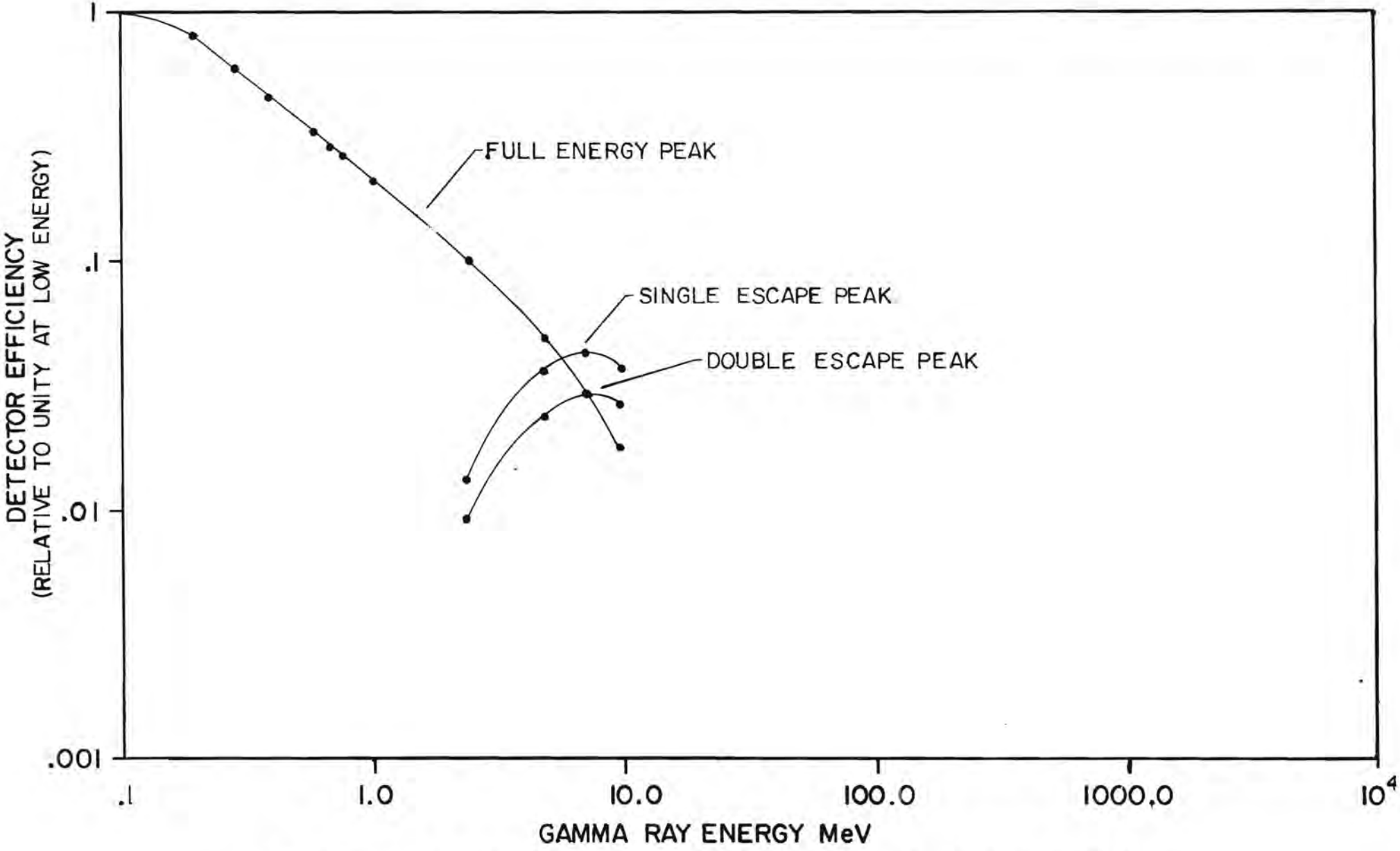

FIGURE 2. CALCULATED EFFICIENCY CURVE OF A 5CM. X 5CM. COAXIAL Ge DETECTOR.

proportional to the energy of the absorbed gamma ray. It is often referred to as the "channel number" in a multichannel analyzer. The accumulated information is stored in a computer as a statistical distribution, the gamma-ray spectrum. A graph of a spectrum, with channel number or gamma- ray energy as the horizontal axis and frequency or intensity of detected events as the vertical axis, reveals a series of narrow peaks sitting on a relatively featureless background. The peaks correspond to the various emitted gamma ray energies which serve to identify the emitting isotopes. Their intensities are correlated with the chemical abundance of the emitter. A spectrum of naturally radioactive uranium ore is shown in Figures 3a-d. The principles of gamma ray spectroscopy with germanium detectors have been extensively treated in the literature.(3)

Ore grade determination.

Ore grade is determined from the net (peak-minus-background) intensities of pertinent peaks, upon application of calibration and correction factors. Ideally, one can optimize results for each ore and host rock combination by optimizing the controllable factors:

-Type and strength of neutron source
-Source-to-detector spacing
-Detector material, resolution and efficiency
-Logging speed
-Irradiation time, delay time, and counting time
-Selected analytical peaks
-Algorithm for determining net intensity of analytical peaks
-Calibration and correction algorithms.

Borehole conditions affect the data and must be taken into account. These include hole diameter, drilling fluid, and casing, if any. Finally, there are effects of the formation, through its physical and chemical properties: density, porosity, composition, water content, and distribution of ore.

Theoretically, if the properties of the formation were sufficiently well known, analysis could be carried out based on first principles. Because there are so many unknowns in that approach, empirical methods have been employed in this investigation. The simplest relationship is:

$$I(i) = k(i)\ C(i) \qquad (1)$$

or

$$C(i) = I(i)/k(i) \qquad (2)$$

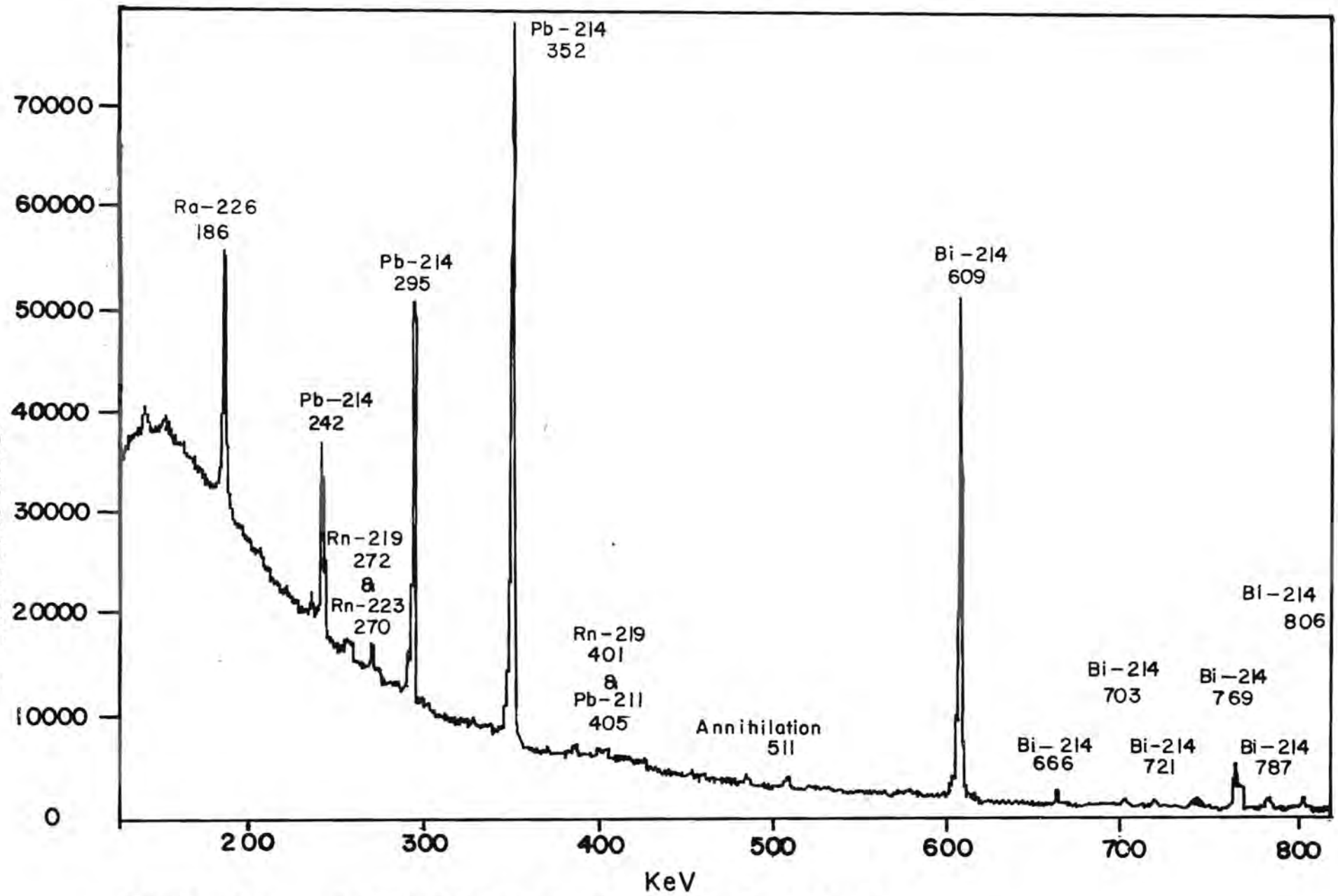

FIGURE 3A URANIUM ORE SPECTRUM, 0 TO 820 keV

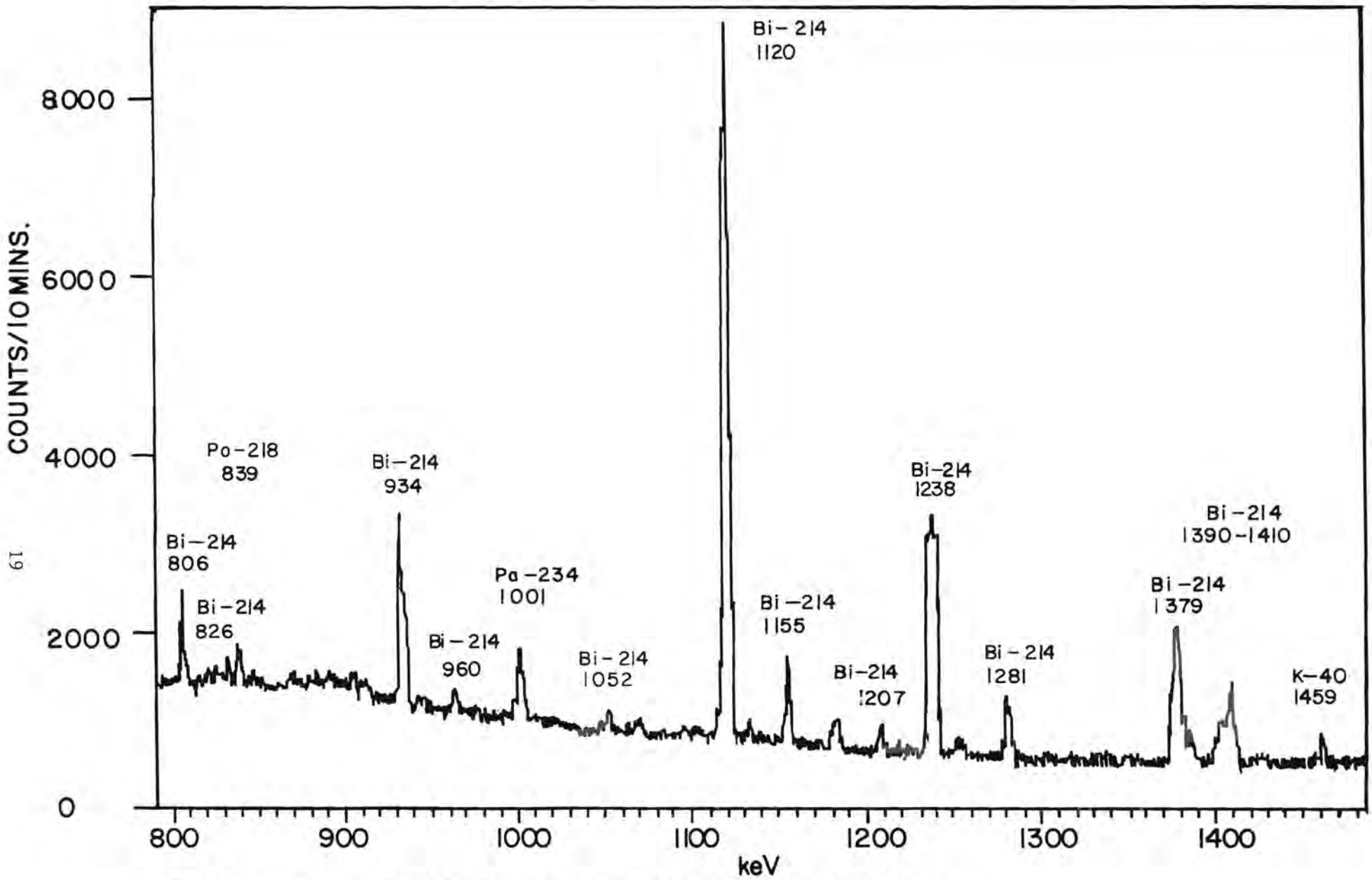

FIGURE 3B URANIUM ORE SPECTRUM, 790 TO 1480 keV

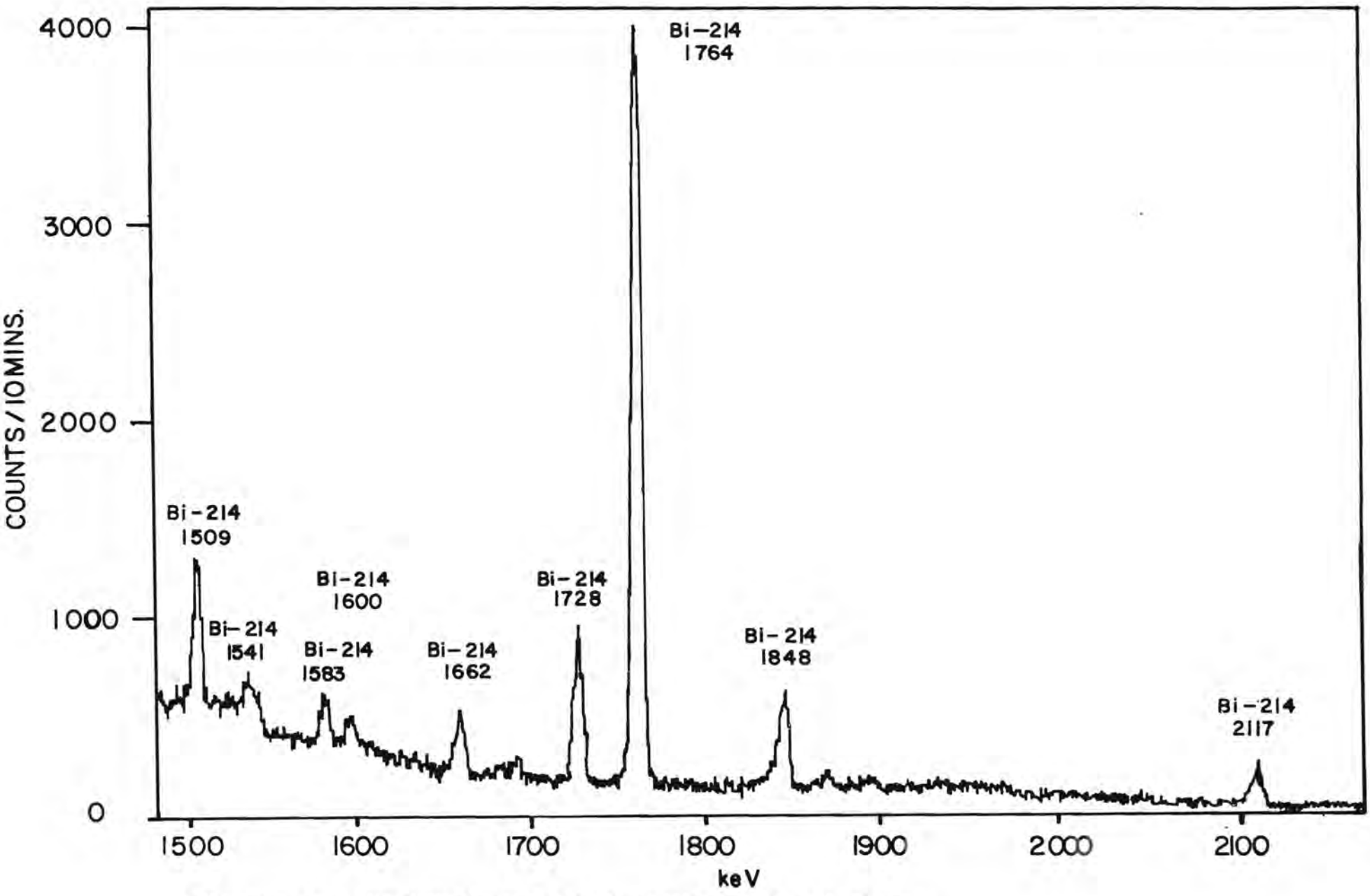

FIGURE 3C URAINIUM ORE SPECTRUM, 1480–2180 keV

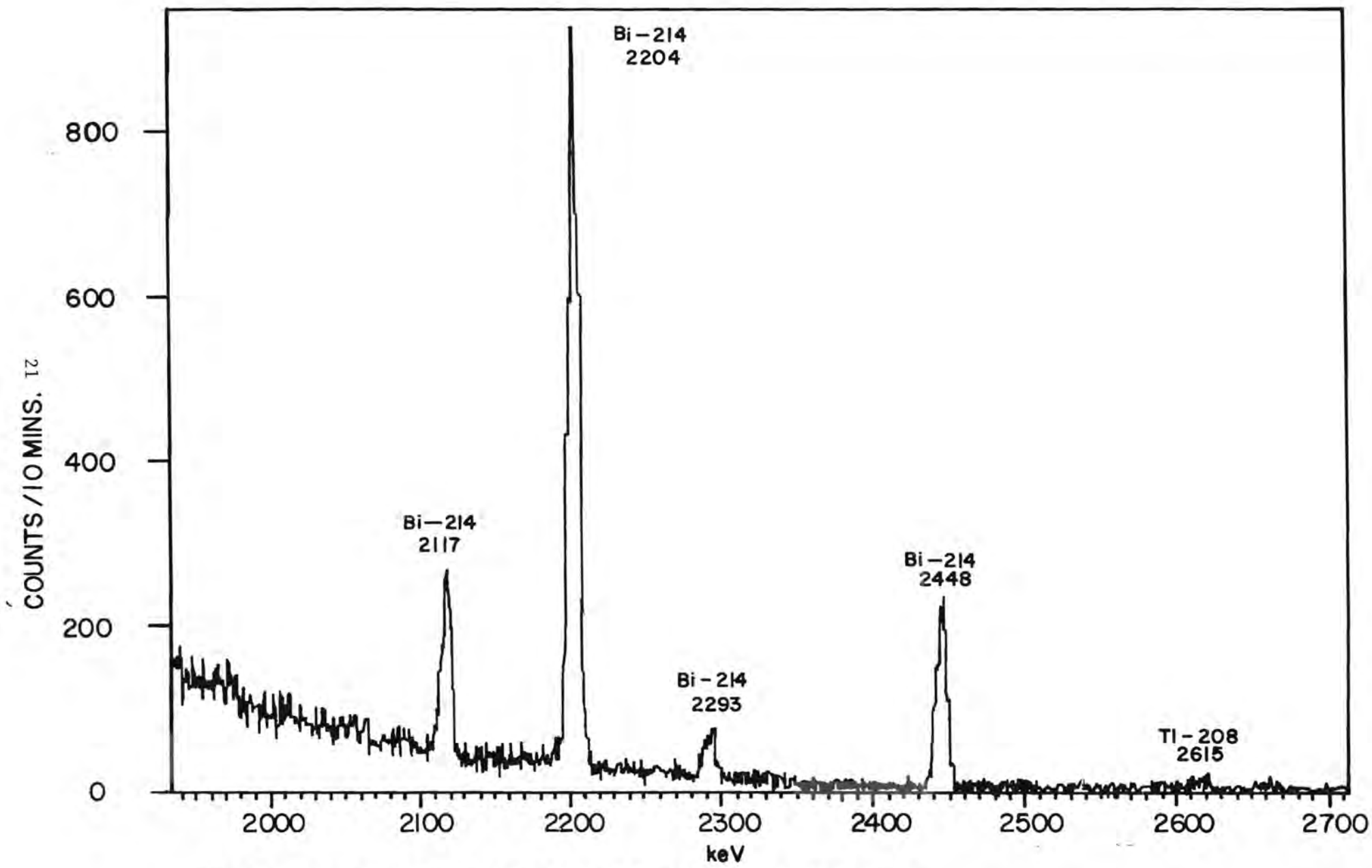

FIGURE 3D URAINIUM ORE SPECTRUM, 1930 TO 2710 keV

where I(i) is the net intensity of gamma rays pertinent to element i.
C(i) is the concentration of element i,
k(i) is the calibration constant, or sensitivity for element i.

Equation 2 is appropriate for low or moderate concentrations in a uniform formation and uniform borehole. The physics of the entire process is lumped into the constant k. One factor that has a strong effect on k in neutron capture work is the amount of hydrogen in the formation. Hydrogen, more than any other element, helps slow, or thermalize, neutrons and thereby affects the neutron spatial distribution and energy distribution. It is present mainly as bound or unbound water. The presence of hydrogen can be monitored by the germanium detector by means of the observed intensity of the 2.223 MeV gamma ray from the reaction:

neutron + proton $\longrightarrow$ deuteron + gamma ray photon (2.223 MeV).

It has been shown that if equation 2 is rewritten as:

$$C(i) = I(i)/k'(i)\sqrt{I(H)} \tag{3}$$

where $k'(i) = k(i)/\sqrt{I(H)}$ and I(H) is the net intensity of the 2.223 MeV gamma ray, then k' is relatively insensitive to the water content in dry, low-porosity rocks. This is because I(i) stays nearly proportional to I(H) if just the water content varies (26)

The analytical capability of ore grade determination by spectroscopy is characterized by two parameters: the sensitivity k, and the zero-grade background counts I(B), at the position in the spectrum where the analytical peaks normally appear. These two parameters vary with the controllable and uncontrollable logging factors and govern the lowest detectable ore grade as well as the precision of measurement at any ore grade. If other things are equal there is a tradeoff between the precision of the determination and the logging speed. Slower speeds will buy improved precision. The lowest detectable ore grade (LDOG) may be expressed:

$$LDOG = 2\sqrt{I(B)}/k(i) \tag{4}$$

(95% confidence or 2 level) and the absolute statistical precision of element i is given by

$$P(i) = 2\sqrt{I(i)+I(B)}/k(i) \tag{5}$$

(95% confidence level) and in percent relative terms by

$$RP(i) = 100\ P(i)/C(i) \tag{6}$$

where RP(i) is the relative precision (2) of element i expressed as a percent of the concentration of the element.
Equation 6 combined with equations 2 and 5 becomes

$$RP(i) = 200 \sqrt{I(i)+I(B)}/I(i) \quad (7)$$

$$RP(i) = 200 \frac{\sqrt{1+I(B)/I(i)}}{\sqrt{I(i)}} \quad (8)$$

at the 95% confidence level.

Equation 8 shows that RP(i) decreases as the ratio I(B)/I(i) decreases and as I(i) increases, in a square root relationship. Since a smaller RP(i) means better relative precision, changes that increase I(i) and/or decrease I(B)/I(i) will improve the analytical precision. For example, an increase of source strength or detection efficiency will increase I(i) but leave I(B)/I(i) unchanged. Better detector resolution means a lower I(B)/I(i) ratio. Slowing the logging speed in prompt gamma and natural gamma ray work will provide more counts within a given interval of depth and so will improve the precision of ore grade determination.

There are several major limitations that affect the accumulated number of useful counts in a given period of time. First, there is a limit on the total acceptable counting rate. As the counting rate increases above some tens of thousands of counts per second the analog electronics becomes too busy, resulting in excessive dead time. Second, in order to keep the rate of damage to the detector from fast neutron interactions at a safely low level, the source-to-detector distance must not be too short. Third, the source strength is limited to that which can safely be handled in the field. Fourth, the detector has size limitations imposed by the diameter of the sonde and available detector manufacturing capability. Fifth, the logging speed should not be impractically slow. These limitations mean that although in principle it is possible to optimize the logging variables for any given sought element, there is no guarantee that the element can usefully be assayed in-situ by this method. In most cases reported here our evaluations indicate that most industry requirements can be met.

PHASE I

The objective of Phase I of this contract was the development of a borehole logging system based on high resolution neutron activation analysis or neutron capture gamma ray spectroscopy. The logging system consisted of the following subunits:

- Intrinsic (high-purity) germanium gamma ray detector
- Replaceable solid cryogen canister for maintaining the detector at low temperature
- Downhole electronics
- Uphole electronics, including a computer, for analysis and control
- Californium-252 neutron-emitting radioisotope source
- Shielding and safe handling facilities for the neutron source
- Surface support vehicle, or logging truck.

A block diagram of the logging system is shown in Figure 4.

Borehole Probe

A prototype high resolution gamma ray spectroscopy borehole probe was designed, built and tested, along with support hardware and software. A 5.1 cm (2 in.) diameter, fieldworthy probe, based on germanium detector technology, was constructed.

The borehole probe was constructed in two sections: the detector section and the electronics section. The sections could quickly be joined together for logging and decoupled for maintenance and service. The physical layout of the probe is shown schematically in Figure 5.

Detector Section

The detector section, called the cryosonde, had the following design goals:

- Maximum diameter, 5.1 cm (2 inches).
- Continuously operable for 8 hours, minimum, between servicings.
- Detector to operate without appreciable loss of resolution.
- System resolution better than 2.5 KeV FWHM (full width of peak, measured at half maximum amplitude) determined at 1.33 MeV.

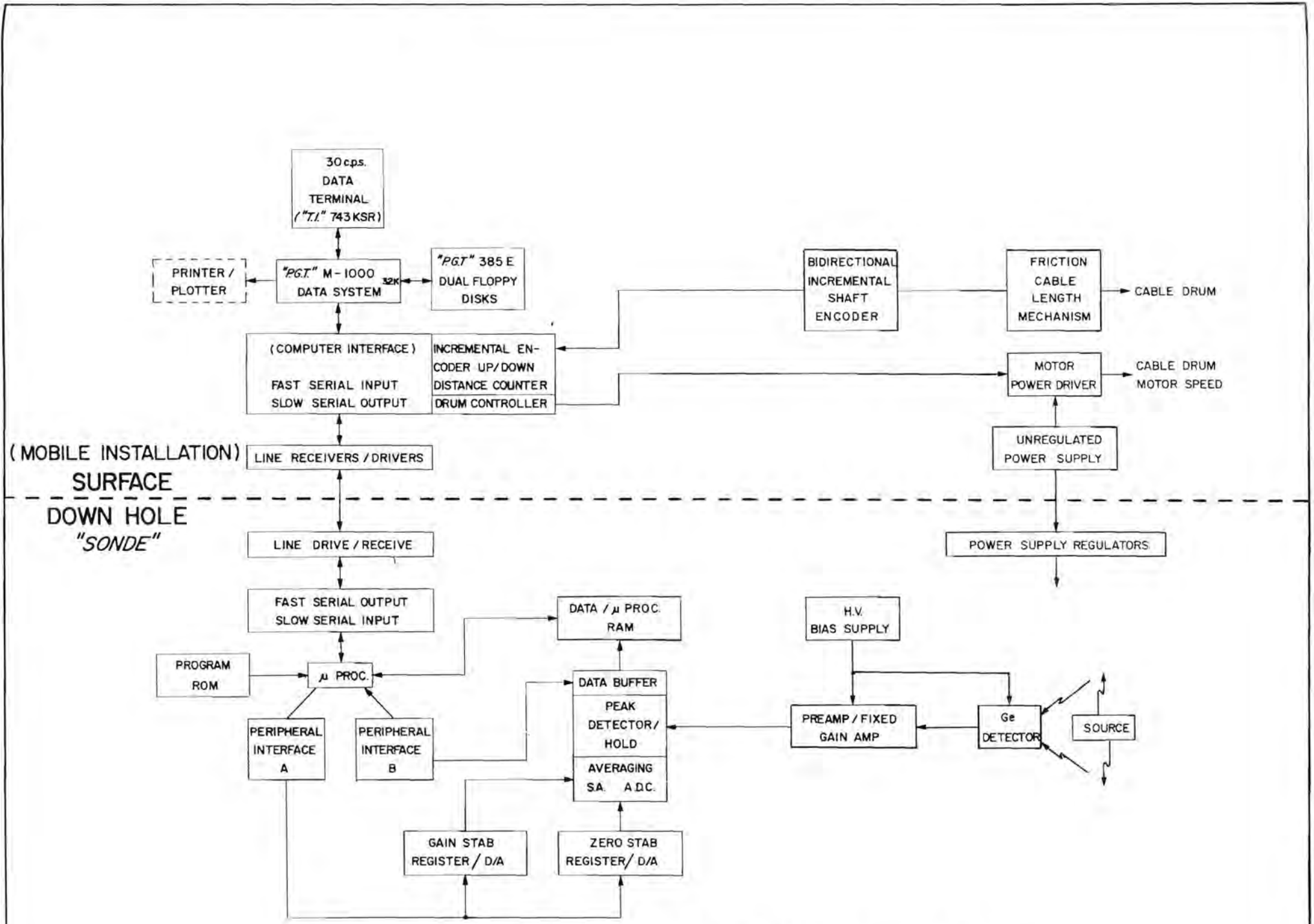

FIGURE 4. BLOCK DIAGRAM OF THE LOGGING SYSTEM

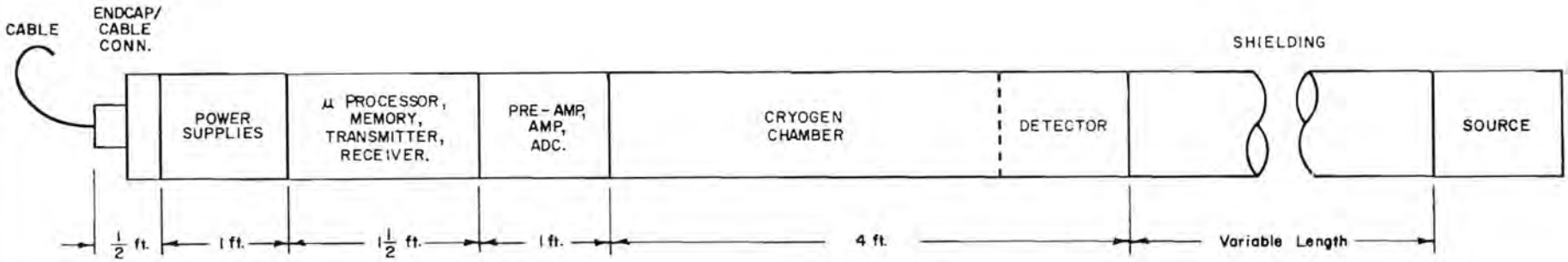

FIGURE 5. DIAGRAM OF THE PHYSICAL LAYOUT OF THE PROBE

The detector section was designed and constructed during the first half of Phase I. It measured 5.1 cm (2 in.) diameter by 122 cm (48 in.) long. The outer casing was 1.6 mm (0.062 in) thick stainless steel. It housed the germanium detector, the field-effect transistor input stage of the preamplifier, and the cryogen canister. The germanium detector was of the p-type, closed-end coaxial configuration and had an efficiency of 9 percent relative to a 7.6 cm x 7.6 cm NaI(Tl) scintillator at 1.33 MeV gamma-ray energy.

In designing the downhole cryogenic system we investigated two basic approaches. One used a solid cryogen that melted at a suitable cryogenic temperature, and the other used a large thermal mass (or copper) which had enough thermal inertia to allow sufficiently long operation in the borehole.

A major technical decision involved the choice of cryogen. The cryogen acted as a heat sink to keep the detector cold enough for high-resolution spectroscopy. Liquid nitrogen, a commonly used cryogen in the laboratory for cooling germanium detectors, could not be used in deep boreholes because of problems associated with venting the evolved nitrogen gas against hydrostatic pressure if the borehole contained water or mud.

Several different cryogens that relied on the solid-to-liquid heat of fusion were evaluated. An acceptable cryogen had to meet the following basic requirements: 1) melt at a sufficiently low temperature to permit successful operation of the intrinsic germanium detector and 2) freeze at a higher temperature than 77°K (the boiling point of liquid nitrogen), so that liquid nitrogen could be conveniently used to refreeze the cryogen during uphole servicing.

Propane was tested first. It had the advantage of low melting point (only a few degrees above LN temperature), but had the disadvantages of being flammable and having a relatively high gas-liquid equilibrium pressure at room temperature. Isopentane, freon, and solid copper were also tested. Isopentane, a liquid at room temperature, had the unfortunate ability to supercool at 77°K without freezing. Its melting point, 115° K, was relatively high. The fluorocarbon R-12 proved to be a nearly ideal cryogen since it exerted a pressure of only 80 pounds per square inch when in equilibrium with the liquid phase at room temperature. Its melting point of 106° K although below that of isopentane, always froze if cooled to 77°K. It had the highest heat of fusion per cubic centimeter of all the cryogens we tested.

The single phase system (the copper mass) required elaborate mechanical support to permit ruggedness and good thermal insulation, and did not yield holding times that were comparable to the melting solid systems.

We were able to meet our design goal of 8 hours holding time using either of two readily available cryogens: propane, and R-12.

Table 1

Holding (working) times of cryogen cannisters in probe.					
Cryogen	Melting Point degrees K	Detector Temp., degrees K	Time to Reach Temperature Plateau, hrs.	Time at Plateau, hrs.	Total Holding Time, hrs.
Propane	85	92	1-1.5	5-5.5	6.5-8.5
R-12	112	119	3-3.5	5.5	8.5-9.5

In the second half of Phase I the germanium detector was fabricated, mounted, and tested in the cryosonde. The holding times were not noticeably affected by the addition of the detector and FET stage. The detector resolution in the probe was about 2 KeV FWHM at 1.33 MeV energy for a detector that had measured 1.8 KeV FWHM in a laboratory cryostat.

Electronics Section

The electronics section formed the upper compartment of the probe in its vertical position. It had the same outer diameter as the detector section, 5.1 cm, and was 1.8 m (6 ft.) long. Major design goals included:

- -Maintenance of high-resolution capability at depths of 1830 m (6000 ft.) or less, at count rates exceeding 60,000 counts per second.
- -Minimal spectral drifts during normal field operation
- -Reliability in field operation
- -Moderate power consumption
- -Size constraints dictated by the 5.1 cm diameter casing.

The following functional subassemblies were included in the electronics section: pulse preamplifier, spectroscopy grade linear amplifier with base line restoration and pole-zero cancellation, 0 to 3000 volts detector bias supply, successive-approximation analog-to-digital converter, microprocessor with buffer memory, read-only memory (ROM) for the program, cable transceivers, and low-voltage power supplies. These subassemblies are described in detail below, but first we shall tell how the design goals and other motivations influenced some of the engineering decisions.

We wanted to be able to look at the in-situ gamma-ray spectra at the surface in order to examine the data and control the means by which it would be processed. One way to accumulate a spectrum at the surface would have been to transmit the analog output signals from the amplifier over a long coaxial cable extending from the sonde to a multichannel analyzer at the surface. We knew from experience that this approach had two serious drawbacks. First, upon transmission of the analog signal over a few thousand feet of coaxial cable the energy resolution would become degraded. Second, we wanted to use only 4-H-0 cable, a 4.8mm (3/16 in) diameter 4-wire armored cable commonly used in the logging industry. By contrast, if we were to have used coaxial cable it would not only have been more expensive and less fieldworthy, but it would also have imposed an undesirable uniqueness on the entire system. Such a sonde would have had the disadvantage that it could have been used only with a specially outfitted truck.

Our decision to use a single 4-H-0 cable made it necessary to transmit digital information at a rate of no more than 32,000 bits per second. This in turn meant that the sonde had to house the multichannel analyzer, consisting of an analog-to-digital converter and a microprocessor-based data storage retrieval, and transmission system.

The analog-to-digital converter (ADC) had to meet the following requirements: 1) approximately 4000 channels resolution, 2) spectroscopy-grade specifications, including good differential nonlinearity, and 3) small enough in size to fit into the sonde. The Wilkinson type of ADC, frequently employed in nuclear spectroscopy laboratories, had the requisite differential nonlinearity, but would have been difficult to fit into the confines of the sonde and would have imposed limits on high counting rate performance. We chose to employ the successive-approximation type of ADC, which is physically small and has a pulse-processing ("conversion") time that is short and independent of pulse amplitude.

In the system the accumulated 3968-channel digitized spectrum was sent up the cable every few seconds to the truck-mounted computer, where the data was held for further processing. The overall system resolution at the 1.3 MeV line was typically about 2 keV FWHM.

All the low-voltage power supplies in the sonde were pulse-width-modulated DC-to-DC converters because of the characteristically low power consumption of that type of design.

The computer not only stored and processed the spectra but also controlled the drawworks. The system could perform continuous logging at computer-controlled optimal speed and discontinuous (stepped) logging, depending on instructions.

Sonde Electronics

Figure 6 shows the functional block diagram for the sonde. Included are some signal names along with timing information. First, overall signal processing is discussed, followed by descriptions of individual PC boards including MAIN AMP/PREAMP, DMA/PUR ADC CHANNEL THRESHOLD, AVERAGING ADC, and MICROPROCESSOR Boards.

Here is a list of abbreviations we shall use.

ACIA	Asynchronous communications interface adapter (Motorola Corp.)
ADC	Analog-to-digital converter
AMP	Amplifier
D/A	Digital-to-analog converter
DEC	Digital Equipment Corporation
DMA	Direct memory access
EPROM	Electrically programmable read-only memory
FET	Field-effect transistor
PC	Printer circuit
PIA	Parallel interface adapter (Motorola Corp.)
PREAMP	Preamplifier
PTM	Programmable timer module (Motorola Corp.)
PUR	Pulse pileup rejector
RAM	Random access memory

Detector signals are processed on the Main Amp/Preamp Board where they are shaped with a 2 μsec time constant and routed to the ADC for analysis. The pulses are also routed to the DMA/PUR ADC Channel Threshold Board from a point prior to integration by the shaping circuits to provide FAST CHANNEL and Fast Discriminator signals. FAST CHANNEL is used by the ADC threshold detector, while the fast discriminator triggers a counter on the Microprocessor Board which keeps a total pulse count. Also on the DMA/PUR Board is a pile-up rejector which prevents the ADC from processing a pulse which has been distorted by another pulse trailing too closely behind it.

The Averaging ADC converts analog pulse signals to digital signals which can be processed by the Microprocessor Board. There are 4096 RAM memory locations corresponding to 4096 ADC channels. Channel addresses are incremented through DMA each time a pulse falls in a particular channel.

Channel data are transferred uphole to a computer over an asynchronous serial communications line at 31.2K baud. Data is read out sequent- ially, then cleared following readout. The uphole computers were either D.E.C. LSI 11/2 or computer automation LSI-2.

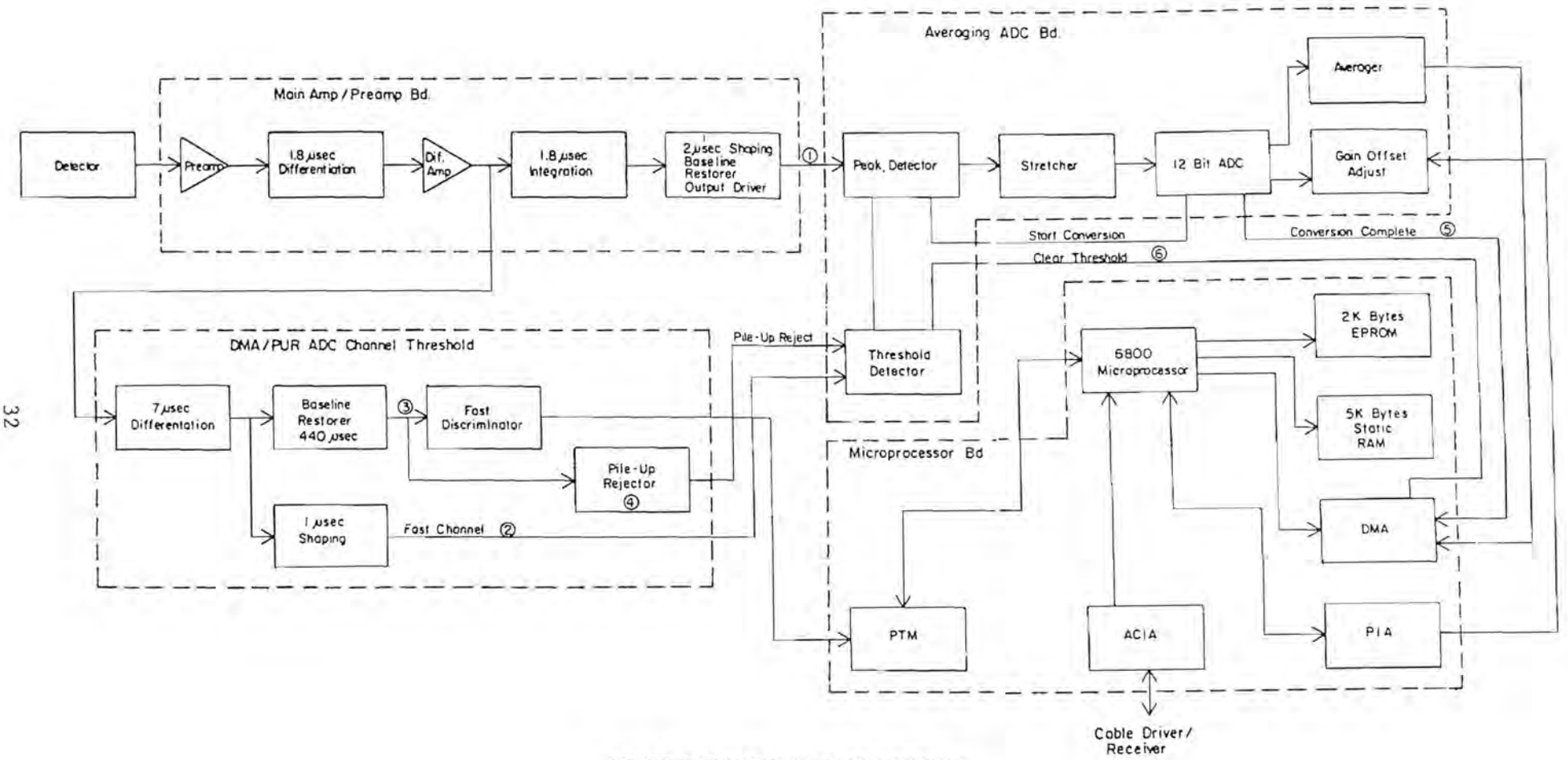

FIGURE 6 FUNCTIONAL BLOCK DIAGRAM OF SONDE

Preamplifier:

The preamplifier is charge-sensitive -- the voltage output is proportional to the charge input regardless of the input capacitance. Discrete components are used to meet requirements for low noise and high speed. The detector is DC coupled to the input FET of the preamplifier.

The relatively fast leading edges of the preamplifier output pulses contain all the radiation energy information. The amplitude of the voltage "step" at the leading edge of the output pulse is directly proportional to the absorbed energy of the gamma ray photon striking the detector. The relatively slow trailing edges of the preamplifier output pulses are a result of circuit properties.

The preamplifier contains an RC differentiator having a 1.8 μsec. time constant. This stage removes the DC offset from the preamplifier signal and shortens the trailing edges of the pulses, thus permitting higher count rates.

The preamplifier also contains a differential amplifier with a single stage of gain. Here again discrete components are used for low noise and high speed.

Shaping Amplifier:

The shaping amplifier is a two-stage active filter amplifier employing RC shaping to provide Gaussian output pulse of 2 μsec nominal time constant. The output pulse width is approximately 10 μsec.

Baseline Restorer:

A gated asymmetric baseline restorer is used immediately following the shaping amplifier. Negative restoration is "hard" while positive restoration is "soft" in order to avoid interference with positive pulse signals.

Output Driver:

The output driver consists of an operational amplifier and transistor push-pull pair. Although it feeds the nearby ADC, it is capable of driving up to 15m (50 ft.) of 100 ohm coaxial cable.

Fast Channel:

A fast amplifier/discriminator section is provided for baseline inspection and pulse pileup rejection. The "fast channel" includes the following stages:

Differentiator:

The differentiator limits the width of the amplifier pulses, which must be kept narrow to prevent degradation of the pulse pair resolving time (1 μsec).

Fast Discriminator:

The fast discriminator is used to determine the total pulse count. It sends a one-shot pulse to the microprocessor when triggered by a fast channel event just above the electronic noise. The total output of the fast discriminator indicates total gamma ray counting rate.

There are two fast channels on the circuit board. The second one is routed to the ADC and is discussed in the section below on Fast Channel Shaping Amplifier.

Baseline Restorer:

The fast channel baseline restorer removes any DC offset on the trailing edges of pulses coming from the differentiator. It is a relatively soft restorer, having a time constant of 440 μsec, and will remove a slowly varying DC component without affecting pulse shape.

Pile-Up Rejector:

Upon pulse detection by the fast discriminator, a 6.5 μsec one-shot is activated in the pile-up rejector. If a second pulse occurs within the 6.5 μsec window, the PILE-UP REJECT signal is sent to the ADC to prevent processing of the first pulse. Since the time between threshold and peak of a main amplifier pulse is about 6 μsec, a pulse occuring within 6 μsec of a previous pulse will distort the previous pulse. The pile-up rejector prevents the processing of such distorted pulses. The pile-up rejector is triggered by the fast channel so that PILE-UP REJECT is imposed before an ADC conversion takes place.

Shaping Amplifier:

A 1 μsec shaping amplifier adds integration to the fast channel to filter the pulse signal before it is sent to the ADC for threshold detection. Since threshold detection is very sensitive to noise, the additional shaping is necessary, although it is done at the expense of widening the pulse. This signal to the ADC is called ADC FAST CHANNEL.

Analog-Digital Convertor (ADC)

The main functional parts of the ADC subassembly are shown in the block diagram of Figure 7.

Threshold Detector:

The threshold detector starts the ADC process by triggering on the leading edge of an incoming pulse when a threshold level is exceeded. Triggering is done on a "fast channel" pulse from the DMA/PUR ADC Channel Threshold Board. Narrow pulses reduce the problem of threshold time walk. They result in triggering at a relatively constant time relationship with respect to the peak of the pulse. Use of fast, narrow trigger pulses permits sufficient time between threshold and peak, even for smaller amplitude pulses, for the ADC holding capacitor to become charged to full peak value.

Upon threshold detection of a pulse, the peak detector is enabled, and upon peak detection the ADC is activated. Conversely, resetting the threshold detector resets the peak detector, which in turn inhibits ADC processing. The threshold detector can be reset either by a CLEAR THRESHOLD signal from the microprocessor or a PILE-UP REJECT signal from the DMA/PUR ADC Channel Threshold Board. CLEAR THRESHOLD is used to initialize the ADC at system start up and following an ADC conversion, while PILE-UP REJECT inhibits conversion in the event of pulse pileup.

Peak Detector:

The peak detector is enabled by the threshold detector when a pulse crosses threshold. Once enabled, it will start an ADC conversion sequence upon detection of the peak of a sonde main amplifier pulse.

The threshold detector activates the pulse stretcher and the averaging circuit. About 4 μsec later, the time necessary for the ADC circuitry to settle, a START CONVERSION signal is sent to the ADC.

Stretcher:

The pulse stretcher holds the peak value of a main amplifier pulse on a holding capacitor so that the value can be sampled by the ADC.

12-Bit ADC:

The ADC is a successive approximation type, with a conversion time of 10 μsec. Fast conversion speed permits high throughput. The fixed conversion time makes dead-time calculations easier.

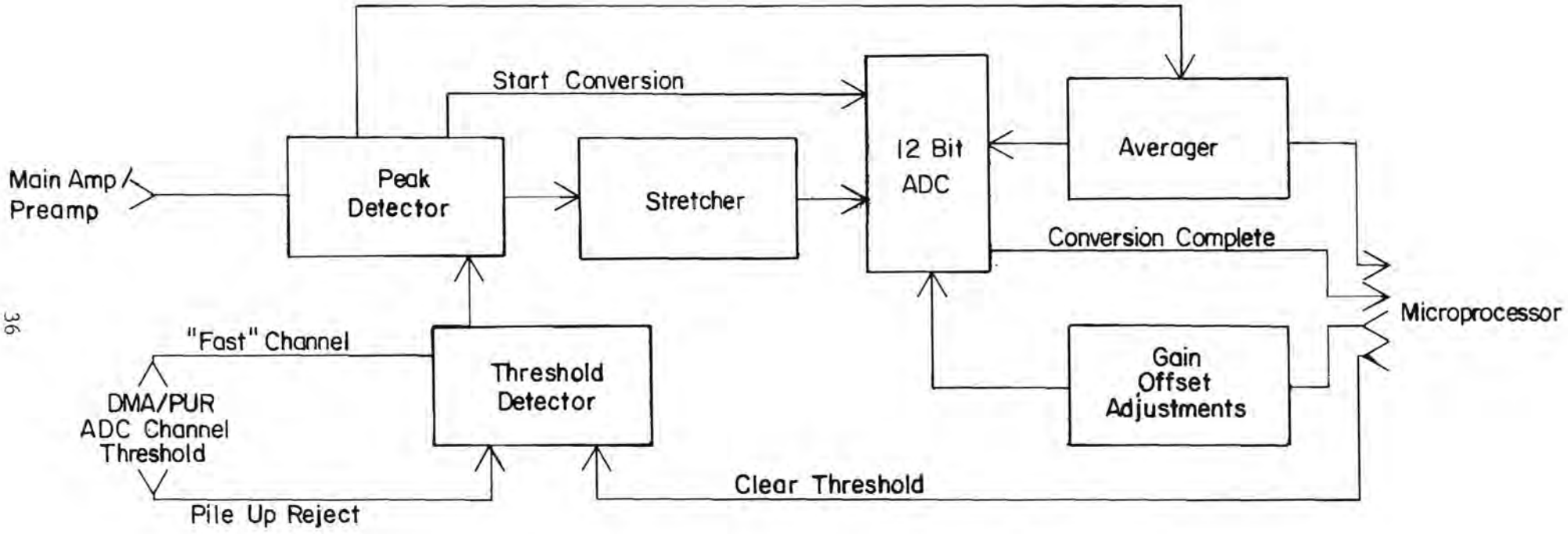

FIGURE 7. BLOCK DIAGRAM OF ANALOG-TO-DIGITAL CONVERTER SUBASSEMBLY.

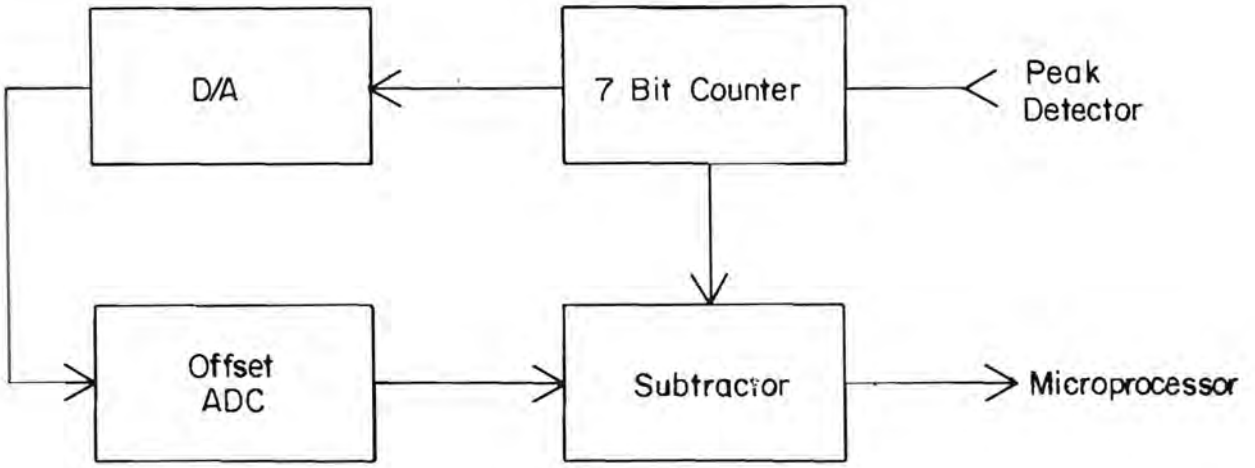

FIGURE 8. BLOCK DIAGRAM OF AVERAGER

The ADC provides 12-bit resolution, or 4096 channels. Gain and offset errors can be zeroed during calibration.

Gain and Offset Adjustments:

ADC gain and offset adjustments were under the control of the microprocessor through two D/A's. The microprocessor periodically fed the D/A's following calibration updates.

Microprocessor

The Microprocessor board is based on the Motorola 6800 Microprocessor, which runs at a clock frequency of 2 MHz. Figure 9 shows the block diagram of this board. On-board support chips include a Peripheral Interface Adapter (PIA) which is used to control ADC offset and gain adjustment D/A's, a Programmable Timer Module (PTM) which is used to count fast discriminator pulses, and an Asynchronous Communications Interface Adapter (ACIA), which controls asynchronous communications with the LSI-11 at 31.8K baud.

System memory consists of 5K bytes of static RAM plus 2K bytes of EPROM. Data acquisition from the ADC is through a DMA controller, which automatically updates ADC data in RAM. When an ADC digital value is received upon CONVERSION COMPLETE from the ADC, the contents of the location in RAM corresponding to that channel is automatically incremented, i.e., for each one of 4096 ADC channels, a channel address in memory keeps a running total of all conversions received for that channel. Periodically, normally every 2 or 3 seconds the entire spectrum is sent uphole and the RAM zeroed. If an overflow occurs at a particular channel address during data accumulation, an interrupt to the process or is initiated and the operator is alerted. Overflow occurs when channel count reaches 256 (8 bits).

After the DMA memory update, a CLEAR THRESHOLD is issued to the ADC so that another pulse can be processed. If an overflow occurs, CLEAR THRESHOLD is delayed so that the processor can process the Overflow Interrupt.

Schematic Diagrams

Figures 10 through 16 are interconnection and electronics schematic diagrams for the logging system.

Data Processing System

The design goal was a computer-based data processing system mounted in the logging truck. It had to be capable of accepting data in serial form over the logging cable and, in the initial stage, processing the data into a semiquantitative

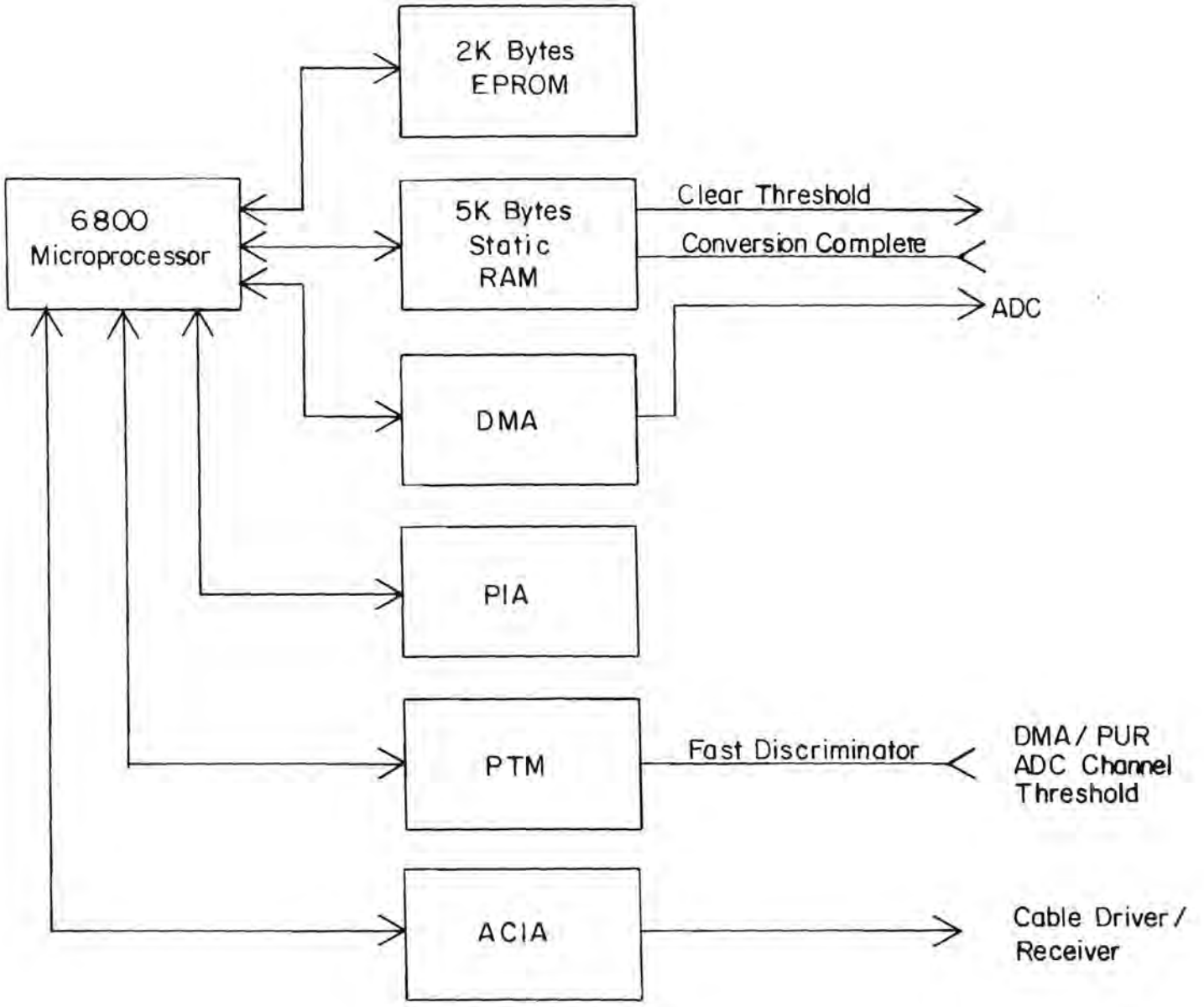

FIGURE 9 BLOCK DIAGRAM OF MICROPROCESSOR CIRCUIT BD.

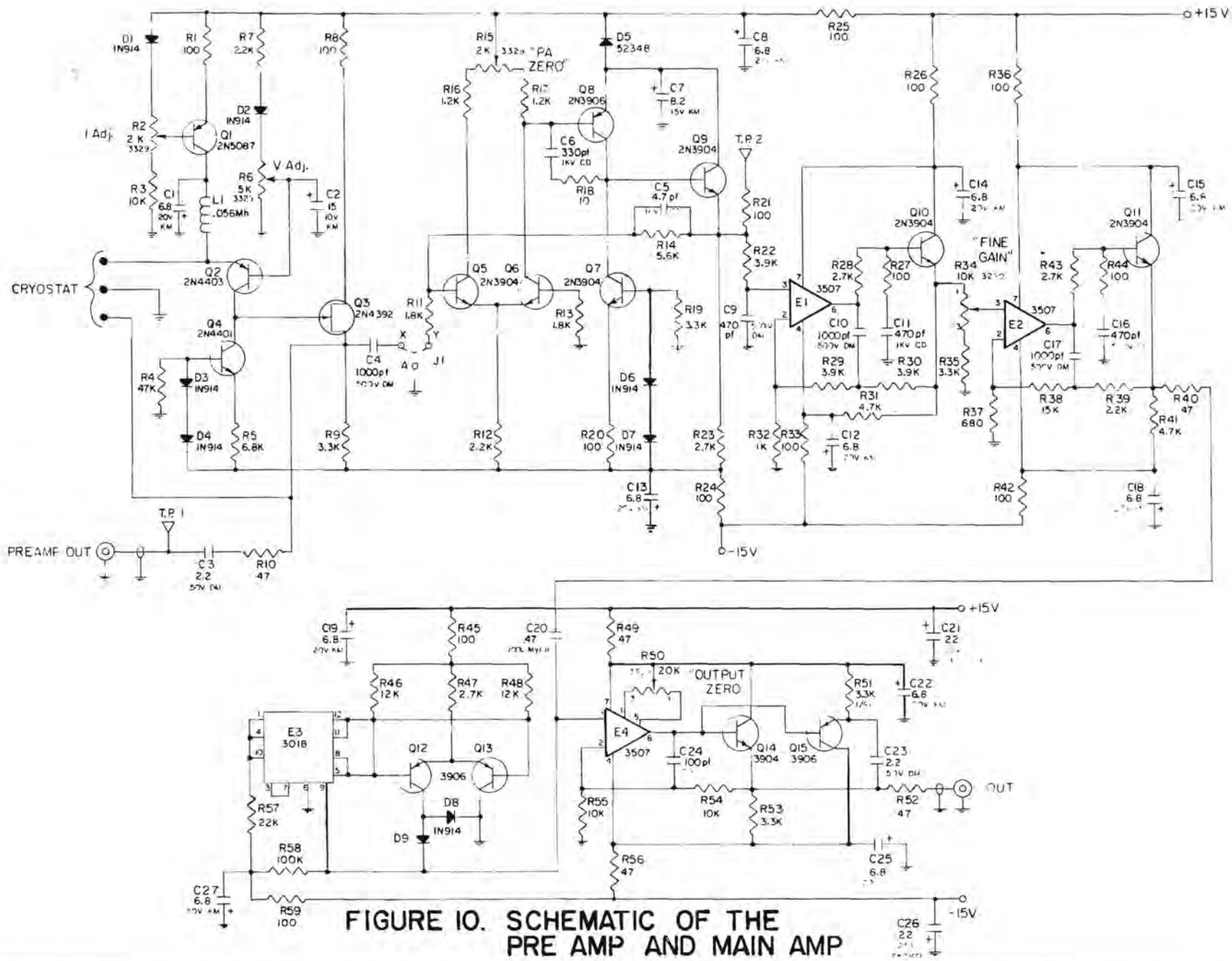

FIGURE 10. SCHEMATIC OF THE PRE AMP AND MAIN AMP

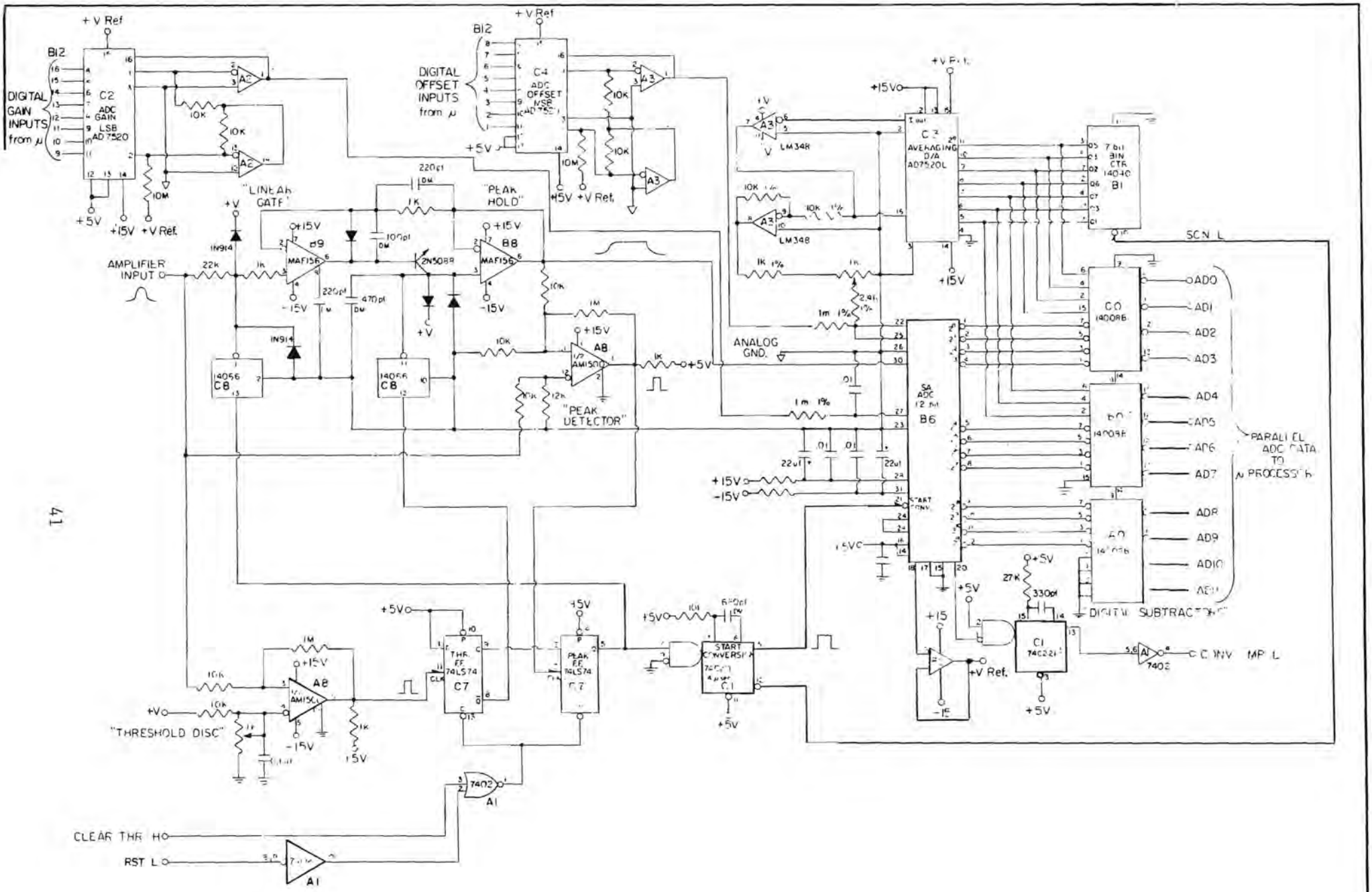

FIGURE 11. SCHEMATIC DIAGRAM OF ADC

FIGURE 12. SCHEMATIC DIAGRAM OF DIRECT MEMORY ACCESS, PILEUP REJECTOR AND ADC CHANNEL THRESHOLD.

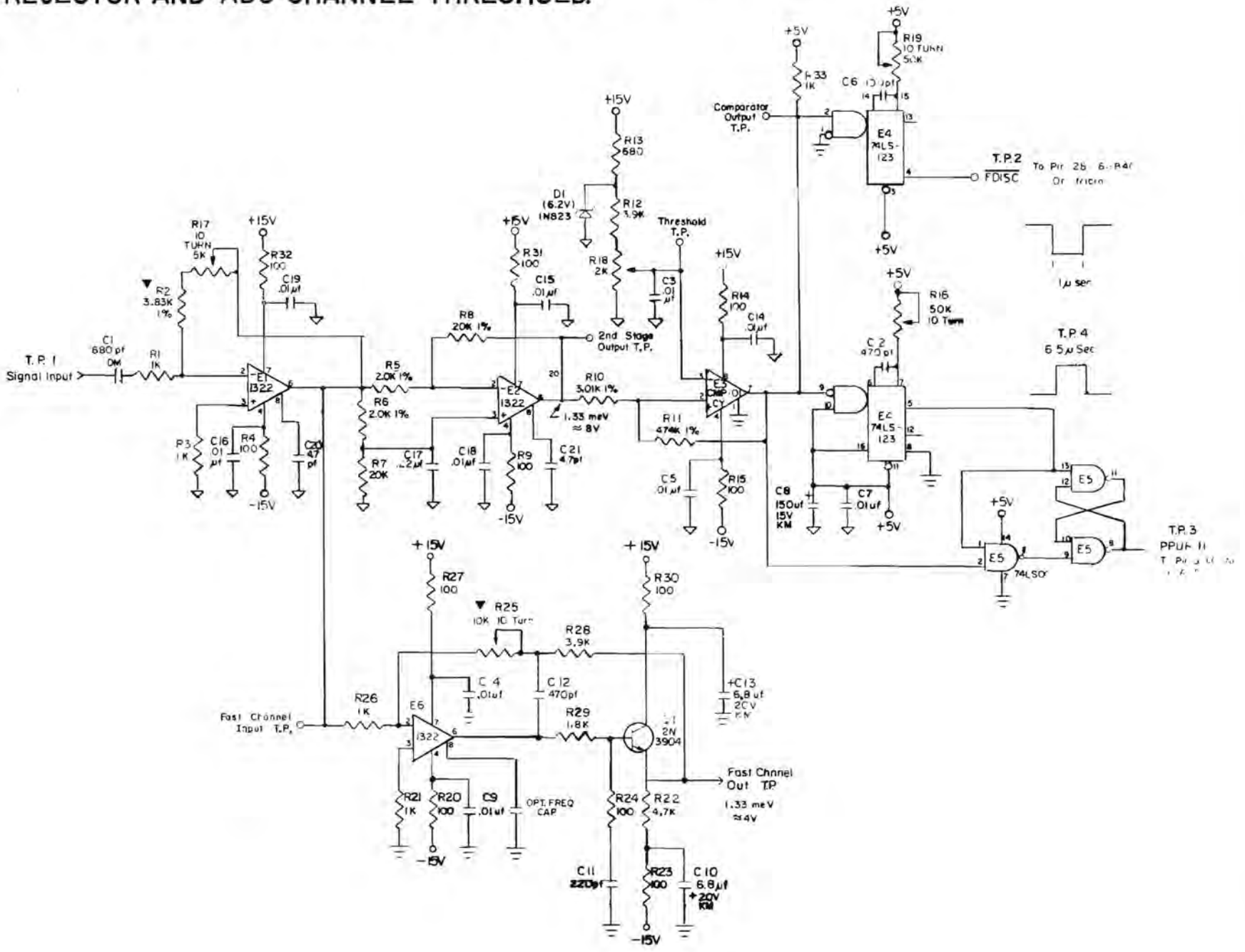

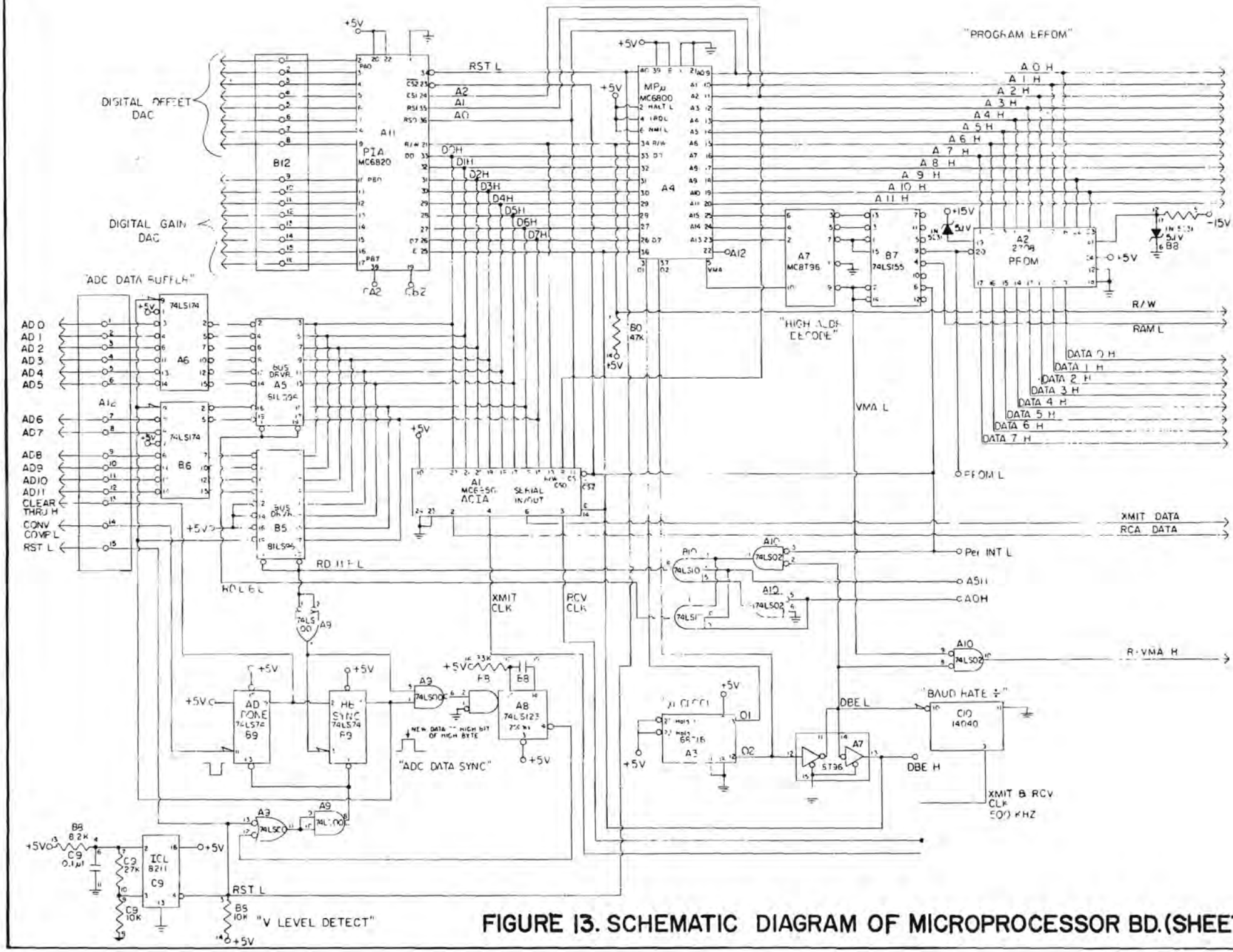

FIGURE 13. SCHEMATIC DIAGRAM OF MICROPROCESSOR BD. (SHEET 1)

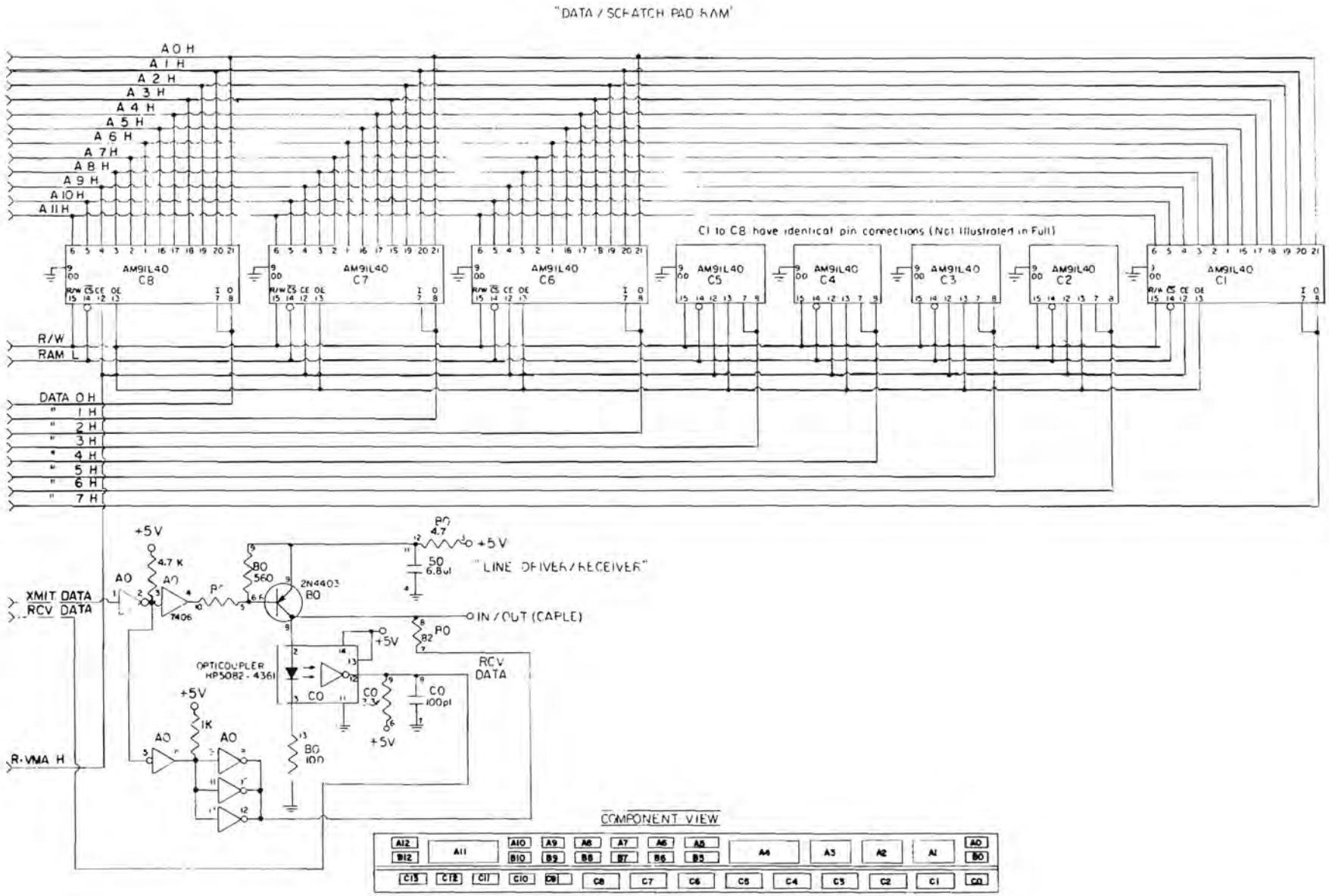

FIGURE 14. SCHEMATIC DIAGRAM OF MICROPROCESSOR BD. (SHEET 2)

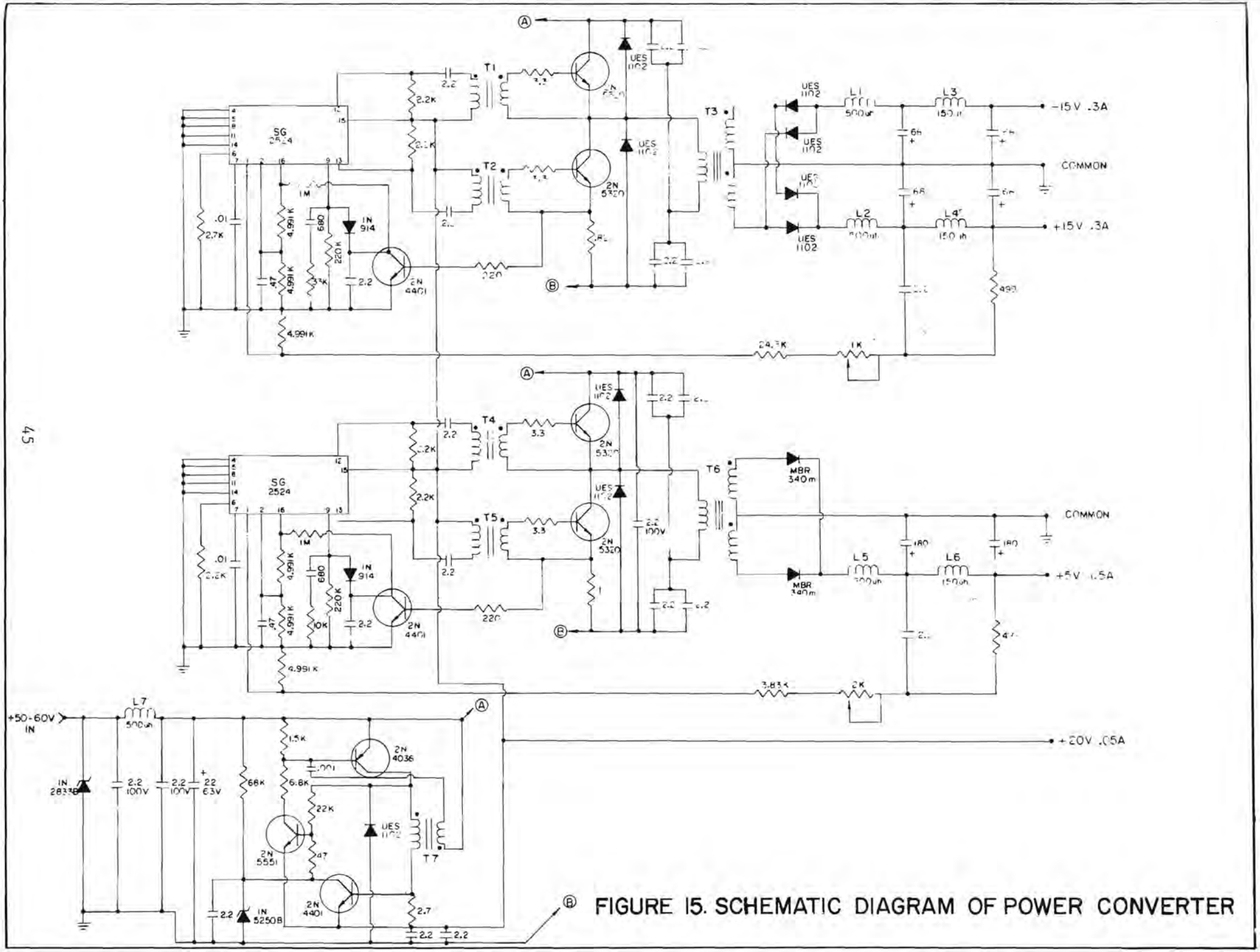

FIGURE 15. SCHEMATIC DIAGRAM OF POWER CONVERTER

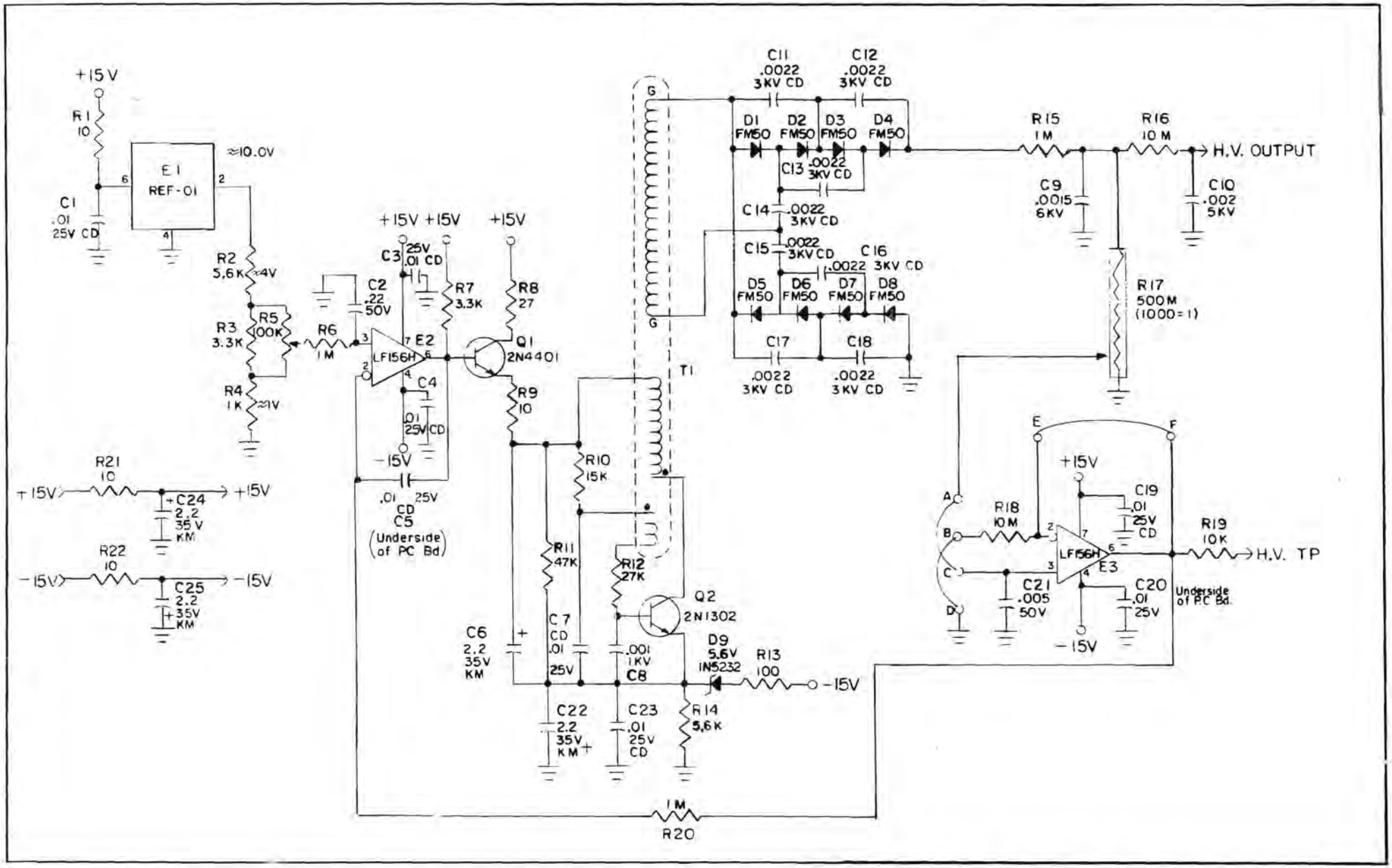

FIGURE 16. SCHEMATIC DIAGRAM OF POWER SUPPLY

ore grade analysis. It was intended that further software development would provide accurate quantitative analysis, corrected for the lithology of the formation. In addition, the computer was to analyze the data continuously to develop gain and offset control signals for the downhole microprocessor and was to control the microprocessor.

The appropriate surface electronics for processing data were mounted in the logging truck.

The block diagram of the components of the truck system is presented in Figure 17. After preliminary processing in the sonde, the signals are sent up the cable and distributed according to energy in a 3968 channel field (or spectrum) and stored in the computer. In order to maintain energy calibration, three peaks in the spectrum are chosen by the operator and checked by the computer at one or two minute intervals during each logging run. These peaks are selected from prominent peaks always present in the spectrum. They are chosen to span as much of the spectrum as possible. For instance, in an iron formation the stabilization peaks might be at 0.511 MeV, (annihilation radiation), 2.223 MeV (hydrogen) and the 7.632/7.646 MeV doublet (iron). The three peaks are used both to provide a redundency check and to diminish the effects of low statistics on the offset and gain calculations. Their centroids are calculated and the gain and zero offset of the downhole system are calculated. If the gain and offset differ from their initial values, the computer calculates corrections and sends the information to the downhole microprocessor.

Using this procedure we were able to maintain the energy calibration over a relatively wide temperature range. It should be noted that the system drifts were primarily caused by the warming up of the detector during a logging run, not by electronic instabilities. The stabilization and recalibration procedures worked extremely well.

A second program consisted of locating, identifying and summing all significant peaks in the spectrum. This was done in three steps. The first step was background subtraction. This step started with the application of a second derivative digital filter. Since the background was relatively flat, the doubly differentiated background regions were nearly zero, peaks showed up as central positive excursions with negative side wings. Background regions were located on both sides of significant peaks. The background under each peak was estimated by a level representing the weighted average of the two side regions.

After the peaks were located, backgrounds subtracted, and centroids calculated, they were identified by comparison with a table of gamma ray energies. The peak areas and statistical uncertainties were provided to the operator along with the isotopic or elemental identity.

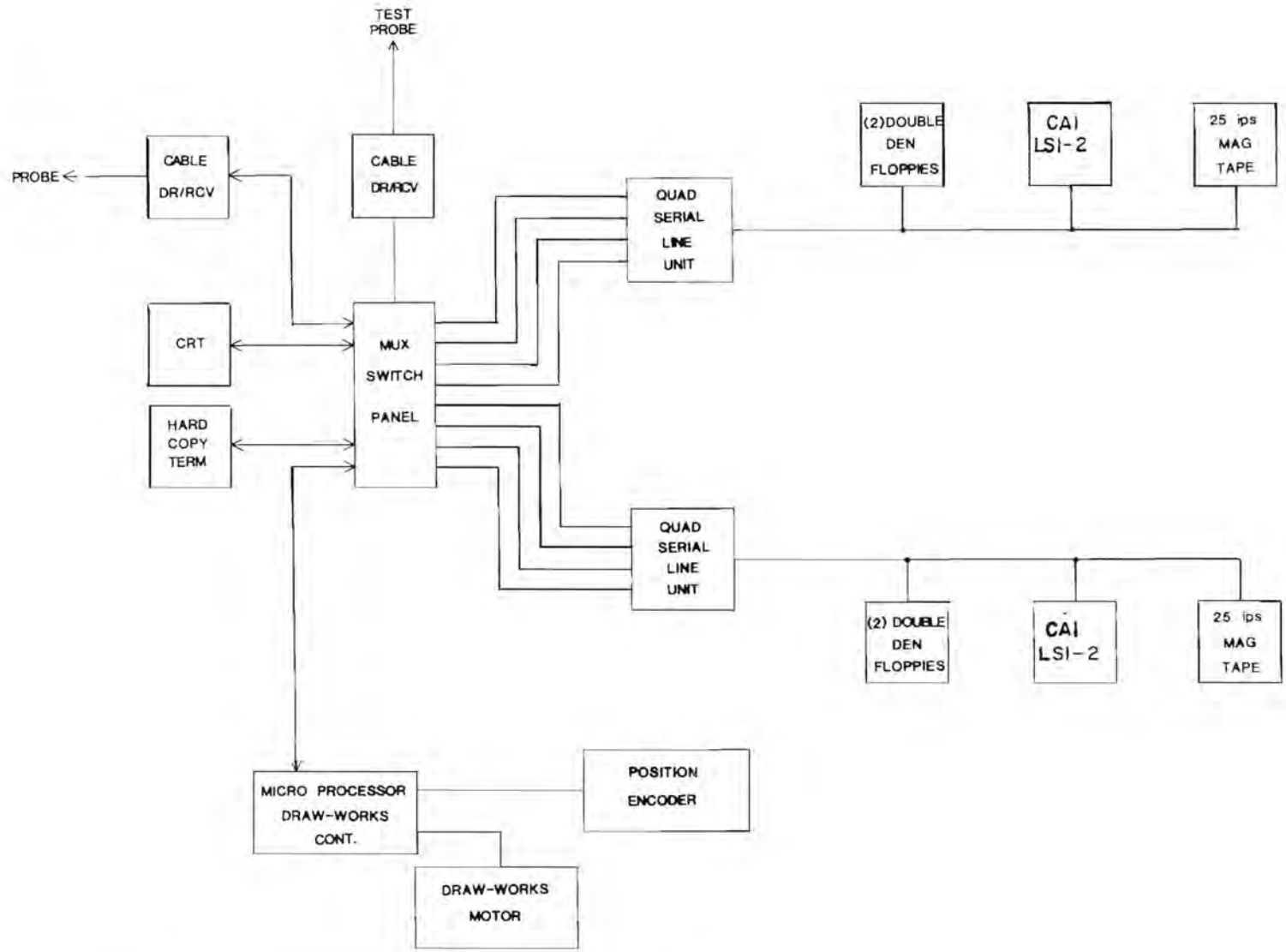

FIGURE 17. BLOCK DIAGRAM OF LOGGING SUBSYSTEMS IN THE TRUCK

The third step was to convert the peak areas into elemental concentrations. This conversion to quantitative analysis was done during the Phase II field tests, and the software was refined as Phase II progressed.

We emphasize what we stated in our original analysis of this program: there is no theoretical path available that can take us directly from measured gamma ray intensities to quantitative analysis. The development of standards (either laboratory standards or field coreholes having core analyses) for the purpose of calibrating the probe was one of the major tasks of Phase II.

Neutron Source

Californium-252

Californium 252 was the neutron source used in all our neutron activation work. It is a man-made isotope which decays spontaneously, producing both alpha particles and neutrons. Only the neutrons penetrate the source capsule. The Californium source was selected for several reasons. It was readily available and relatively inexpensive. It was safer to use and easier to license than other radioisotope neutron sources such as plutonium-beryllium. The average energy of neutrons produced by Californium-252 is 2.35 MeV, which is significantly lower than that of a plutonium-beryllium source or an accelerator. In neutron capture work it is advantageous to start with neutrons having relatively low energies because gamma ray backgrounds are lower, thermalized neutrons are concentrated in a smaller volume nearer to the detector, and the detector which is subject to damage by energetic neutrons can be safely located closer to the source.

On the other hand, there are advantages to using an accelerator to generate neutrons. It can be pulsed. It is easier to handle. Finally, several important applications require energetic neutrons.

Table 2 lists the major nuclear properties of Californium-252. (37)

Table 2

Nuclear Properties of Californium-252.	
Effective half-life	2.646 ±0.004 years
Alpha decay half-life	2.731 ±0.007 years
Spontaneous fission half-life	85.5 ±0.5 years
Average neutron energy	2.348 million electron volts
Average alpha particle energy	6.117 million electron volts
Gamma emission rate	1.3×10^{13} photons per second per gram
Decay heat (51.1% from fission, 48.9% from alpha decay)	38.5 watts per gram
Neutrons per spontaneous fission	3.76 neutrons
Specific neutron activity	4.4×10^{9} neutrons per second per curie
Neutron emission rate	2.34×10^{12} neutrons per second per gram

Summary

The logging system met all of its design goals. The next step was to transfer it to the logging truck prior to Phase II.

Source Design

The neutron source was to be strong enough to yield an acceptable data rate. It was to be made by a certified supplier to meet NRC regulations. Its storage container had to permit wasy and safe attachment to the sonde without radiation exposure of personnel or risk of losing the source downhole.

The source supplier was Monsanto. With their consultation we designed a container that will be used for shipment by common carrier and for transport to field sites in the surface support vehicle. It is about 30 inches in diameter and 36 inches high. The source was designed to be mounted in a rotatable shutter having a chain and sprocket linkage that permitted it to be screwed into the sonde from outside the shield. Only after the source was attached to the sonde the shutter could be released and rotated to a position that permitted the sonde to be lowered into the borehole.

The source size was chosen to be 25 micrograms of Californium-252. This size was selected from consideration of maximizing safety in handling, minimizing the potential radiation damage to the detector, maintaining adequate analytical sensitivity, and retaining detector resolution. The theoretical and experimental procedures describing the optimization process have been reported. (27)

We ordered two Cf-252 sources from Monsanto. One was the 25 microgram source for use in most of the field tests. The second source was 2.5 micrograms. It was used in preliminary tests to troubleshoot the system and to get most of the borehole standards data. These data aided the extraction of quantitative data from the field logs.

Phase I Performance Tests

The entire system was tested for holding time, system resolution, proper logical functioning of the microprocessor, including its control of gain and offset of the ADC, quality of transmission over 3000 feet of 4-H-O cable, and full two-way communication with the computer at the surface.

The cryosonde (detector, cryostat and first stage of FET preamplifier) was tested with laboratory electronics (last stages of preamplifier, main amplifier, HV supply, ADC etc.) The resolution was 2.1 keV for 1.33 MeV gamma rays. Then the downhole electronics package in its entirety was tested using a laboratory germanium detector. The resolution, observed with the PGT-1000 surface computer connected through 3000 feet of 4-H-O cable was between 2.0 and 2.1 keV at 1.33 MeV. Finally, the completely assembled system exhibited about the same resolution, 2.1 keV FWHM at 1.33 MeV.

The autocalibration system, which provided gain and offset corrections to compensate for drifts as described above was found to work well. Little or no electronic drift was observed (as evidenced by little change in the offset and gain correction signals) when the detector was maintained at constant temperature. During a typical warmup the correction signals changed in a continuous pattern that was related directly to the changing detector temperature. (Note: As the germanium crystal warms up, the energy bandgap decreases slightly. This increases the number of electron-hole pairs produced by the gamma rays, tending to shift the photopeak slowly toward higher energy if not corrected).

The microprocessor performed its function as intended. Incoming ADC events were processed with priority, and the buffer memory was systematically interrogated during ADC idle time.

No losses were encountered during transmission over the logging cable up to the maximum specified data rate of 31.8K baud per second.

PHASE II

Field Tests

Summary of Goals and Accomplishments

The primary objectives of the field tests were: 1) to test and improve the performance and reliability of hardware and software, 2) to observe the characteristics of various neutron-induced gamma ray spectral techniques using the Cf-252 source and germanium sonde, and 3) to quantify the capabilities of the germanium sonde pertinent to the following ores and minerals of commercial interest: uranium, iron, coal, copper, silver and gold.

By the end of the project a great amount of experience had been gained in all phases of the work. Some of the main objectives were reached but not all. Most successful was the progress made in hardware and software development, the identification of an immediately useful application (uranium logging), and the acquisition of basic data pertinent to neutron-stimulated gamma ray logging for the ores and minerals studied.

The uranium logging technology that was developed, in part, under this project was considered by the contractor to have significant advantages over other methods. After completion of the field test, the contractor initiated a commercial uranium logging service based on it.

The iron and coal results were considered to be technically successful but of little immediate value to the mining industry. The method was not judged by the authors to be currently cost competitive with other methods available in both iron and coal work. Moreover, the method could not distinguishbetween the different valence states of iron, between different types of ores such as magnetite (Fe_3O_4) and hematite (Fe_2O_3). Knowledge about the type of ore is essential to the industry, since mining and processing costs are ore-dependent.

Results for silver, gold, and copper were incomplete for various reasons. Of the three, the delayed-gamma-ray data on borehole neutron activation of silver showed a great deal of promise but had large uncertainties because of unreliable chemical assays of borehole material. The prompt-gamma work on gold revealed that the method had unusably low sens[illegible]. There were other problems in the gold study: an important gold-bearing zone that should have been logged was not logged because of erroneous chemical assays. The investigation of copper suffered from the absence of a more active source. Because of that, no delayed-gamma work was attempted on copper. Theoretically, the delayed-gamma method was expected to be more sensitive than the prompt-gamma method.

In summary, it was felt that the field tests produced valuable preliminary data, indicated some of the potentialities and limitations of the method, and pointed up specific areas of investigation that could benefit from further work.

Field Test Procedures

Our experimental procedures were developed over the duration of this research. Calibration, data collection, and data reduction procedures became efficiently automated. A typical field test consisted of setup, calibration, passive (natural gamma ray) logging, prompt gamma-ray neutron activation, and in a few cases delayed-gamma-ray neutron activation.

Two vehicles were generally used in the field tests that employed neutron sources. One was the mobile laboratory housing the sonde, computers, drawworks, generators, and associated electronic systems. Figure 18 pictures the logging vehicle used in this work. The other a truck with californium 252 sources in their casks. In use the cask holding the stronger source was placed astride the borehole. The sonde was connected to the source through a port that permitted logging through the cask. That is, the sonde and cable could pass through the cask. When the second smaller source was used, its cask and shielding was set up near the borehole. Then the sonde was coupled to the source and the sonde/source assembly rapidly moved to the borehole. The assembly was controlled by guy lines manipulated by operators who were positioned about 10 to 20 feet from the source. Radiation measuring instruments and personal dosimeters were employed to verify that exposures of personnel to radiation were within allowable limits.

In a typical field test the area was roped off and posted as a radioactive safety zone. The whole setup was monitored according to Nuclear Regulatory Commission (NRC) regulations, conforming to appropriate safe standards for such an operation. The detector was calibrated on the surface with a cobalt-60 source prior to lowering the sonde into the borehole.

The detector energy resolution, when the sonde was in operation, was monitored by observing one of the prominent gamma-ray lines commonly present. Often the aluminum 1779 keV line or the prompt 2223 keV line of hydrogen was used. Degradation of the resolution indicated incipient detector warmup and signalled that it was time to raise the sonde to the surface and replace the cooling canister.

The gain and threshold of the 4000 channel analog-to-digital converter (ADC) were set to cover the energy range, 200 keV to 3560 keV, in delayed (n, γ) studies. In the prompt-gamma mode of operation the values were adjusted for the energy range of 150 keV to 9750 keV.

Typically, passive logs were first run at approximately one foot per minute in the borehole to determine baseline levels of natural radioisotopes. This was done because activity from the decay products of naturally occurring potassium, thorium and uranium formed part of the background in activation spectra. The passive counting situation in the

FIGURE 18

borehole is schematically illustrated in Figure 19.

Prompt (n, γ) logging required the determination of the appropriate spacer length separating the source from the detector. The spacer protected the detector from damage by fast neutrons in two ways. First, its tungsten shadow shield scattered neutrons coming directly from the source. Second, it put the detector at the optimum distance from the source so that adequate gamma-ray count rates were achieved without appreciable neutron damage to the detector. The optimum spacing depended on the source strength and the neutron scattering properties of the formation. Since the presence of hydrogen in the formation (in bound or unbound water or in organic matter) had a powerful slowing effect on neutrons, shorter spacers were used in porous rock formations and longer spacers in hard rock.

Neutron capture is the most prevalent interaction that results in characteristic gamma rays useful in neutron activation analysis. Fast neutrons such as those produced by californium-252 are slowed in the formation to thermal energies, approximately 0.025 eV, prior to capture. The mean slowing down time and the mean free path to first collision are functions of the composition of the formation and the original energy of the neutron. In granite the mean slowing down time is about 300 usec with mean free path of 6.5 cm. In water the mean slowing down time is only about 4 μsec. Therefore the amount of water in and around the borehole significantly affects the calibration of the probe and the quality of results.

Four factors are particularly significant in the delayed activation mode: the source-to-detector distance, the period of activation, the delay before counting and the counting period. The source-to-detector distance can be optimized by maximizing the gamma flux subject to limits on the allowable fast neutron flux at the detector (16). For example, if damage is established in a germanium crystal after neutrons per square centimeter have struck the detector,and a lifetime of 1400 hours is acceptable, then no more than 20 fast neutrons per square centimeter per second are allowed.

The period of activation was chosen, if convenient, to be one to three times the half life of the pertinent radioisotope. Delay time could not be less than the time to move the detector to the point of activation, but it was sometimes made long enough to reduce interferences from shorter lived radioisotopes.

Extraction of the desired net counts from each spectrum was accomplished by means of a computer subroutine contained within the logging program. This subroutine performed a least squares fit of the data to a mathematical function that represented a Gaussian peak shape superimposed on a linear background. The program was capable of fitting three

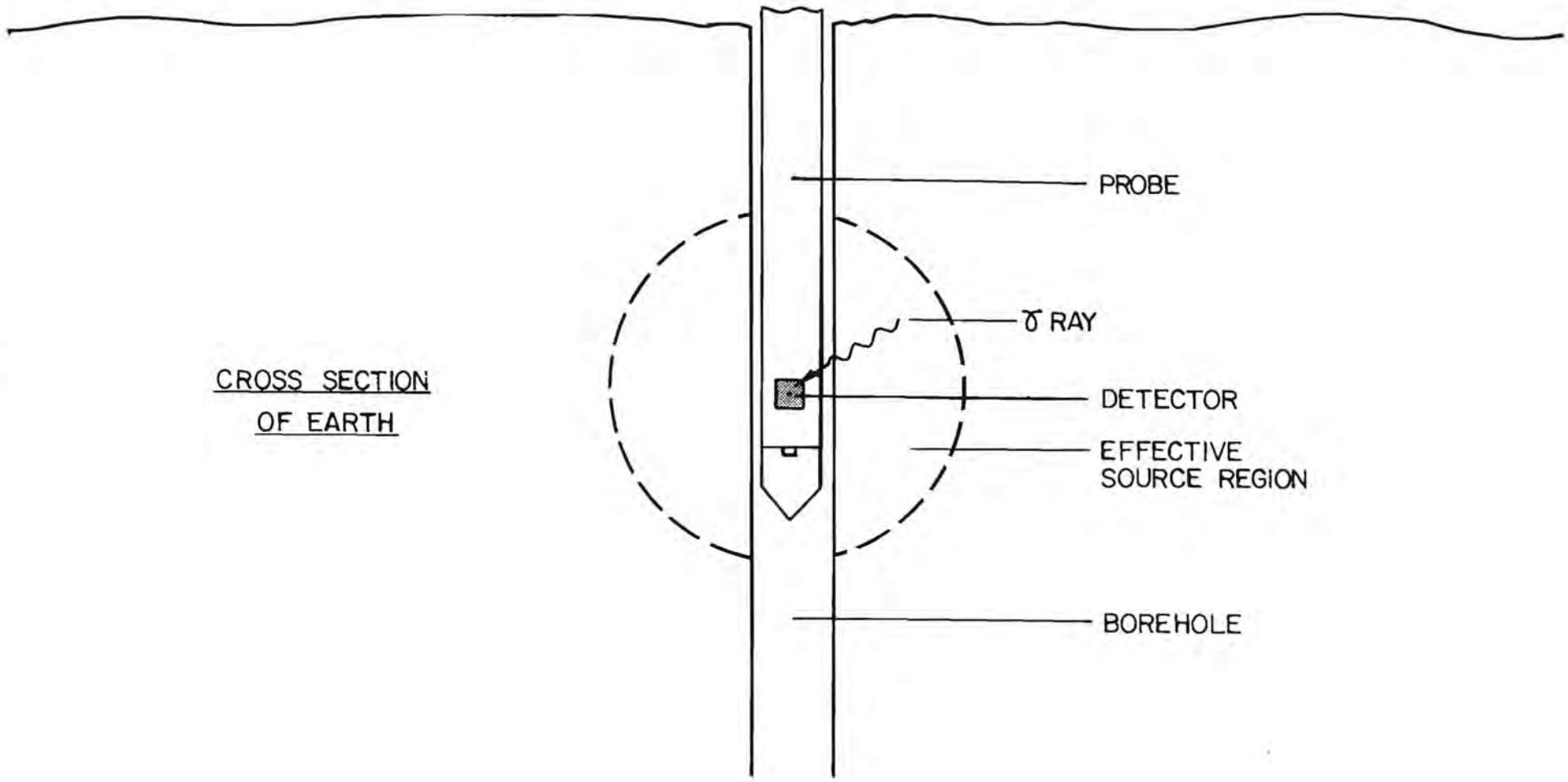
CROSS SECTION
OF EARTH
PROBE
γ RAY
DETECTOR
EFFECTIVE
SOURCE REGION
BOREHOLE

FIGURE 19

preselected peaks per pass through a spectrum. Of these, two peaks were used by the program to calibrate the spectrum. The third peak was the peak to be analyzed.

The experimental data were then compared to core assays or other reference standards, from which calibration factors were developed. Finally, limits of detectability were estimated from the statistical uncertainties associated with photon counting, and so represent the best attainable results for the system under the stated logging conditions. Actual uncertainties were worse by unknown amounts because they included the combined effects of all sources of error, some of which were inestimable from the limited data.

We now describe the field tests pertinent to the various ores and minerals. These are organized not in chronological order, but are rather grouped by logging technology: passive logging (uranium), prompt gamma rays (iron, coal, copper), prompt and delayed gamma rays (silver, gold).

Iron: Reston, Virginia, and Dover, New Jersey

Objectives

The main objectives of the iron tests was to field test the equipment for the first time with the Cf-252 neutron source. Iron ore provided a good material for this purpose. We expected the characteristic signal from iron in iron ore to be readily and unmistakably seen because 1) commercially important iron ore grades were high in iron content, 2) the neutron capture cross section (probability of neutron interaction) was relatively high, and 3) the resulting prompt gamma ray spectrum of iron exhibited a readily discernable doublet structure. We felt that iron ore would be an excellent test material upon which to examine various experimental parameters, such as the effect of source-to-detector spacing on signal intensity, background intensity, and sample volume.

Background

The reaction of interest is that of thermal neutron capture by Fe-56 written symbolically as:

$$(Fe^{56}) + n \longrightarrow (Fe^{57}) + \gamma$$

Natural iron is 91.8% Fe-56. The Fe-56 isotope has a thermal neutron capture cross section of 2.6 barns. The newly formed Fe-57 promptly emits gamma rays. About 22% of the captures result in gamma ray emissions at 7.646 MeV and about 27% at 7.632 MeV (17). The resulting spectrum from each of these gamma rays contains, in addition to the full-energy peak, single- and double-escape peaks. The last two represent irretrievable loss of one and two 0.511-MeV annihilation photons, respectively, emitted following the pair production interaction within the detector. There is also a Compton-scattering continuum, representing inelastic photon collisions with electrons in the detector. A portion of a spectrum highlighting the full-energy and escape peaks of the Fe-56 doublets is shown in Figure 20.

Calibration Test Pits, Reston, Virginia

This portion of the investigation was carried out in close cooperation with Frank Senftle and his group at the U.S. Geological Survey at their test pits in Reston, Virginia. The purpose was to test the effects of the source-to-detector spacing and to calibrate the sonde in preparation for the field tests.

Test holes were constructed in the following way. Into an existing 89cm (35 inch) diameter pit were stacked, by means of an overhead crane, five cylindrical iron ore standards one on

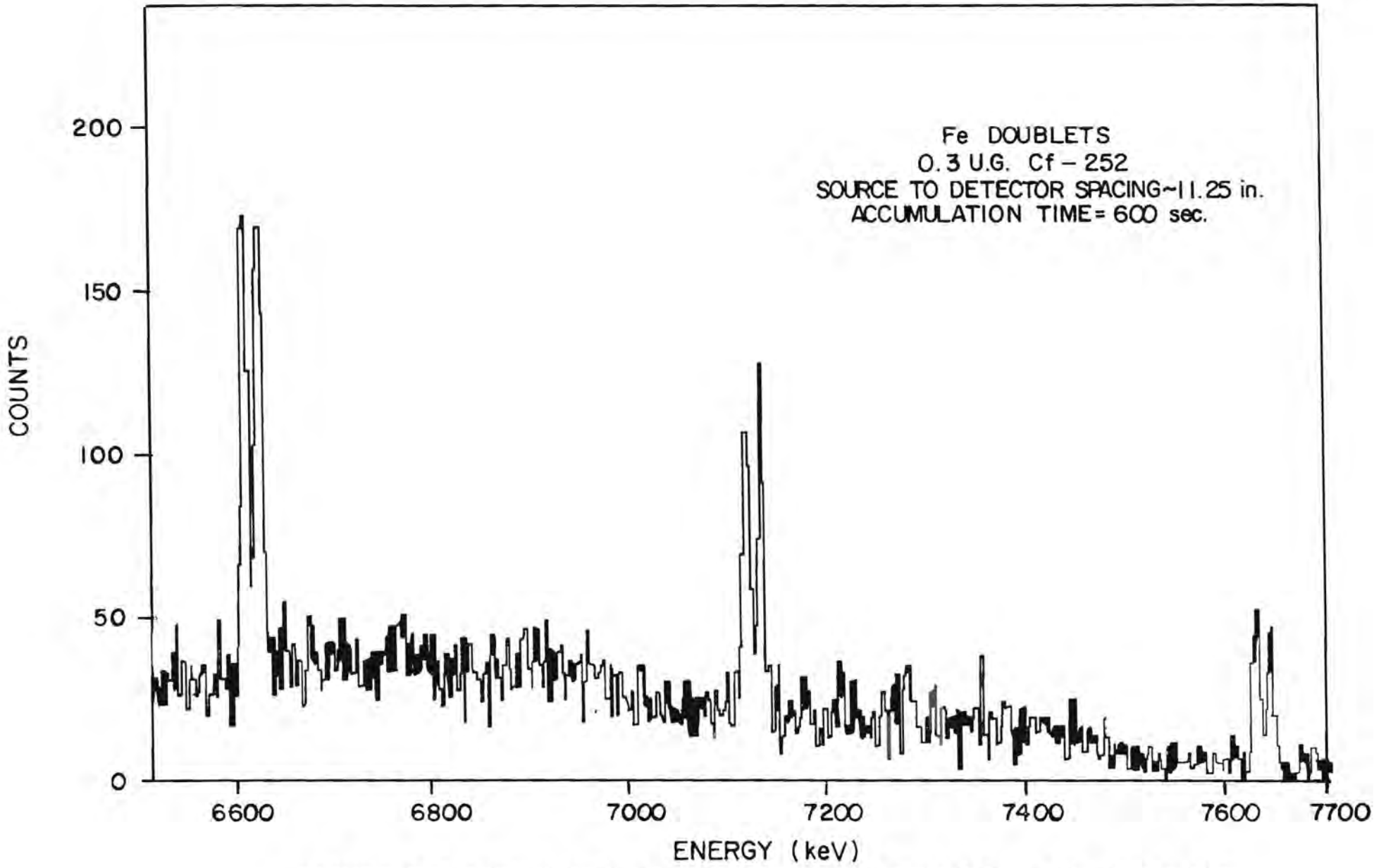

FIGURE 20. PORTION OF NEUTRON-CAPTURE GAMMA RAY SPECTRUM OF IRON, FROM 6.6 MeV, SHOWING THE FULL ENERGY DOUBLET AND THE ESCAPE PEAKS.

top of another. Each standard had dimensions 76cm (30 inch) diameter x 76cm high and had a 13cm (5 inch) axial open core. A 13cm diameter ABS plastic pipe passed through the cores of the stack to form an inside liner; it was sealed to the pit at the bottom. Standards were prepared: six containing 12% Fe, six with 27% Fe, and six with 49% Fe. Individual standards weighed less than 1050 kg (2300 lb). The stack formed a simulated borehole. Variety was achieved by rearrangements of the ordering of the standards in the 380 cm (150 inch) high stack.

The standards were prepared as iron-ore-loaded castings. Concentrated iron ore from Dover, N.J., the site of the field tests to come, was thoroughly mixed with Portland cement, sand, and the least amount of water necessary to achieve a good solid casting, in order to keep the hydrogen content to a minimum. Steel lifting cables were cast into each piece. The castings were steam-cured, then sealed with silicone to stabilize the hydrogen content.

Table 3 lists the calculated compositions of the three ore-grades standards for the major elements exclusive of hydrogen and oxygen.

Table 3

Lab Analysis of simulated iron-ore standards. Composition,(wt %)			
ELEMENT	LOW	GRADE MEDIUM	HIGH
Fe	12.0	27.0	49.0
Ca	8.0	8.0	7.0
Si	19.0	11.0	4.0
Mg	2.3	1.8	0.8
Al	4.5	2.8	0.9

The following elements were present in concentrations lower than 0.1%:

Cu, Cr, Mn, Ni, Ba, Mo, Cl, Na, V.

In all tests the borehole model was filled with water. Depth was measured from the top of the stack to the detector position. For calibration purposes, a 600-second spectrum was first collected at the center of each ore grade stack. Then the stack was logged point-by-point through the ore grade interfaces in 30 second periods of data acquisition per point.

We next investigated the interrelationship among the source strength, source-to-detector spacing, and relative sensitivity. We tested a variety of source strengths, ranging between 0.3 ug and 100 ug of Cf-252 (7 x 10 and 2.3 x 10 neutrons/sec, respectively), in combination with spacings that gave total counting rates of about 3000 counts/sec. and total neutron fluxes at the detector of 20 neutrons per sq. cm per second or less. This insured low rates of neutron damage to the detector. We found that the analytical sensitivity to iron varied only by a factor of 2 under these conditions, even though the source strength varied by a factor of 300.

Field tests, Dover, New Jersey

The iron-ore field tests were carried out at the Halecrest Co. mine in Dover, N.J. In the first tests our objectives were to check the reproducibility of the system, to establish procedures for safe handling of the sources in the field, and to collect spectra pertaining to a wide range of ore grades.

In order to study the reproducibility of the system, spectra were collected from six successive depths in the borehole, 10 minutes at each depth. The depth intervals were 6.1 m (20 ft). A 0.3 ug Cf-252 source was used, spaced 29 cm (11.3 in) from the detector. After spectra from all the depths were recorded, the sonde was pulled up and the sequence was repeated two more times. In each spectrum the three pairs of iron doublets, the full-energy peaks at 7.646 MeV and 7.632 MeV and their single- and double-escape peaks, were readily discernible. A double-Gaussian peak-fitting procedure was applied to extract the double-escape peaks at 6.624 MeV and 6.610 MeV from background. The hydrogen line at 2.223 MeV was also counted. Net intensities of these spectra are presented in Table 4. From the data of Table 4 we judged that the reproducibility was consistant with statistical counting errors.

Table 4

Ten-minute net counts of iron and hydrogen capture.

Depth (ft)	RUN 1 Net Cts. ±%Stat Error	RUN 2 Net Cts. ±%Stat Error	RUN 3 Net Cts. ±%Stat Error
IRON DOUBLET AT 6.610 MeV			
168	115 ± 35 pct	42 ± 96 pct	177 ± 23 pct
148	731 ± 7	704 ± 7	717 ± 7
128	741 ± 7	797 ± 7	863 ± 6
108	575 ± 9	582 ± 8	485 ± 10
88	560 ± 9	557 ± 9	456 ± 11
68	569 ± 9	485 ± 10	606 ± 8
IRON DOUBLET AT 7.121 MeV			
168	99 ± 29	89 ± 33	49 ± 60
148	369 ± 10	328 ± 12	406 ± 9
128	398 ± 10	471 ± 9	470 ± 9
108	302 ± 12	374 ± 10	299 ± 12
88	312 ± 12	367 ± 10	314 ± 12
68	347 ± 11	336 ± 11	339 ± 11
IRON DOUBLET AT 7.632 MeV			
168	78 ± 27	28 ± 71	19 ± 103
148	203 ± 13	198 ± 13	167 ± 14
128	270 ± 10	232 ± 11	178 ± 14
108	124 ± 18	96 ± 24	140 ± 17
88	168 ± 14	106 ± 21	146 ± 16
68	104 ± 23	132 ± 17	152 ± 16
HYDROGEN PEAK AT 2.223 MeV			
168	12429 ± 1	12246 ± 1	12443 ± 1
148	11606 ± 1	10763 ± 1	11294 ± 1
128	12780 ± 1	12446 ± 1	12142 ± 1
108	12008 ± 1	11625 ± 1	12187 ± 1
88	10913 ± 1	11132 ± 1	10816 ± 1
68	13030 ± 1	12534 ± 1	12444 ± 1

These tests provided our first information on the reliability of the sonde in the field. Data were collected without interruption during a 6-hour period. In that time we observed no significant electronic drift and no significant degradation of resolution.

Later, another series of measurements were carried out at this site. A hole was cored and logged to a depth of 18.3 m (60 ft.). The core was sampled according to protocol in order to get the best local value of iron in each 30.5cm (one-foot) interval from 5.2m (17 ft.) depth to 17.4m (57 ft.). The samples were analyzed for iron by X-ray fluorescence spectrometry at Princeton University. Throughout the core the rock type was layered metamorphic rock with the layering sharply angled to the core axis. The iron appeared as magnetite in thin layers between thicker layers of quartz-feldspar-biotite gneiss. Prompt-gamma-ray logs were obtained from 30-second spectra obtained at successive 30.5cm (one-foot) intervals. Net intensities and backgrounds for the full-energy doublet were again extracted by means of Gaussian peak-fitting and straight-line background-fitting. Hydrogen counts were also routinely monitored because Senftle had found in dense rock that better correlations with chemical analysis were obtained when prompt gamma ray net intensities were ratioed to the square root of the hydrogen counts than when they were not ratioed. (26)

Comparisons between the prompt-gamma data and the core analyses have been analyzed for the ratioed and unratioed iron gamma ray intensities. These comparisons exhibit good qualitative correlations. Considering the uncertainties of counting, sampling and depth measurement it is impossible to draw any conclusions regarding the relative merits of ratioed and unratioed presentations.

The sensitivity of the system for prompt gamma analysis or iron was approximately 0.2 net iron counts at the double-escape doublet per second per weight percent iron. The 2-sigma uncertainty resulting from counting statistics in a 30-second count was about ± 6 weight percent Fe at the 20 weight percent level. A slightly improved statistical error would have been obtained if data from the single-escape and full energy peaks had been combined with those from the full energy peaks; we estimated the 2-sigma error would have been about ± 5 percent instead. Our estimate of the 2-sigma error for a hypothetical 30-second count for an ore grade of 50% Fe is approximately ± 6 wt. pct. Fe, or $\pm 12\%$ relative.

Uranium: Kennedy, Texas

Objective

The primary objectives in the early field tests of the borehole probe were to test the durability of the instrumentation and to observe correlations between signals from the germanium detector and chemical analyses of core samples. Spectroscopic analysis of natural gamma rays from uranium-238 decay products held special attraction because of its technical and operational simplicity, since stimulation by neutrons was not involved.

Background

Three naturally radioactive parent isotopes are commonly found in rocks: Uranium-238 (U-238), Thorium-232 (Th-232) and Potassium-40 (K-40). Various daughter isotopes of U-238 and Th-232 are also radioactive. The daughter products from uranium decay provide a number of gamma ray emission energies extending up to 2.5 MeV. A typical high-resolution gamma ray spectrum of uranium ore, taken with a germanium detector is shown in Figure 3a-d, in which the peaks are labelled by their emitting isotopes.

The principal members of the U-238 decay chain are shown in figure 21. In a geochemically stable environment, the daughter products of U-238 are in equilibrium with the parent isotope. In that case a measure of the total activity-that is, the gross gamma count-can be a good indicator of uranium content provided that the thorium and potassium emissions are negligible. In many formations, however, a dynamic geochemical system has existed in recent geological history. Some of the decay products have markedly different chemical mobilities compared to the parent uranium. At least four isotopes have been identified in the uranium decay chain where fractionation of the daughter product nuclides can be expected to occur as a result of differential leaching in wet, or temporarily wet, environments. If such leaching has occurred within the last 240,000 years, then a degree of radiochemical disequilibrium will be found. In that situation conventional gross gamma measurements will give wrong assays.

Flowing ground water in sandstone ore deposits typically produces a crescent-shaped zone of oxidation, if looked at in a vertical cross section cut along the direction of flow. In surficial geological environments, this action removes one or more members of the uranium decay chain. The whole deposit may be dynamic. Such conditions of disequilibrium are often found in, for example, roll-front deposits that commonly occur in South Texas and Wyoming.

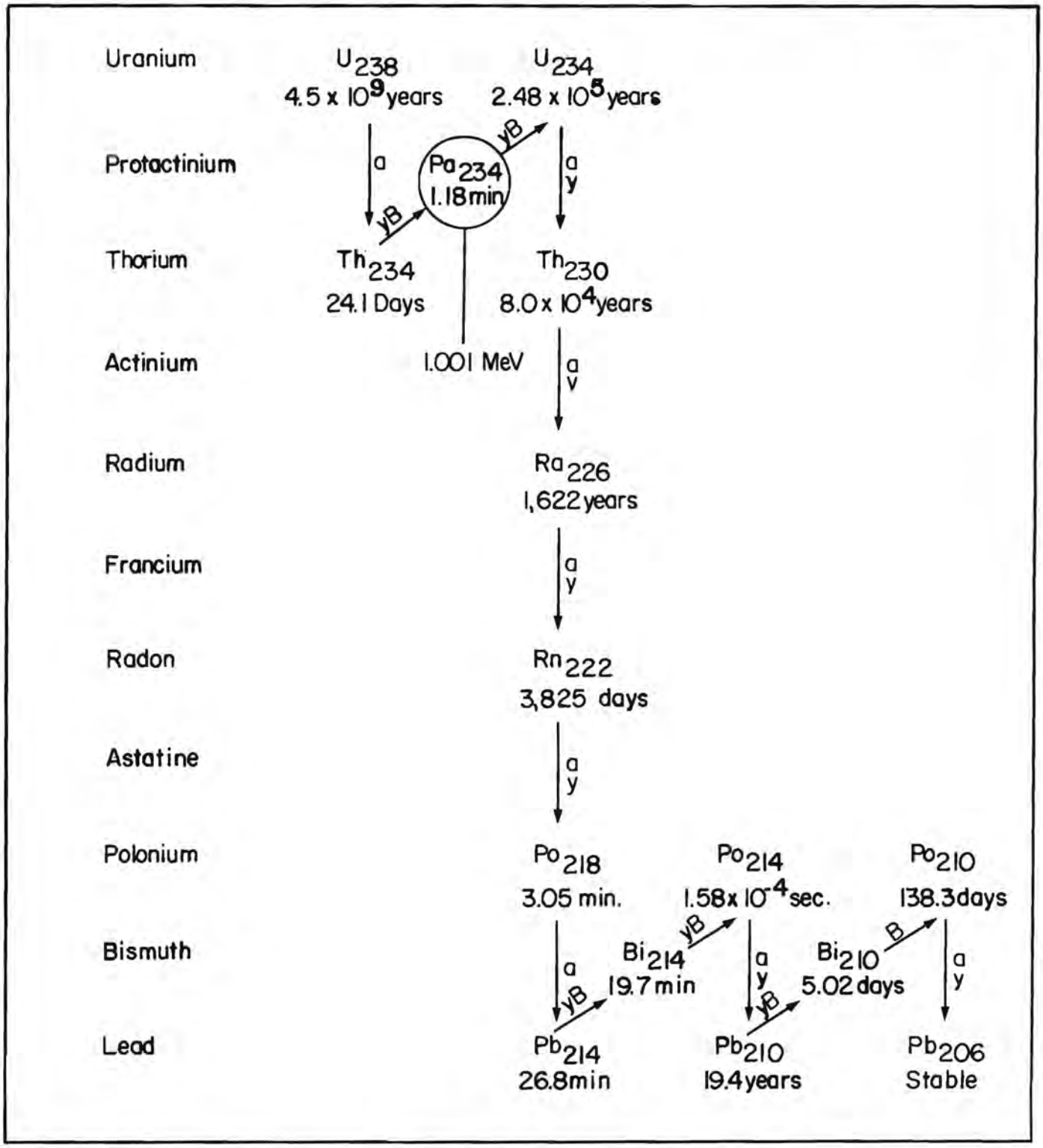

FIGURE 21.
RADIOACTIVE DECAY OF U^{238}.

As noted above, if there is a condition of disequilibrium, then the measurement of the emissions of a decay product will not accurately indicate the concentration of the parent uranium. Because of the physics of the decay chain, the traditional natural gamma measurement used in uranium exploration is predominately a measure of the gamma rays associated with Bismuth-214.

In a geological context, only three of the daughter products of Uranium-238 can be certain to exist in a state of equilibrium with the parent isotope: Thorium-234, Uranium-234, and Protactinium-234. Of these, only Pa-234 has a usable gamma ray for logging purposes. The use of the 1001-keV photon from Pa-234 for tracking uranium has been discussed by Tanner et al (35) and Brodzinski and Wogman (2). Statistically, the 1001-keV gamma ray is produced in only 0.59 percent of the uranium decays, which means that counting rates are low for this gamma ray. On the other hand, it has the advantage that its photon energy is great enough so that a relatively large volume of the borehole surround near the detector sampled. Gamma rays of 1001 keV can penetrate the formation as much as 20cm (8 in.).

Field Tests

Thirty 25cm (10 in.) diameter boreholes in a shallow sand uranium deposit were drilled, cored, and cased. The water table was such that all of the holes were water-filled to within a few feet of the surface. The sonde was used without significant interruption over a five week period at the site. Spectra were collected at 30cm (one-foot) intervals in all the regions for which core analyses were available. Additional regions of the boreholes were selectively logged in stepped fashion at various footage intervals. Some continuous logging was also attempted.

Concurrent with these tests was a series of field tests, cosponsored by Conoco, the Bureau of Mines, and Department of Energy for comparing the various procedures for direct borehole assay of uranium (35). These included natural-gamma high-resolution spectroscopy, delayed-fission-neutron (DFN) counting, and prompt-fission-neutron (PFN) counting. Although the PGT high-resolution sonde was still in its initial testing stage, it gave results that compared favorably with the other methods.

The results from the Kennedy field tests showed that the borehole sonde's logs and the core assays correlated very well, even in those holes that exhibited poor correlation between gross gamma measurements in the borehole and core analysis-where disequilibrium was suspected. Occasionally, slight discrepancies of one or two feet of depth between the borehole sonde and core sample assignment were noted. Such discrepancies were not unexpected, given the inaccuracies in

depth measurement associated with core drilling and with the early drawworks mechanism. The borehole sonde assays and the core assays were finally plotted so that major features were forced to line up, eliminating depth discrepancies. When this was done and the ore grade depth profiles compared with the 1.001 MeV gamma ray count rate, excellent correlation was seen. From these data a value for the calibration constant, k, was obtained in the equation,

$$\text{Ore grade} = I/k,$$

where I = intensity, or count rate of the gamma-ray line.

The value of k was found to be approximately 7 counts per weight percent U-238.

Figures 22(a) and 22(b) show several assay logs, corehole assays and gross gamma logs plotted together. As noted above, precise correlation was not to be expected because of differences in the sample volumes and because of imprecisions inherent in gamma counting and chemical analysis.

Gross gamma, or "natural gamma", measurements were derived from the spectra of the borehole sonde and compared with independent natural gamma logs obtained by means of a traditional gamma logging tool. Natural gamma log data were supplied by Conoco. The gamma tool was sensitive to gamma ray activity but had no energy discrimination. We derived equivalent data from the germanium borehole sonde in two ways. One way was to record the count rate of all detected events the signal of which exceeded an electronic threshold. The second way was to record individual intensities of the major peaks in the spectrum belonging to Bi-214. The two methods correlated well with each other and with the gamma log. the "counts-above-threshold" method had three advantages over using spectral information: 1) it was simpler to implement; 2) it provided better precision; and 3) its basic information was more akin to that of the natural gamma tool, being unselective of the uranium, thorium and potassium gamma rays.

After the system had been calibrated, the natural gamma count yielded the "equivalent" ore grade in weight percent U_3O_8 or "EU_3O_8". This reflected what the ore grade would have been under equilibrium conditions. The ratio of EU_3O_8 to the true assay value, called the disequilibrium factor (DEF) was readily computed from the germanium borehole sonde data. This factor was judged useful to the geologist interested in past geochemical movements of the uranium. Most of the holes logged in this investigation exhibited disequilibrium to a significant degree.

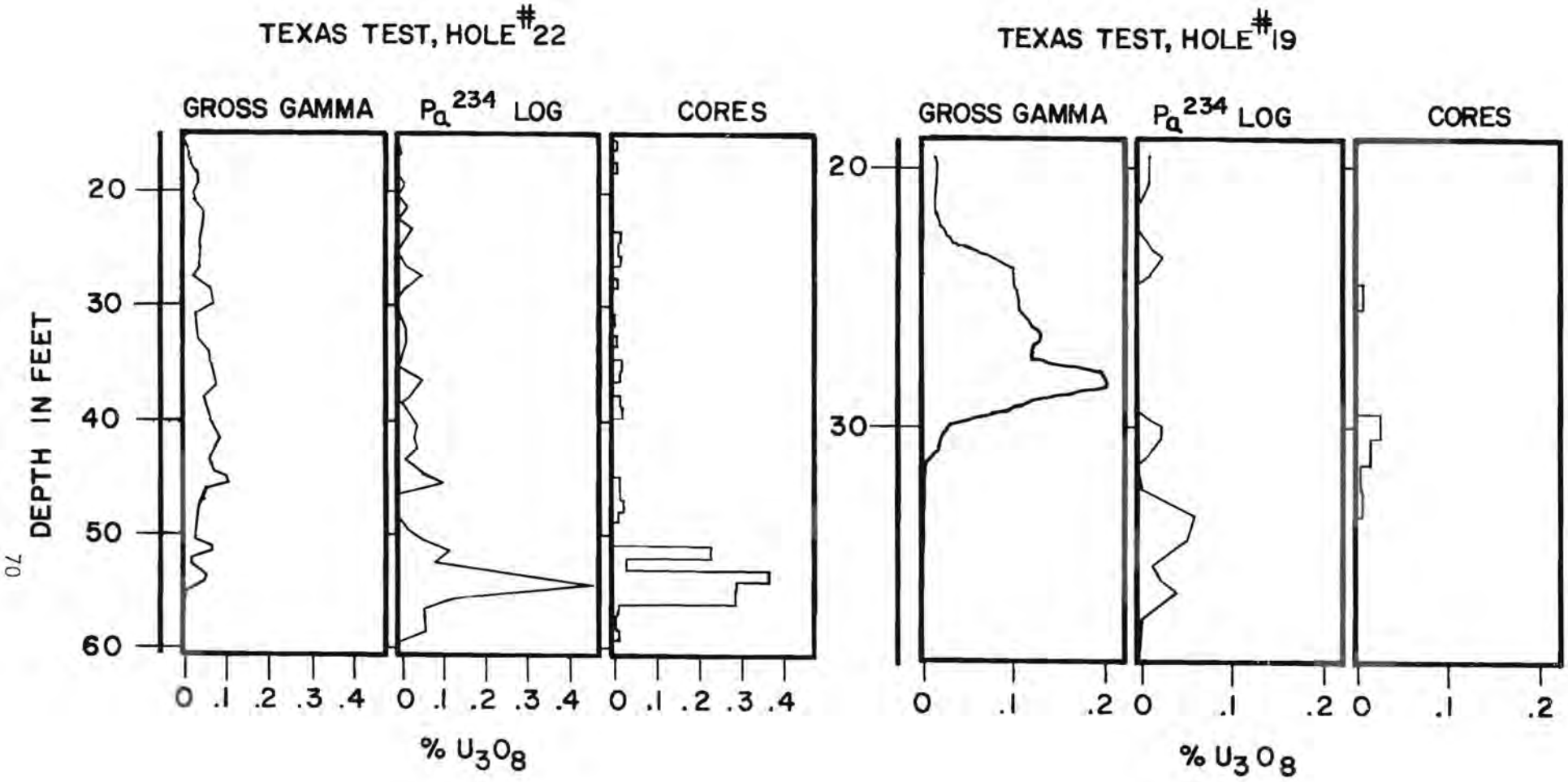

FIGURE 22 (A) COMPARISON OF TYPICAL U_3O_8 ASSAYS USING THE P_a^{234} 1.001-MeV GAMMA RAY LOG vs. CORE ANALYSIS AND GROSS GAMMA RAY ANALYSIS IN A SHALLOW SAND ROLLFRONT DEPOSIT.

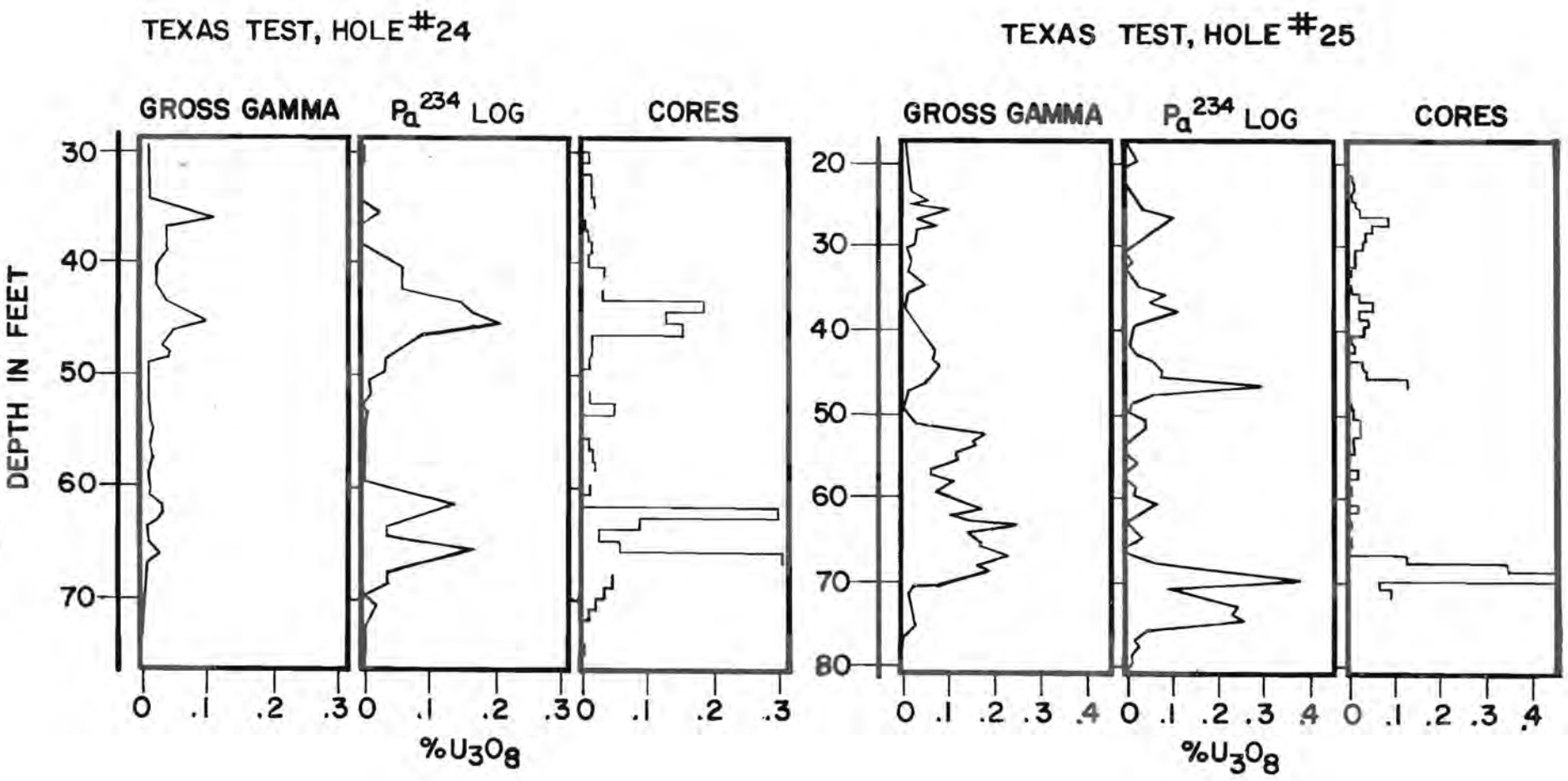

FIGURE 22(B) COMPARISON OF TYPICAL U_3O_8 ASSAYS USING THE P_a^{234} 1.001-MeV GAMMA RAY LOG Vs. CORE ANALYSIS AND GROSS GAMMA RAY ANALYSIS IN A SHALLOW SAND ROLLFRONT DEPOSIT.

We concluded that the germanium probe using gamma ray spectroscopy for the 1.001 MeV line of Pa-234 was a direct and efficient means of in-situ uranium ore grade determination, and had particular value in ore bodies exhibiting disequilibrium. Logging speeds averaged about 4.6m (15 ft) per hour in ore zones and 305m (1000 ft) per hour in barren zones.

Coal: Graysville, Pennsylvania

The coal field tests were performed in cooperation with the U.S. Steel Corporation at the minesite in Graysville, Pennsylvania. The work reported below covers the same investigation that has been documented by Mikesell, et al (19) and substantially follows their account.

Objectives

Our main objectives in the coal tests were to gain further experience with 1) the logging equipment that had been developed up to that time, 2) neutron-induced prompt gamma-ray logging procedures in general, and 3) the application of prompt gamma-ray logging procedures to coal, an important energy-related mineral. The objective of the U.S.G.S. was to extend their previous research in this application (24), in particular to examine the effects of increased borehole diameter on the quality of results.

Summary of Conclusions

All the technical objectives were achieved. The depth and the width of the coal seam and its partings were determined from the aluminum and potassium logs. From spectral data we obtained ash content and elemental analysis. The increased ratio of borehole diameter to probe diameter degraded the analytical precision by a moderate amount, owing to the effects of water in the hole.

Background

Coal is an abundant mineral in the U.S. and an important source of energy. Although coal strata can be identified and located by means of conventional logging tools, the chemical and physical properties of coal are usually determined from core samples. Some of the logging service companies offer in-situ determinations of BTU and ash content using resistivity, self-potential, and neutron logs. Impurity levels of sulfur and other undesirable elements are of great interest to the coal mining industry. No logging tools of sufficient specificity now exist for in-situ assays of those elements.

Neutron-induced gamma-ray spectroscopy possibly could provide specific, simultaneous analysis for a number of elements. Senftle, et al (24) has found that the BTU content and the ash content could be quantitatively inferred from the gamma-ray spectrum, if reasonable assumptions are made about the unobserved oxygen content. These determinations were achieved by means of simple, empirical formulas. That investigation was carried out with a germanium detector and a Cf-252 source in a close-fitting borehole. In field work,

boreholes are not likely to be close-fitting, and are usually full of water. The response of the sonde was expected to be sensitive to the borehole diameter because the hydrogen in water strongly affects the neutron flux, effectively reducing the sample size. However, the magnitude of this effect in coal had not been empirically determined.

Field Tests

The borehole, located in the Pittsburgh seam, Green County, Pennsylvania, had a diameter of 25.4cm (10 in). The detector section of the probe had dimensions 5.1cm (2 in) diameter by 122cm (48 in) long, exclusive of neutron source and spacers.

A short phenolic plastic section containing a 6.35 cm lead shadow shield was fastened to the bottom of the sonde. Phenolic and/or nylon spacers were screwed into the bottom of this section to change the source-to-detector distance. The source section, which held an additional 10.6 cm lead shadow shield directly above the Cf-252 source, was placed below the spacer located farthest from the detector. Four sources of different sizes (0.23, 2.7, 25 and 96 ug Cf-252) were used in the experiments; the source-to-detector distances used are shown in Table 5.

Table 5

The source-to-dectector distances used with different 252-Cf sources.

Source Size (μg)	Source-to-Detector Distance (cm)	Length of Pb Shadow Shield (cm)
0.23	19.9	6.35
2.7	50.2	16.95
25	73.8*	16.95
25	61.0*	16.95
96	74.3	16.95

* Used for borehole log only.
**Used for spectral analysis in the coal seam.

On the day before the experiments were performed, the hole was bored to a depth of about 9m below the main bench of the

coal seam, which extended from 225.5 to 227.4m below the surface. About 7.5m south of the main borehole, a 4cm diameter exploratory borehole (No. F-31) was bored to a depth just below the coal seam. The part of the core from this hole that intersected the seam was used for the chemical analysis of the coal. As shown in Figure 23, pyrite and carbonate rocks were noted both above and below the main bench of the coal seam.

Depth and Lithology Measurements

Before operating the sonde with a neutron source, natural gamma-ray spectra were collected every 0.3m starting just above the roof coal. At each location, a complete spectrum was made in a collection time that varied from 1 to 5 minutes. The total count-rate data shown in Figure 23 were useful to determine the depth of the coal, and the full width at half-maximum of the count depression in the seam was a fairly good measure of the width of the seam. The only spectral peak in the spectrum that could be used for the same purpose was the 1461 keV line of K-40. Bi-214 activity from parent U-238 and Tl-208 activity from parent Th-232 were also observed but they did not mark the coal boundaries as well as did the K-40 log. For instance, the activity of Bi-214, although low in the coal, was high at the top and bottom of the main bench, and that of Tl-208 was highest in the shale just below the coal.

Later, the same section of the hole was logged, using a 25 μg Cf-252 neutron source and a source-to-detector distance of 73.8cm, while the sonde was drawn upwards. A spectrum was accumulated for 60 seconds at each station. The hydrogen capture-gamma-ray line at 2223 keV and the aluminum decay-gamma-ray line at 1779 keV marked the coal seam reasonably well, as was shown by Senftle et al. (24) The aluminum log showed the presence of a narrow clay parting (not shown in the geologic log) almost in the center of the main bench. Although the counting statistics in 60 seconds were rather poor for the silicon, iron, and sulfur lines, some useful information was obtained. Similar to the results of Nargolwalla et al (20), the 3539 keV line of silicon was noticeably absent in the upper and lower benches of the coal. The iron and sulfur lines at 7632 and 5420 keV respectively, although less intense in the coal, showed anomalies that corresponded to pyrite horizons.

The earlier report (24) pointed out that the hydrogen anomaly occurs slightly above the coal, but that the aluminum anomaly corresponds very well with the location of the coal seam. This difference was entirely explicable in terms of the different gamma ray energies, which affected the apparent depth. The largest number of hydrogen gamma rays were produced when the source was at the center of the seam. Because of their relatively high energy, the gamma rays readily penetrated the coal, and arrived at the detector, which was above the center of the irradiated volume by the amount of the

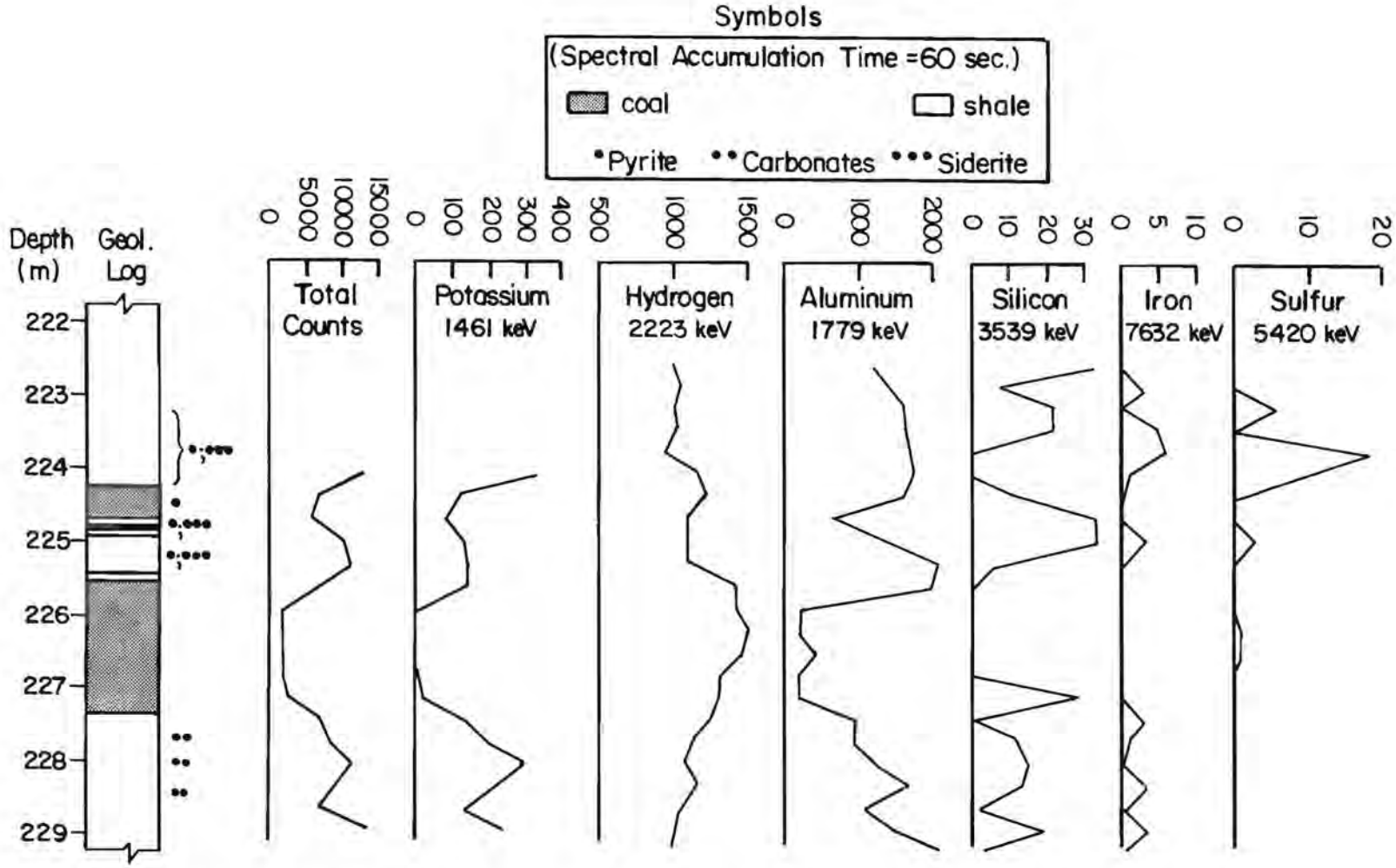

FIGURE 23 COMPARISON OF THE GEOLOGIC LOG WITH THE TOTAL COUNT AND ELEMENT LOGS ABOVE, THROUGH AND BELOW THE PITTSBURGH COAL SEAM, GREEN COUNTY, PA. (19)

source-to-detector distance. However, the aluminum gamma rays having a lower energy than those of hydrogen, originated from a smaller volume near the source so that the depression in the aluminum activity corresponded more closely to the center of the coal seam. Because the sonde was moving upward in the hole, there was no residual decay-gamma activity from previously-irradiated points in the hole. The depression in the silicon log, which was based on the 3539-keV gamma-ray, was displaced even further than the hydrogen anomaly, an expected result of the still higher energy (3539 keV) of the silicon gamma-ray. These effects were particularly noticeable in the upper, narrower bench of the coal.

Consequently, to determine the depth of the seam, we recommend use of the low-energy gamma-lines of K-40 or of aluminum.

Spectral Analysis of Coal

Individual spectral analyses in the coal seam were obtained with the 0.23-, 2.7-, 25-, and 96- μg Cf-252 neutron sources. The spectrum obtained with the 2.7 μg source appeared to be in error and was discarded. The counting statistics were best when the 0.23 μg source was used because of the correspondingly short source-to-detector distance. All spectra were accumulated for 3600 seconds. The quantitative analysis of the coal was made from the spectral data by the method described in reference 24. Because some important changes were made in the method of calculation, we briefly describe the technique again.

Method of Calculation

The gram fraction, f, of any element in the coal is given by the expression,

$$f = NW/\sigma\phi MLg\varepsilon It \qquad (9)$$

where

N = number of counts in a given peak
W = atomic weight
σ = the total elemental capture cross-section in barns
ϕ = the termal neutron flux in the sample in neutrons/cm2sec
M = mass of the sample in grams
L = Avogadro's number
g = geometric factor
ε = relative system efficiency
I = intensity of the gamma ray in number per neutron capture
t = irradiation or data accumulation time in seconds

Further, it was previously shown (8,24), that for j elements in the the coal matrix

$$f = \frac{NW}{\sigma\varepsilon I}\left[\sum \frac{N_j W_j}{\sigma_j \varepsilon_j I_j}\right]^{-1} = \frac{A}{\Sigma A_j} \qquad (10)$$

where the A-factor for each element is the appropriate ratio, $NW/(\sigma\varepsilon I)$. Equation 10 is thus an expression for the mass fraction of any element in the coal; the expression is independent of the neutron the sample size, the geometry, and the spectral accumulation time. If one could evaluate the denominator, ΣA_j, in equation 10, one could calculate the mass fraction of any element for which an A-factor can be determined.

An "ultimate analysis" of coal specifies percentages of five elements plus the ash concentration, the sum of which is 100 percent. Thus, if an A-factor can be determined for these six components of the coal, their mass fractions can be expressed as functions of ΣAj, summed, and the sum equated to 1. As the factors for five of the six components that make up ultimate analysis can be evaluated from the capture gamma-ray spectrum, the values of Aj can be evaluated and then used to determine the mass fraction of any other element for which an A-factor can be determined.

The ash term in equation 10 includes all the minor and trace elements in the coal, some of which are below the detection threshold and therefore cannot be calculated directly. However, the major cation elements in coal ash are aluminum, silicon, and iron, all of which have relatively intense lines in the capture gamma-ray spectrum. Several empirical equations are reported in the literature (1,18,40) showing the relationship between aluminum, silicon, or the sum of these two elements, and the ash content in coal. Senftle, et al used a relation suggested by Loska and Gorski (18) that gave the ash content as a function of the sum of the percentages of alumina plus silica. Mikesell, et al found that including the percent Fe_2O_3 in the relationship gave consistently better results (24). However, because of the large amount of iron in the construction material of the sonde, the number of counts in the iron peaks tended to be higher than that expected from the formation, particularly when short source-to-detector distances were used. This situation made the true iron level difficult to determine accurately. To examine the ash relationship further advantage was taken of the large number of ash analyses in the literature for many coal seams. Thirteen analyses for the Pittsburgh coal seam within a 100-mile radius of the area in which we were working were used to find the relationship between total ash and the sum of the

alumina and silica concentrations (41). A simple proportion gave a good fit, allowing the ash term in equation 10 to be evaluated as follows:

$$f(\text{ash}) = 1.742\, f(Al_2O_3) + f(SiO_2), \qquad (11)$$

where f is the mass fraction.

The only important term in equation 10 that could not be evaluated directly from the capture gamma-ray spectrum was the oxygen term. Oxygen did not yield any observable capture gamma-ray lines because of its relatively small thermal-neutron capture cross section. Therefore, it was necessary to employ an indirect technique to obtain the mass fraction of oxygen. An attempt was made to study the analyses of Pittsburgh seam coal in order to find a relationship between oxygen and one or more elements in the coal for which there existed a measurable line in the capture gamma-ray spectrum. Such a relationship could not be found. Finally, simply the average oxygen content in the literature was used. As previously shown, the error was distributed over all the terms in equation 10; therefore, this procedure did not introduce undue error into the calculated components of the coal. The average of 13 oxygen analyses pertaining to the above-mentioned Pittsburgh seam samples (41) were employed here.

It should be pointed out that the analyses shown in the literature give oxygen-by-difference, which is not the true value of oxygen in the coal (9). However, the oxygen-by-difference should be used in equation 10 if the analyses of the other elements are to conform to the ultimate analyses reported by coal chemists. If oxygen were measured directly, for example by fast neutron reaction with 14-MeV neutrons, then the value of the other elements would be biased away from the chemists' values and would require correction.

Calculation of System Efficiency

The efficiency term in our equation 9 was obtained experimentally in reference 24 from borehole spectra and normalized to published point-source efficiency curves for laboratory germanium detectors of a size and geometry similar to those of the detector in the sonde. It was assumed that, because only high-energy spectral lines were used, the attenuation coefficient in the ore would be essentially independent of energy. In this work lower energy spectral lines have been included, and the assumption became less valid because the lower energy gamma rays suffered greater attenuation than those of higher energy. Also, the problem was complicated by the fact that the borehole sample was an extended source rather than a point source. As a result, we

dealt with the "system efficiency"; that is, the applicable efficiency curves could differ markedly from the point source efficiency curves. Consequently, the system efficiency in the coal seam was inferred from the multiplicity of chlorine lines in the borehole spectrum and their known relative intensities. (34)

Chlorine has a substantial number of well documented lines spread across the energy range of interest, as shown in Table 6, and so can conveniently be used to determine a full-energy peak system efficiency curve as shown in Table 6. In a high-resolution spectrum these peaks are free of significant interference from the full-energy, single-escape, and double-escape peaks from other elements in coal. Except for the 6111-keV line, they are also free of interference from other chlorine peaks. The counts in 6111-keV line were corrected for the single-escape peak at 6109 keV. Also shown in Table 6 are intensity values reported by Spits and Kopecky (34). These were used to calculate the system full-energy peak relative efficiency curve shown in figure 24.

Table 6

Selected interference-free chlorine lines in coal.

Full Energy, keV	Line Intensities, gamma rays/100 neutrons absorbed (Spits & Kopecky, 1976)
789	15.0
1165	25.7
1951	18.7
1958	12.1
2865	6.0
4980	3.53
5716	5.14
6111*	19.7
7790	8.61

*Doublet of 6111-keV full-energy and 6109-keV single-escape peaks of chlorine.

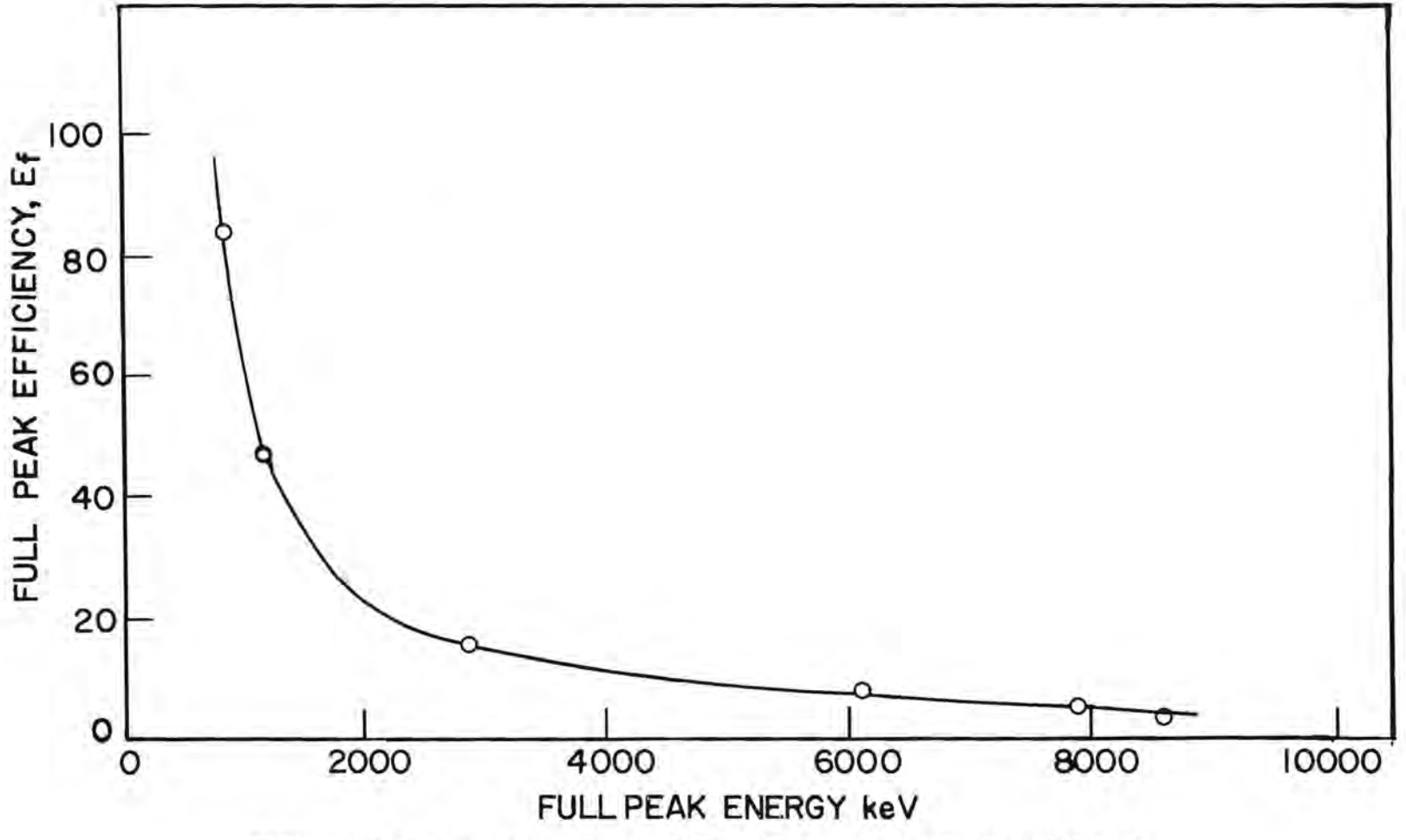

FIGURE 24. RELATIVE FULL ENERGY PEAK EFFICIENCY (19)

To determine the single-escape and double-escape efficiency curves, the ratio of the peak areas of the single-escape-to-full-energy and double-escape-to-full-energy peaks as a function of the full-peak energy was plotted as illustrated in figure 25. These curves were similar to those obtained by Seyfarth et al (31). A polynominal fit was made to each set of data and the appropriate excape peak efficiencies were calculated by normalization to the data in figure 25. These efficiencies were then used in the calculation of the A-factor for the elements.

Results and Discussion

In reference 24, a specific peak in the spectrum was used for each element. The given peak was chosen on the basis of its intensity and lack of potential interference from other peaks. In the present experiments, the counting statistics were relatively poor. It was assumed that a better determination could be obtained if as many peaks as possile for each element were used to obtain an average A-value.

For example, Table 7 lists the spectral peaks used for each element analyzed, and the A-value obtained with the 96 µg source. Table 8 shows the elemental analyses of the coal. The chemical analyses shown were made on core samples from the test hole located near the main borehole. The average oxygen concentration of 13 coals in the region, as noted above, were employed for the analyses of data collected using three differenct californium sources. The results were better than one might have expected, considering the unfavorable geometry, uncertain centering of the sonde in the hole, and the fact that the chemical anaylses were determined from coal samples out of a hole 7.5 m away. The results got progressively better as the source size increased from 0.23 ug to 96 µg Cf-252, but were not as good as those obtained in a close-fitting hole (24).

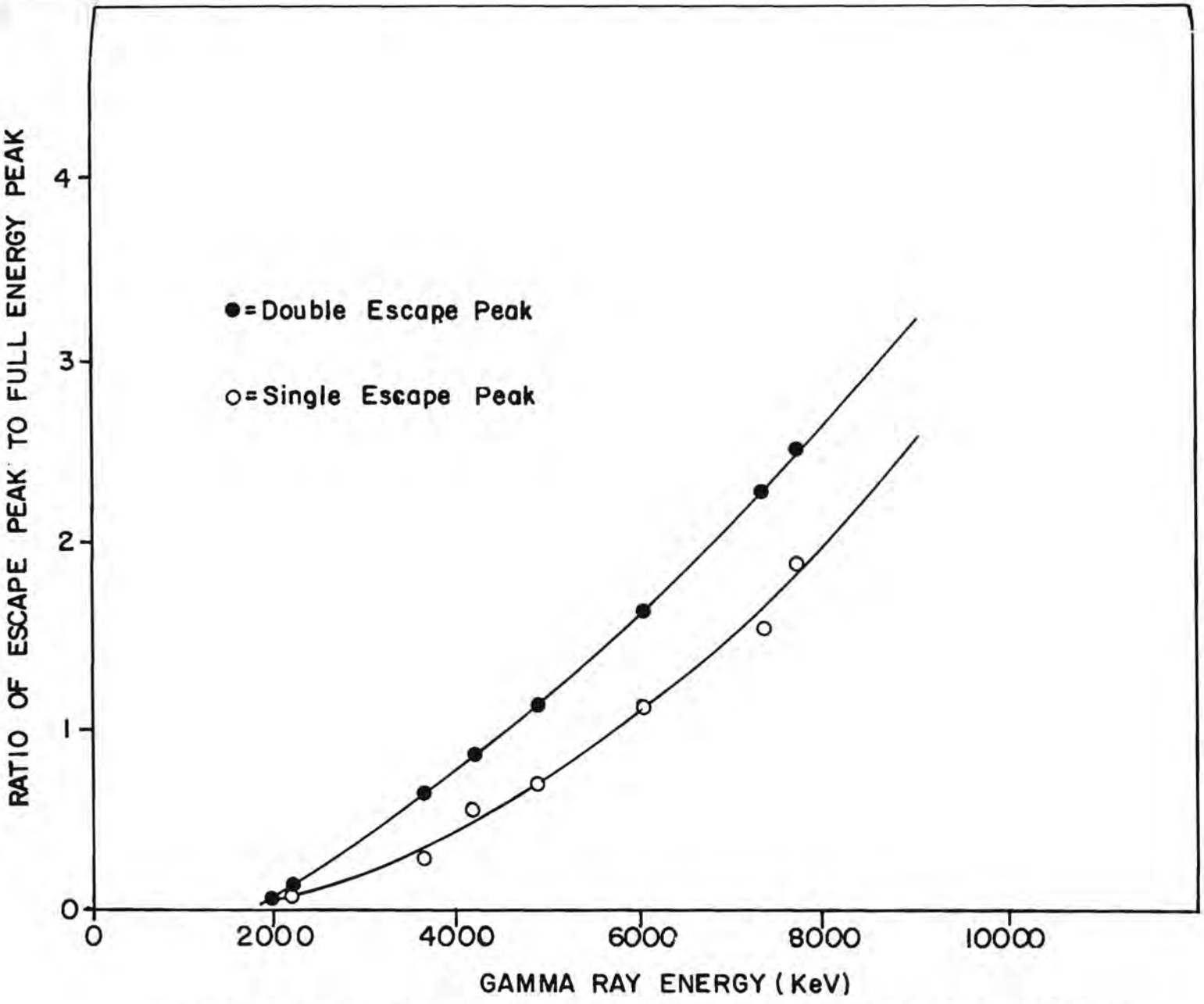

FIGURE 25. RATIO OF ESCAPE PEAK INTENSITIES TO FULL ENERGY PEAK INTENSITY FOR A TYPICAL Ge DETECTOR

Table 7

Full(f), Single(s), and Double Escape(d) Peak Energies and Calculated A Factor for Data Obtained with the 96 μg 252-Cf source.		
Element	Peak Energies (keV)	A Factor
Carbon	3684(f), 3173(s), 2662(d) 4944(f), 4433(s), 3922(d)	1239.5
Hydrogen	2223(f), 1712(s), 1201(d)	101.4
Sulfur	5420(f), 4909(s), 4398(d)	25.78
Nitrogen	4508(f), 3486(d) 5267(f), 5568(d)	59.6
Aluminium	7212(s) 1779 (decay line)	21.47
Silicon	3539(f), 3028(s), 2517(d)	17.74

Table 8

Elemental Analyses of a Coal Seam from Capture Gamma-Ray Spectra using 252-Cf Neutron Sources of Different Sizes in an Oversize Borehole.				
Element	Capture Gamma-Ray Analyses (%) 0.23μg	25μg	96μg	Chemical Analysis as received (%)
Carbon	62.0	68.0	71.9	75.9
Hydrogen	7.1	6.2	5.9	5.45
Sulfur	0.7	1.3	1.5	1.39
Nitrogen	3.8	4.1	3.5	1.54
Oxygen	9.3	9.3	9.3	7.73
Aluminum	3.3	1.0	1.2	1.01
Silicon	1.7	2.1	1.0	2.02
Ash	17.1	11.0	7.9	7.98

The gradual improvement of the results with larger sources is understandable in an oversize borehole if one keeps in mind that the source-to-detector distance must be increased as the source size increases. In all the spectra, the total counting rate was approximately the same, and the contribution of borehole water (primarily hydrogen) to the total count was greater for the smaller source sizes. The effect of the relatively large amount of water in the oversize borehole decreases for larger source-to-detector distances (larger sources); so better analyses were obtained with the larger sources. However, even for large sources, the deleterious effect of water on the signal-to-background ratios was significant.

Conclusions

Borehole logging of a coal seam by means of germanium gamma-ray spectrometer and a Cf-252 source can provide the following information.

1. Identification, depth and width of the coal seam. These are obtained from logs of the 1779-keV aluminum gamma-ray counts and the 1461-keV potassium-40 counts.

2. Quantification of the significant elements in coal ash including sulfur, aluminum, silicon and iron, but excluding oxygen.

3. Determination of the ash content.

4. Determination of the carbon and hydrogen content of coal and consequently, the BTU content.

Trace quantities of impurity metals in coal could not be directly determined within practical measurement times.

The data suggest that pyrite probably can be determined at the level of a few percent or more, if care is taken to minimize the amount of structural iron in the probe near the detector. Water present in an oversize borehole worsens accuracy compared to a close-fitting borehole and affects the optimum source strength and source-to-detector distance. These last parameters vary with the borehole diameter.

If the direct determination of oxygen were of special importance, along with the determination of other elements, it would be necessary to employ an accelerator to generate 14.4-MeV neutrons, which can directly stimulate gamma-ray emission from oxygen. They do so by inelastic scattering, producing 6.13 MeV gamma rays.

Copper: Kearney, Arizona

Objective

The purpose of the copper field test was to obtain basic data and to investigate the applicability of the germanium tool to neutron activation logging of copper ore in a major deposit in southwestern U.S.

This objective was not fully realized because only one method was tried, that of prompt gamma rays following neutron capture. A second method, involving the 5.1-minute delayed gamma rays of neutron activation of Cu-65, was not attempted, because a sufficiently strong Cf-252 source was not available at the scheduled time of the test, as a result of delayed delivery. Therefore, we considered our results, while valid as far as they went, to be incomplete, since laboratory studies by others and theoretical calculations indicated that the delayed-gamma method ought to be superior to the prompt-gamma method for in-situ determinations of copper (15,20,33).

Background

The copper mining industry utilizes core drilling extensively for orebody delineation and exploration. Because of the sampling problem with coring, in-situ borehole analysis has been thoroughly investigated by the copper industry (11,15). The larger volume sampled by in-situ neutron activation procedures, 0.1 to 1.0 cubic meters, depending on photon energy and rock density, is more representative of the orebody matrix than are core samples, which are much smaller. An effective neutron activation logging procedure could therefore represent a considerable cost saving for copper exploration, improve the efficiency of exploration, and be less subject to sampling errors, compared to core analysis.

Activated copper emits several prompt gamma rays that are usable for gamma-ray logging. The most prominent prompt gamma-ray energies in keV, ordered by decreasing sensitivity of the system, are: 278, 7915, 7637, 609 and 385 keV. The reaction is:

$$Cu + n \longrightarrow Cu + \gamma \qquad (12)$$

Activated copper produces a delayed gamma ray at 1039 keV with a 5.1 minute half-life, a consequence of the reactions,

$$Cu^{65}\ (n,\gamma)\ Cu^{66} \xrightarrow[\beta,5m.]{} Zn^{66} + \gamma(1.039\ MeV)(8\%) \qquad (13)$$

Use of prompt and delayed gamma rays has been investigated in the laboratory pertinent to logging copper ores (15). That study concluded that prompt gamma-ray analysis does not have the sensitivity to detect concentrations of copper in the 0.1

to 1.0 weight percent range as desired for logging. On the other hand, their delayed gamma-ray studies indicated that enough statistically significant counts were present in the peak to achieve adequate precision. Working with a laboratory model consisting of sand penetrated by copper wires, Jensen et al concluded not only that the 5.1-minute activity should be exploited, but also that a sodium iodide scintillator probably would provide better detection limits and accuracy than a germanium detector (15).

Field Tests and Analysis

At Kearney Arizona, spectra were acquired in two holes that had been cored, Borehole Nos. 1128 and 1129. A 2.4-microgram Cf-252 neutron source (5.6×10 neutrons/sec) was used in all the tests. The source-to-detector spacing was 30cm (12 inches), resulting in a total count rate of approximately 1500 counts per second. The following information was extracted from the spectral data: 1) net copper counts in the 7915-keV peak, 2) net hydrogen counts in the 2223-keV peak, and 3) total counts (gross gamma). Net counts in the peaks were determined by applications of a peak-and-background-fitting computer program, a procedure necessitated by the relatively weak signal. Two other prominent prompt gamma rays of copper were also evaluated in this work: the lines at 609 keV and 278 keV. However, each gave results that were poorer than those of the 7915-keV line because of interferences and background levels.

Since the prompt gamma-ray signal was weak, spectra were accumulated over rather long periods of time. First, two one-hour calibration measurements were carried out at the 16.2m (53 ft) and 19.2m (63 ft) depths in Borehole 1129. Next, in Borehole 1129 spectra were acquired at regular depths in 5-foot increments, over the cored region from 15.2m to 33.5m (50 to 110 ft.) The procedure was a little different in Borehole 1128. There, two spectra were accumulated. Each represented one hour of data acquisition, an assemblage of ten 6-minute counts at successive 30cm (one foot) intervals; so that a 3.0m (10 ft) section was sampled. This was done for the 15.2m to 18.3m (50 to 60 ft) interval and the 18.3m to 21.3m (60 to 70 ft) interval. Corresponding laboratory analyses of the cored sections were provided to us by the Kennecott Copper Corporation for tool calibration and evaluation.

In analyzing the data we followed the reasoning of Senftle et al (26) that if hydrogen (present in free or bound water) is the principal agent for slowing neutrons, then the ratio of the analyte signal to the square root of the hydrogen signal is approximately proportional to the concentration of the analyte. This is expressed, for copper (Cu), by application of equations (1) and (3):

$$C(Cu) = \frac{I(Cu)}{K(Cu)} = \frac{1}{K'(Cu)} \frac{I(Cu)}{\sqrt{I(H)}} \qquad (14)$$

where C(Cu) is the copper concentration in weight percent,
I(Cu) is the net counts per unit time of the copper signal,
I(H) is the net counts per unit time of the hydrogen signal, and K and K are calibration constants.

From equation 14 we get

$$K'(Cu) = \frac{I(Cu)}{C(Cu)\sqrt{I(H)}} \qquad (15)$$

which we used to determine the calibration constant based on chemical analyses of core samples.

We simply took the calibration constant, k'(Cu), to be the average value found from applying equation 15 to the calibration measurement at 63 ft. in Borehole 1129 using the core assay's C(Cu) value. This gave k'(Cu) = 0.30, which was then applied to the rest of the prompt gamma data to yield our results for C(Cu).

The results are summarized in Table 9 and plotted in figures 26a,b. We observe in Fig. 26 that the prompt-gamma results correspond fairly well to the core analyses at most, but not all, depths. The largest discrepancy was at the 28.7m (94 ft) depths in Borehole 1129. We do not know the cause. Significant discrepancies may have been flukes or perhaps were related to sampling errors associated with small core samples. Gross gamma counts were used only to monitor the consistency of the data, to make sure the equipment was not experiencing problems. None of our datum points showed any unexpected behavior in the gross gamma counts. Consequently, we had no reason to question our derived copper concentration results at any depth.

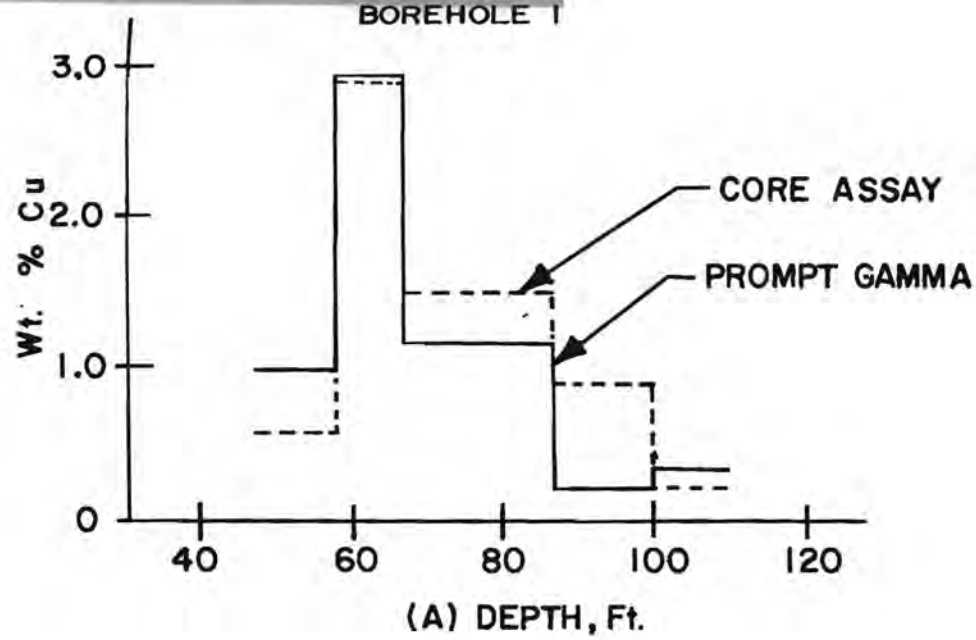

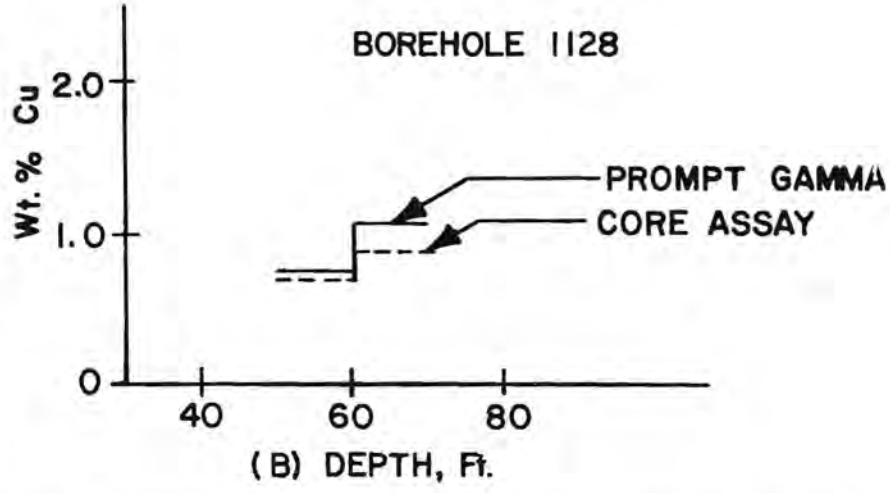

FIGURE 26 COMPARISON OF 7915-KeV PROMPT GAMMA RAY LOG AND CORE ANALYSIS FOR COPPER IN TWO BOREHOLES.

Table 9

In-situ prompt gamma ray calibration and logging data for copper determination.

1 Depth ft.	2 Core Assay (Wt % Cu)	3 Data Collection Time (sec)	4 I(cu) (7915 KeV) (Net cts/hr)	5 I(H) (cts/hr)1/2	6 I(Cu) I(H)	7 Prompt Gamma Analysis assuming k' = 0.30 (Wt % Cu)	8 Cu Core-gamma (Wt % Cu)
"CALIBRATION" MEASUREMENTS							
Borehole 1129							
53.0	0.60	3600	44.4 ± 18.2	156.6 ± 0.6	0.284 ± 0.117	0.95 ± 0.37	+0.35
62.9	2.90	3600	132.5 ± 16.7	153.8 ± 0.6	0.862 ± 0.112	2.87 ± 0.37	-0.03
"LOGGING" MEASUREMENTS							
47- 58	0.60	3600	45.3 ± 16.2	154.7 ± 0.6	0.293 ± 0.107	0.98 ± 0.36	+0.38
58- 67	2.90	1200	137.4 ± 16.4	155.7 ± 0.6	0.882 ± 0.111	2.94 ± 0.37	+0.04
68- 77		1800	52.6 ± 12.8	190.1 ± 0.5	0.277 ± 0.069	1.16 ± 0.15	-0.34
77- 87	1.50	1800	87.0 ± 12.9	210.3 ± 0.5	0.414 ± 0.063		
87-100	0.87	2700	14.5 ± 9.5	216.5 ± 0.5	0.067 ± 0.044	0.22 ± 0.15	-0.65
100-110	0.24	3600	21.0 ± 12.0	214.4 ± 0.5	0.098 ± 0.056	0.33 ± 0.19	+0.09

Comparison of columns 7 and 8 of Table 9 gives a quick check on the consistency of the prompt gamma assays with the lab assays. Column 8 is the absolute difference between the two assays. Column 7 contains the plus-or-minus one sigma uncertainty owing to statistical errors in gamma counting. Qualitatively, for the prompt gamma and chemical assays to be considered consistent with each other, the absolute values of the numbers in column 8 ought to be less than twice the error figures in column 7; and column 8 ought to exhibit randomly distributed positive and negative values. The first criterion is satisfied at most datum points. Because of the limited amount of data, no conclusion can be reached on the distribution of deviations. Finally, looking at the two depths (53 ft and 63 ft) in borehole 1129 where prompt gamma measurements were repeated, we note that the data reproduced well.

Uncertainties

Under the assumption that the terms k'(Cu) and $\sqrt{I(H)}$ in Equation 14 were approximately constant, which was probably valid, at least within any given formation, then the uncertainty in C(Cu) was directly related to the uncertainty in the net copper counts, N(Cu), which is equal to I(Cu)t, where t is the duration of the measurement. If equation 14 is expressed as a difference equation and if it is assumed that k'(Cu) and I(H) are constants, then

$$\Delta C(Cu) = \frac{\Delta I(Cu)}{K} \tag{16}$$

Dividing by equation 14, we get

$$\frac{\Delta C(Cu)}{C(Cu)} = \frac{\Delta I(Cu)}{I(Cu)} = \frac{\Delta I(Cu)t}{I(Cu)t} = \frac{\Delta N(Cu)}{I(Cu)t} \tag{17}$$

If we further assume that the principal error in N(Cu) comes from counting statistics, and we associate $\sqrt{N(Cu) + N(b)}$ with this uncertainty, where N(b) is the background counts under the Cu peak, then

$$\Delta N(Cu) = \sqrt{N(Cu) + N(b)} = \sqrt{I(Cu) + I(b)\ t} \tag{18}$$

Substituting equation (18) into equation (17) leads to

$$\Delta C(Cu) = \frac{C(Cu)}{I(Cu)} \frac{\sqrt{I(Cu) + I(b)}}{\sqrt{t}} = \frac{\sqrt{I(Cu) + I(b)}}{K(Cu)\sqrt{t}} \qquad (19)$$

where I(b) is the background count rate at the copper peak. Equation 19 shows that the relative uncertainty in the copper concentration decreases inversely with the square root of the measurement duration. Extending the counting time improves the answer. But there will be a practical lower limit on the logging speed. It must not be unacceptably slow. From equation 19 we rewrite $\Delta C(Cu)$ as follows:

$$\Delta C(Cu) = \frac{\sqrt{I(b)R(pb)}}{K(Cu)\sqrt{t}} \qquad (20)$$

where R(pb) is the peak-to-background ratio of raw (peak plus background) count rate to background count rate under the peak.

We define the lowest detectable amount (LDA) of Cu to be that computed at the 2-sigma level if only background counts are present; that is, when R(pb) = 1. It follows that

$$LDA(Cu) = \frac{2\sqrt{I(b)}}{K(Cu)\sqrt{t}} \qquad (21)$$

In this work K(Cu) was between 45 and 95 counts per hour per wt% Cu.

The quality of the results presented here could readily be improved by a factor of 3 to 5 simply by using a source that is stronger by a factor of 9 to 25. As equation 7 shows, LDA (Cu) decreases inversely as the square root of the source strength because K and I(b) are diectly proportional to the source strength. Counting rates of 25 x 1500 = 37,500 counts/second are within the capabilities of this system. Table 10 lists some expected LDA's for a variety of logging speeds and measurement times (depth intervals for which the analysis will provide average values), under the assumption that the source activity would be 9 times that used in these tests, or 21.6 μg of Cf-252.

Table 10

Estimated lowest detectable amounts of copper by means of in-situ prompt gamma ray analysis.*

Logging Speed, ft/hr.	Depth Averaging Interval, ft.	LDA Wt % Cu
20	10	0.35
20	5	0.50
20	2.5	0.70
10	10	0.25
10	5	0.35
10	2.5	0.50
5	10	0.17
5	5	0.25
5	2.5	0.35

*The following conditions are assumed: 21.6 g Cf-252 source, 10%, 3 KeV FWHM Ge detector, 30 cm source-to-detector spacing, 13,500 cps total counting rate, analysis of 7915-KeV copper line, and peak shape fitting for obtaining net intensity.

We emphasize that in-situ quantitative assays are complicated by variations in the matrix. The neutron flux at any point depends on the neutron slowing-down properties of the medium. The absorption of radiation in the rock is also matrix-dependent. The results presented in this section are merely indicative of the capabilities of prompt gamma ray spectroscopy for copper logging.

We concluded from the data that the prompt gamma method using a Cf-252 neutron source and germanium spectrometer would only be of marginal value in copper-ore logging because it is not fast enough at the desired level of precision.

Technically, delayed gamma ray spectroscopy remains a promising method for in-situ copper ore analysis. Future work ought to include extensive field tests using delayed gammas. The question of which detector, germanium or sodium iodide, would ultimately provide the best analysis in actual boreholes remains to be answered. Indeed, the answer may depend on the type of orebody being examined. For example, the 9.5 minute, 1014-keV gamma ray from neutron activation of aluminum will interfere with the 5.1 minute, 1039-keV gamma ray from copper much more in a NaI(Tl)-detector system than in a Ge-detector system. A comparative study of different types of detectors in a variety of boreholes would provide needed answers.

Silver: Crede, Colorado

Objective

Our main objective was to field-test the applicability of the germanium spectroscopic probe for borehole analysis of silver ore through the use of prompt and delayed gamma rays following neutron capture. Other objectives were to evaluate the new cask design for the 22-microgram Cf-252 source and to evaluate newly developed hardware and software for automated logging.

Background

In the last few years silver has received a great deal of publicity and economic interest because of rapid changes in market price.

Silver is not only a precious metal but is also a strategic material. It has favorable technical properties for neutron activation. Senftle et al (23) have suggested a neutron activation procedure for in-situ determination of silver, based on the 658-KeV delayed gamma ray that is emitted in the following sequence of reactions:

$$Ag^{109}(n,\gamma)\ Ag^{110} \xrightarrow[\beta,24s.]{} Cd^{110} + \gamma(658\ keV)$$

In addition, several prompt gamma rays belonging to the neutron capture process seemed to be good candidates for evaluation because of their photo energies and emission probabilities. Consequently, we investigated the suitability of prompt and delayed gamma rays for silver logging.

Field Tests: Procedures and Results

Delayed Gamma-Ray Tests

In the delayed gamma-ray tests a 22-microgram Cf-252 source (5.1×10^7 neutrons per second) was attached to the bottom of the sonde at the end of a 152cm. (5 ft.) nylon spacer, so that the source-to-detector distance was about 162cm. (5.3 ft.). The gamma ray of interest was the 24.2-sec, 658 keV line.

The logging sequence was as follows. The sonde was held at a given depth and the source was allowed to irradiate the borehole surround for 60 seconds. Then the sonde was lowered 152cm (5 ft.) so that the detector was now positioned in the center of the previously irradiated volume. Starting at about 10 sec. after the end of the irradiation, the system counted delayed gamma rays for 60 seconds. The source was irradiating a location 152cm further down hole during this time.

Repetition of the cycle gave a series of assays in 152cm steps down the hole. After the sonde reached the lowest desired depth it was raised back uphole to a point 30cm (1 ft) below the starting point of the previous series and another 152cm-stepped series of counts performed. After 5 such series, each offset 30cm from the next one, we had collected 60-second spectra at 30cm (1 ft.) intervals over the whole assayed zone.

Spectrum calibration was important in all our tests because the ratios of net counts to background counts for the gamma-ray peaks of interest were relativey small, often much less than 1. Peak-fitting computer programs were employed to glean the best possible net count rate data from each spectrum. It was crucial in this procedure for the computer to know the exact location of the analyzed peak in the spectrum.

The photon energy scale of each of the delayed-gamma-ray spectra was calibrated on two of the outstanding peaks that appeared in all the spectra, the 511-KeV annihilation photons and the 1778-KeV peak from the activation of aluminium in the host rock.

Cuttings from the test borehole were chemically assayed for silver in 5-foot sections. The assays were performed by the assay laboratory of Chevron Resources.

Comparison of the experimental data with the assays of the cuttings followed the usual procedure: 1) calibration of the tool against the assay data and 2) computing in-situ probe assays based on this calibration. The tool was calibrated by averaging the foot-by-foot probe data over 5-foot intervals that matched the intervals from which the cuttings were sampled and analyzed. Data from selected intervals were used to obtain the calibration constants in the expression,

$$C(Ag) = \frac{I(Ag)}{K'\sqrt{I(H)}} \qquad (22)$$

where C(Ag) is the silver assay in Troy ounces per short ton. I(Ag) is the average net count rate of the silver gamma rays, I(H) is the average count rate of the prompt 2223 KeV Hydrogen gamma ray, and k' is the calibration constant for the section.

The criterion for selection was that I(Ag) had to be greater than or equal to two times the estimated statistical counting error. Only sections having sufficiently high silver

counts were considered in the analysis. As mentioned earlier in this report, the I(H) factor corrected, to a degree, for count rate variations in the silver counts that were caused, not by variation of the silver levels, but indirectly through variations in the neutron distribution that resulted from changes in the amount of water present. The prompt gamma- ray data for hydrogen were obtained in the later, prompt-gamma-ray series of measurements, described below.

Results of the delayed gamma-ray tests are presented in Table 11 and shown graphically in Figure 27. There may have been a small depth discrepancy between our data and the cuttings, which probably resulted from the usual uncertainties regarding assigned depths. In the test borehole the factor I(H), expressed as net counts per 120 sec, varied from a low of 26 to a high of 49, roughly a factor of 2. This indicates that the concentration of water varied with depth to a significant degree.

SILVER INSITU LOGGING

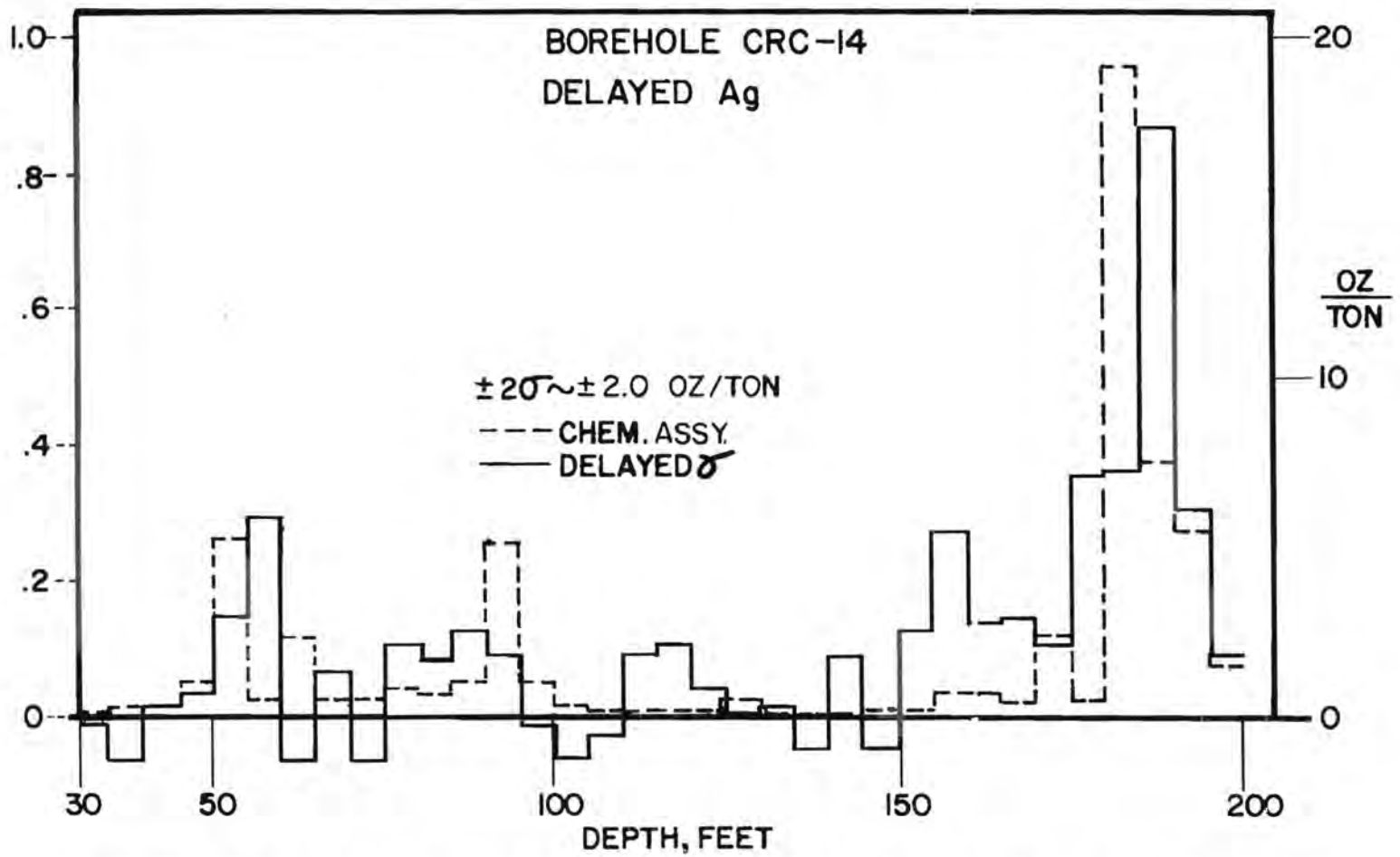

FIGURE 27. COMPARISON OF DELAYED GAMMA-RAY ASSAY AND CORE ANALYSIS FOR SILVER.

Table 11

Comparison between silver in-situ delayed-gamma neutron activation assays and chemical assays in the test borehole

Depth ft.	Net Counts per station (5-ft. avg.)	± 1 Error in net counts	I(Ag) I(H)	1 Error	*In-Situ assay, oz/ton	Chemical assay, oz/ton
30- 35	9.3	7.5	0.235	0.190	-0.24	0.09
35- 40	7.0	7.3	0.176	0.183	-1.18	0.11
40- 45	10.3	7.5	0.269	0.196	0.30	0.33
45- 50	11.8	5.4	0.296	0.136	0.73	1.04
50- 55	15.5	7.4	0.432	0.206	2.91	5.25
55- 60	23.0	6.0	0.623	0.163	5.96	0.50
60- 65	8.0	5.9	0.173	0.127	-1.23	2.38
65- 70	13.0	7.5	0.333	0.192	1.33	0.53
70- 75	7.6	5.7	0.174	0.130	-1.21	0.52
75- 80	15.0	9.2	0.386	0.237	2.17	0.99
80- 85	12.3	7.5	0.354	0.216	1.66	0.75
85- 90	18.8	5.8	0.410	0.127	2.56	1.08
90- 95	17.8	5.9	0.363	0.120	1.81	5.14
95-100	9.0	5.6	0.230	0.143	-0.32	1.01
100-105	7.8	5.9	0.184	0.139	-1.05	0.40
105-110	11.5	6.5	0.283	0.160	-0.53	0.29
110-115	13.8	5.7	0.371	0.153	1.93	0.18
115-120	13.3	7.5	0.380	0.214	2.08	0.08
120-125	11.5	6.1	0.303	0.161	0.85	0.10
125-130	9.7	7.3	0.260	0.196	0.16	0.27
130-135	9.7	7.3	0.272	0.205	0.35	0.17
135-140	6.4	5.5	0.195	0.167	-0.88	0.16
140-145	12.8	6.4	0.363	0.181	1.79	0.21
145-150	7.0	6.6	0.201	0.190	-0.78	0.24
150-155	10.5	6.4	0.349	0.213	1.58	0.37
155-160	17.0	7.5	0.592	0.261	5.46	0.78
160-165	13.5	8.8	0.429	0.279	2.86	0.77
165-170	14.2	5.6	0.434	0.178	2.94	0.44
170-175	12.5	6.4	0.389	0.199	2.22	2.41
175-180	22.3	7.9	0.693	0.245	7.08	0.60
180-185	21.0	9.5	0.705	0.319	7.27	19.11
185-190	41.2	6.6	1.329	0.213	17.24	7.52
190-195	16.8	6.8	0.636	0.258	6.16	5.44
195-200	10.3	7.1	0.373	0.257	1.96	1.50

*Computed: $\text{Assay}_{(\text{oz/ton})} = \left(\frac{I(Ag)}{I(H)} - 0.25\right)/.0625$

The effect of the water correction showed up in the relative amplititudes among data groupings near the 50 ft., 90 ft., and 180 ft. depths. Table 12 compares the average chemical assays in these three regions with the corresponding logging values. Note that the logging-to-chemical assay ratios that are based on the I(H)-normalized intensities exhibit tighter grouping among themselves then do the corresponding ratios based on the unnormalized intensities. This comparison provides qualitative experimental verification of the validity of using the I(H) factor in the analysis.

Table 12

Comparisons between silver in-situ results that do and do not explicitly contain the 1/ I(H) water-correction factor.

ore Zone Depth interval, ft.	*Chemical Assay oz/ton	*In-Situ Assay		Ratio, In-Situ/Chemical	
		+unnormalized, oz/ton	++normalized, oz/ton	unnormalized	normalized
45- 60	6.79	8.2	7.5	1.2	1.1
85- 95	6.22	8.2	5.9	1.3	1.0
165-190	30.08	26.7	29.7	0.9	1.0

* All assay results represent averages over the depth interval.
+ Unnormalized results are based on assumption $C(Ag) = I(Ag)/k$.
++Normalized results are based on assumption $C(Ag) = \frac{I(Ag)}{k' \; I(H)}$

The sensitivity of the delayed-gamma procedure was found to be approximately 0.04 counts per sec. per oz/ton. For a one minute activation-and-data-accumulation duration per point, this sensitivity implied a lower limit of detectability of about 1.6 oz/ton at the 95% confidence level under the conditions of the present test. The above detectability limit could be improved, since it varies inversely with the square root of the count rate. The count rate is proportional to the source strength and detection efficiency, It can be increased by a factor of 24 (6 for the source and 4 for the detector), giving a practical detectability limit of about 0.4 oz/ton, with a Cf-252 neutron source. Approximately the same figure will hold for the precision of measurement for in-situ assays: about +2.2 oz/ton at the 30 oz/ton level with the system used in these tests, and about +0.44 oz/ton at the 30 oz/ton for the hypothetical higher count rate system. These precisions pertain to each measurement point (each foot in this experiment). This corresponds to an average logging speed of about 50 ft/hr at one-foot spacing between stations. Individual errors will fluctuate positively and negatively in a random fashion so that averages over several depths will improve precision further. Accuracy will be worse than the precision figure and will depend in part on the assumed calibration factor at each depth.

Loss and Recovery of Cf-252 Source

In the course of the delayed gamma work the 22-ug Cf-252 source was accidentally dropped down Borehole CRC-17. After several months and multiple efforts at recovery by contractors, the source was finally fished out of the hole. The recovery operation damaged the source encapsulation but did not break it. There was no leakage of radioactivity. Ultimately, the source was returned to the supplier for evaluation and burial. Throughout this effort all the procedures and reportage required by the NRC were adhered to. The loss of the source forced curtailment of the delayed gamma work with silver. Its absence also affected the amount of delayed gamma work later carried out in the gold ore boreholes.

Prompt-Gamma-Ray Tests

Of the several prompt gamma-ray lines associated with silver during neutron capture the line at 5700 keV photon energy was chosen as the most suitable for this investigation. The total neutron emission rate from the 2 microgram Cf-252 source was about 5x10 neutrons/second, the source-to-detector spacing was 30cm (1 ft) and the total counting rate was about 3000 counts/sec. at the detector.

We lowered the sonde with its attached source to the bottom of the region to be logged and counted at the fixed depth for 120 seconds. The sonde was raised 30cm (1 ft) and another 120 second count accumulated. This procedure was repeated at successive 30cm intervals until the entire depth

range of interest was logged. We ended up with a 120-second gamma-ray spectrum for each point.

The photon-energy scale of the gamma-ray spectra was calibrated on the strong, always-present 3539-keV prompt gamma-ray line of silicon from the reaction

The same general procedure of data reduction was used to obtain the assays based on prompt gamma emission as that used for the delayed gamma work: calibration of the tool followed by the application of the calibration constant to spectrum-fitted net intensities to yield the assays. Data was averaged over 5-foot sections and the 1/ I(H) factor was employed to compensate for the effects of hydrogen on the neutron flux. The results of this analysis were tabulated and plotted. However, these results were so erratic. because of large statistical fluctuations in the net intensity, that the tool could not be calibrated. Little, if any, correlation was found between the net counts and the chemical assays. It was considered that the poor results could have been due to interference of the 5700 keV silver line by the nearby 5956 keV line of potassium, so the intensity data was corrected for that interference in the following way. The measured total net intensity at 5700 keV was assumed to be the sum of the net silver counts and a fraction, a, of the net potassium counts:

$$I(5700\ keV) = I(Ag,5700\ keV) + aI\ (K,1460\ keV) \qquad (23)$$

where I(K,1460 keV) is the net counts in the intense, isolated, potassium peak at 1460 keV

$$I(Ag,5700) = I(5700) - aI\ (K,1460) \qquad (24)$$

The coefficient, a, was empirically determined to be $(3.98 \pm 3.31)\times10^{-2}$. In this way I(Ag) was determined, notwithstanding the large error in a. Unfortunately, after the effects of the interfering line had been removed, the results still exhibited no correlation between the net intensities and the chemical assays.

Figure 28 shows the behavior of the prompt gamma results, plotted as net counts in the 5700-keV peak vs. depth. This is to be compared to the chemical assay plot in figure 27. We note that none of the prompt gamma data was statistically significant. This implies that the detectable amount (LDA), although undetermined, was greater than 40 oz/ton for a 120-sec. measurement. More specifically, it implies that LDA is greater than 40 oz/ton at a logging speed of 46m (150 ft)/hr if the data is averaged over 1.5m (5 ft) intervals, or that, at 3m (10 ft)/hr, LDA is greater than 10 oz/ton.

We concluded that practical in-situ assays of silver could be achieved with neutron-induced delayed gamma rays (neutron

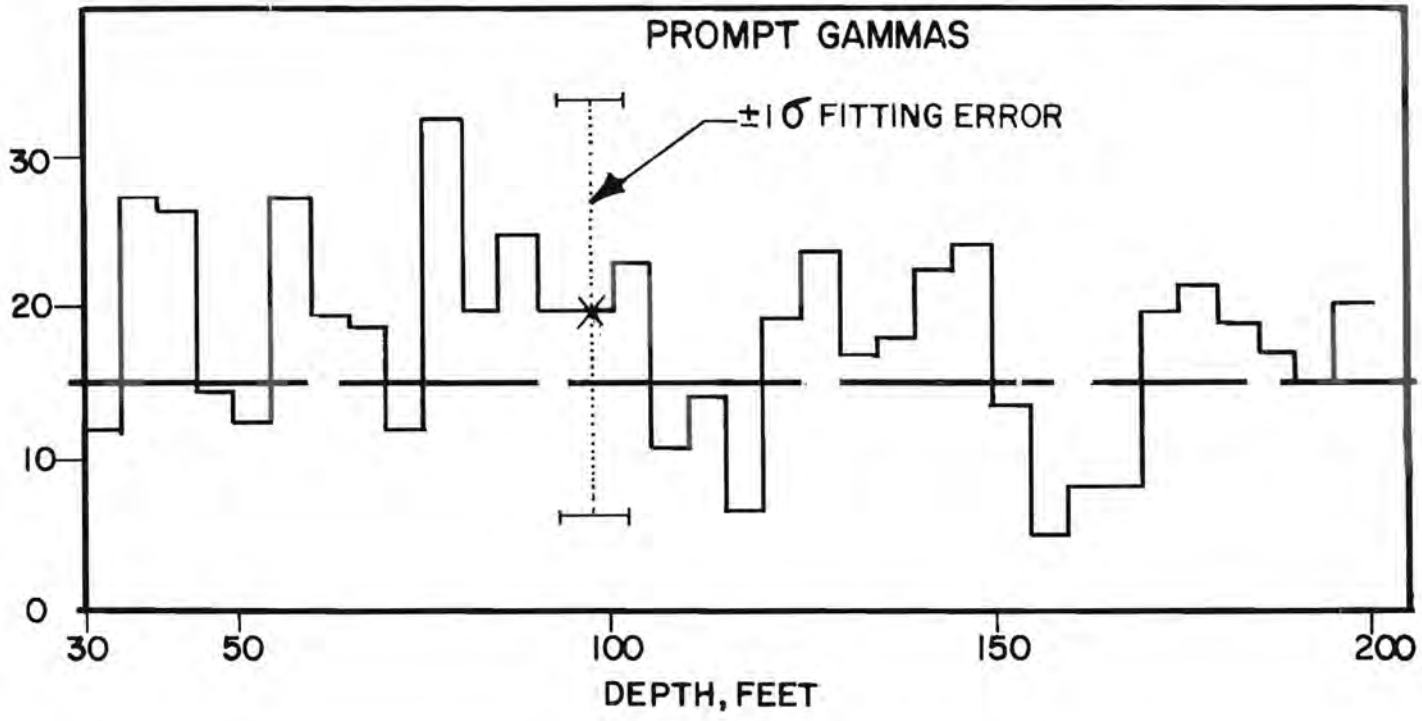

FIGURE 28. PROMPT GAMMA-RAY LOG OF THE SAME BOREHOLE AS SHOWN IN FIGURE 27.

activation analysis), but that adequate silver assays were not obtainable at practical logging speeds when prompt gamma rays of silver were used. Our conclusion about the prompt gammas was based on one line, at 5700 keV, but we believe our conclusion will be qualitatively valid if any other prompt silver line or combination of prompt silver lines were used instead.

The quality and speed of in-situ logging for silver could probably be improved if a pulsed neutron generator were to replace the Cf-252 source. If this were done, several benefits would ensue: 1) better radiation safety and/or less cumbersome shielding for the source of neutrons, 2) availability of continuous and stepped logging, 3) 25% less loss of data by elimination of the approximately 10-second delay between the end of irradiation and the start of counting, which was necessitated by the relocation time of the sonde, and 4) increase in intensity as a result of ongoing technological improvements in downhole accelerators.

Gold: Cripple Creek, Colorado

Objective

Our objective was to conduct in-field tests of gold logging by means of high-resolution gamma-ray spectroscopy with the developed equipment. The study was to include neutron-induced prompt and delayed gamma ray emissions so that the two could be compared, in order to evaluate their relative merits.

Background

In the United States gold occurs in some regions as concentrated veiny deposits, but the major deposits are low-grade, highly dispersed. Deposits of the latter are found in areas of the western U.S., including the region in the vicinity of Cripple Creek, Colorado. Dispersed gold deposits have average ore grades as high as a few tenths of an ounce per ton in some locations. Today, 0.03 oz (Troy) gold per short ton or 1.2 ppm by weight, is considered economically minable under favorable conditions if the price of refined gold is above $400 an ounce. Many gold deposits are found in hard rock where core drilling for assay samples can be relatively costly. An instrumented gold logging technique might have advantages of lower cost and faster reporting of results, compared to coring and assaying. The required accuracy for direct determination of gold in low grade ores is about +0.005 oz per ton, or 0.2 ppm. To satisfy that requirement an in-situ nuclear technique would have to be extremely sensitive. This implies relatively high costs because of the normal trade-off between the data collection time and the associated precision of measurement.

Procedures and Result

We collected data in two boreholes in the Cripple Creek district, where gold occurred as dispersed free gold or gold tellurides. It was relatively homogeneously distributed in hard rock. Delayed gamma-ray emissions as well as prompt gamma-ray emissions were observed following neutron-induced activation of the borehole surround, in separate series of measurements. One of the holes had been rotary drilled and the other had been cored. Chemical analyses of the drill chips and core samples were carried out by the U.S. Bureau of Mines, Reno Research Center, Reno, Nevada, two commercial laboratories, and Texas Gulf Golden Cycle Mining Company. Samples were chemically analyzed for gold by fire assay. Several other elements were determined by emission spectrography.

The field test results turned out to be inconclusive because of errors in laboratory assays, etc., and suggested the need for further work.

Natural Gamma Ray Logs

First a passive spectral log (naturally-emitted gamma rays, no neutron source) was obtained for the zones of interest in each hole, in order to measure the baseline background radiation from the naturally radioactive isotope of potassium, uranium and thorium. We encountered no significant background radiation that might interfere with activation analysis.

Delayed Gamma Rays

Gold, if activated by means of high-energy neutron inelastic collision, emits a 279-keV gamma ray having a 7.2-second half-life. If activated by thermal neutron capture, gold emits a 412-keV gamma ray with a half life of 2.696 days. These processes are expressed in the following reactions:

$$Au^{197}(n,n\gamma)\ Au^{197m} \xrightarrow[\beta,7s.]{} Au^{197} + \gamma(279\ keV) \qquad (25)$$

$$Au^{197}(n,\gamma)\ Au^{198} \xrightarrow[\beta,2.7d.]{} Hg^{198} + \gamma(412\ keV) \qquad (26)$$

Using a probe containing a Cf-252 neutron source and a germanium detector, we looked for each of these two gamma ray lines, as described below. The results were inconclusive, but tended to indicate the following: 1) optimal use could not be made of the 7.2-second half-life radiation in this investigation for two reasons; (a) the 66 microgram Cf-252 source did not provide a high enough neutron flux of adequate energy, and (b) many of the 7.2-second, 279-keV gamma rays were lost during the time it took to move the detector to the irradiated zone. 2) The 2.697-day activity, while observed, seemed impractical to work into a fieldworthy logging schedule. It would take too long to log a hole, even if the borehole were to be irradiated on one day and counted during the following day. We concluded that the best chance for in-situ neutron activation analysis of gold would be a system that would include a pulsed accelerator and would employ the 7.2-second activity.

The activation procedure for evaluating the use of the 7.2-second half-life decay utilized the 66 microgram californium-252 source with a five foot nylon spacer. In this procedure, after 20 seconds of irradiation (approximately 2.6 times the half-life) the sonde was lowered by five feet, thereby positioning the detector in the activated region. After a delay of 25 seconds, including the time to move the

sonde, a spectrum was collected for eight seconds. The procedure optimized the data collection from gold activation while minimizing the accumulation of background from the decay of activated aluminum produced in the following reactions:

$$Al^{27}\ (n,p)\ Mg^{27}$$

$$Mg^{27} \xrightarrow[\beta,9m.]{} Al^{27} + \gamma(1014 \text{ and } 844 \text{ keV}) \qquad (27)$$

$$Al^{27}\ (n,\gamma)\ Al^{28} \xrightarrow[\beta,2m.]{} Si^{28} + \gamma(1778.8 \text{ keV}) \qquad (28)$$

The sonde was then lowered by five feet and the process repeated. Subsequently, logging sequences in the same hole were offset by a foot from the previous one; so that we ended up with foot-by-foot activation data for portions of both holes.

The data analysis for the 7.2-second half-life decay, using the 279-keV line under the stated measuring conditions, was such that the statistical uncertainties limited the conclusions that could be drawn. Of the 285 data points for the 279-keV line in the rotary hole, integrated peak counts at only 5 locations were greater than two times the square root of the background counts, i.e., exceeded the two sigma value of the counting statistics. Contributing to the uncertainty of the quantitative results was the fact that the average ore grade was rather low, about 0.05 oz. per ton. Had it been significantly greater, we might have been able to collect enough counts to determine the sensitivity of our procedure for the 7.2-second activity.

In order to investigate the 2.697-day, 412-keV delayed gamma ray, we irradiated two locations in the rotary borehole, at 336 and 341 feet with the 66-μg Cf-252 source for 10 and 20 minutes, respectively. These locations were counted for 30 minutes the next day. The two spectra showed recognizable peaks at 412 keV, confirming the presence of gamma rays from gold activation, since interfering activation peaks would have died away by then. However, the chemical fire assays for these and other depths were not repeatable and were considered unreliable. As a result, no calibration of counts vs. gold assay was achieved. Figure 29 shows the vicinity of the gold peak at 412 keV in a spectrum obtained in the rotary hole.

A series of activation mesurements were made in the rotary hole with ten minute activation, three hour delay, and ten minute counting times, at 14 depths spaced 5 feet apart, between 82.3m (270 ft) and 103.7m (340 ft). The three-hour delay was chosen as sufficient to allow the activated aluminum to decay to the point where the aluminum-dependent background was substantially reduced. Ten minutes activation and counting

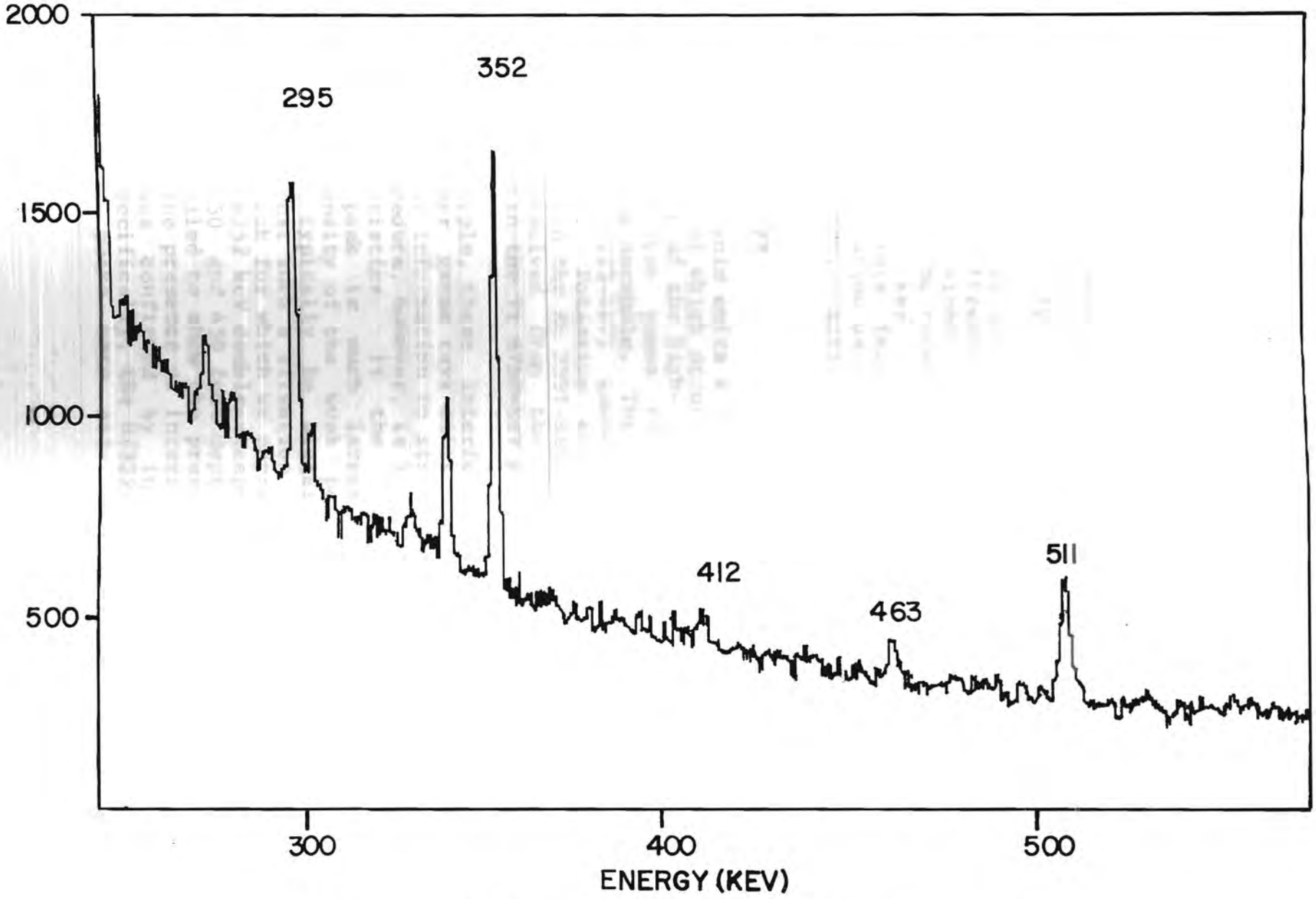

FIGURE 29 DELAYED-GAMMA RAY SPECTRUM
IN THE VICINITY OF THE 412 KeV LINE OF GOLD

was considered the slowest tolerable speed. However, the presence of indium, with a relatively intense 54-minute half-life, 417-keV, gamma ray interfered with the sought 412-keV line. The interference could not be adequately compensated by tracking the 1293-keV line of activated indium and subtracting a proportional number of counts from the combined gold and indium lines near 412-keV. The indium was present in sonde construction. The obvious cure was not to use indium in sondes destined for gold analysis, but we did not try it in this investigation because of time constraints. Naturally occurring actinium-288, a daughter product in thorium decay, has a line at 409 keV. We found this not to be a significant interference in our tests. Of the fourteen data points that we obtained pertinent to the 2.696-day delayed gamma rays in the rotary hole, not one of the "peaks" in the vicinity of 410 keV turned out to have statistical significance. This fact, coupled with the uncertain lab assays, did not allow us to achieve any quantitative results for the 10 min. activation, 3 hr. delay, 10 min. count protocol.

Prompt Gamma Rays

Activated gold emits a number of prompt gamma rays, the more intense of which occur at 215, 248, 261, 1202, 2391, and 6252 keV. Some of the high- energy prompt gamma rays encounter interferences from gamma rays emitted by other activated elements in the borehole. The 1203-keV double-escape peak of the strong H(2223-keV) gamma ray interferes with the Au 1202-keV line. Potassium emits a 2390 keV line which interferes with the Au 2391-keV gamma ray. The 6252-keV gamma ray was unresolved from the 6250-keV single escape peak associated with the Ti 6760-keV gamma ray.

In principle, these interferences may be mitigated by tracking other gamma rays emitted by the interfering elements and using that information to strip out the interfering peak. Such a procedure, however, is limited by the uncertainties of counting statistics. If the relative intensity of the interfering peak is much larger (by a factor of 10 or more) than the intensity of the weak peak of interest, then the errors will typically be bigger than the sought peak. We encountered just such a situation in the case of gold. The only gold peak for which we expected no interference was that at 5230-keV (6252 keV double-escape). Prompt spectra, taken at 130, 330, 350 and 450 foot depths in the rotary hole for one hour each, failed to show the presence of a detectable peak at 5230 keV. The presence of interfering elements, as previously mentioned, was confirmed by inspection of the gamma-ray spectra. Specifically, the H(2223 keV)the K(2073 keV) and the Ti(1381 keV) peaks were all observed with substantial intensities.

Conclusion

The delayed-gamma data were not adequate to determine the sensitivity of the technique for in-situ gold determinations. A sufficient number of peaks attributable to gold were noted under various measuring conditions to suggest the advisability, in future work, of further testing in the field and laboratory. The delayed-gamma work, while inconclusive, suggested that the use of an intense, pulsed, 14-MeV neutron source and the 7.2-second half-life activity offers the best change of success.

Our prompt-gamma tests indicated that this technique is incapable of practical use in gold determinations because of the relatively high backgrounds and interfering peaks that are associated with it.

CONCLUSIONS

A new high-resolution gamma-ray spectroscopic borehole probe was designed, built and tested for in-situ analysis of elements in geological formations by means of neutron-induced and natural gamma-ray emissions. This work was carried out in two phases.

Phase I included the following tasks:

1) The design, construction and testing of prototype probe containing a cryogenically cooled intrinsic germanium detector, having a 5.1cm (2 in) outer diameter, and capable of operating at 3000 ft. for 8-hour periods.

2) The development of associated downhole electronics assemblies for the probe, including low-voltage and high-voltage power supplies, spectroscopy preamplifier and amplifier, analog-to-digital converter, and 4096-channel microprocessor-based multichannel analyzer.

3) The development of a complete logging truck with data processing equipment and electrical mechanical controls for conducting tests of the systems.

4) The development of downhole and uphole software.

5) Laboratory testing and calibration of the prototype system.

Phase 1 was completed in 1978. The prototype probe and system met design specifications. An interim report on Phase I was submitted March 31, 1978.

Phase II consisted of field investigations of the prototype probe for in-situ ore grade determinations of uranium, iron, copper, silver, and gold and analysis of coal. Summarized results of each are presented below. During this time, ongoing hardware and software improvement were incorporated as needed in order to achieve a reliable and smooth running automated logging system.

Iron

The iron ore tests were the first tests in this investigation to employ neutron-induced prompt gamma rays. These tests successfully proved the technical feasibility of the cryosonde and borehole electronics pcakage. The sensitivity of the sonde for iron was found to be approxomately

0.2 counts per second per percent iron using the double-escape doublet at 6.610 MeV and 6.624 MeV. The measurement time needed to achieve +10% (1 sigma) relative precisions at the 50% by weight Fe level was estimated to be about 50 sec.

Uranium

Uranium ore grade was determined by counting the naturally emitted 1.001-MeV gamma ray of Protactinium-234, a close daughter product of Uranium-238. This gamma-ray line, although less intense than lines from other decay products, was more representative of the uranium ore grade than was the traditional gross gamma count, if the ore is not in secular equilibrium with all its daughter products. We found that uranium ore could be logged at +10% to + 20% relative precision at levels exceeding 0.01 weight percent U_3O_8 at practical logging speeds. As a direct result of this work, Princeton Gamma-Tech initiated a commercial uranium logging service in 1979.

Copper

The application of the cryosonde to in-situ logging of copper was investigated using prompt gamma-ray detection. The sensitivity was in the range 45 to 95 counts per second per weight percent copper. The minimum detectable amount was about 0.4 wt % Cu in a one-hour measurement. Although upgrading the system could lead to improved prompt gamma results, we recommend that future efforts concentrate on the delayed gamma technique, which ought to yield significantly better in-situ determinations of copper at faster logging rates.

Silver

Delayed and prompt gammas following neutron stimulation from Cf-252 sources were investigated as a means of achieving in-situ silver assays. The 24.2-sec. half-life, 658-keV delayed gamma ray was found to be an excellent indicator of silver, providing that the effect of hydrogen in the formation was taken into account. Our tests indicated that a hypothetical scaled-up system having a 130 microgram Cf-252 source and a 30% efficient Ge detector (relative to a 3" x 3" NaI cintillator) would be able to step-log at an average rate of one foot per minute and achieve a 2-sigma minimum detectable limit of about 0.4 oz per ton, or 17 parts per million by weight. On the other hand, the prompt gamma tests, based on the 5700-keV gamma-ray line, indicated that the prompt gamma approach using a Cf-252 source was impractical for downhole assaying of silver because of insufficient intensities and poor peak-to-background ratios.

Gold

Delayed and prompt gamma rays following neutron stimulation from Cf-252 sources were studied in a dispersed gold deposit. We concluded that the prompt gammas were not practical for logging because of relatively high backgrounds and interfering peaks. The delayed-gamma work was inconclusive because of calibration problems. Furthermore, of the two radioisotopic half-lifes that were considered suitable candidates, one (7.2 sec.) was too short for practical step-logging work with a Cf-252 source and the other (2.697 day) was probably too long to be of practical value for field work.

Coal

Borehole logging of a coal seam with the cryosonde and including, a) natural gamma logging and, b) prompt gamma ray logging with a Cf-252 neutron source, provided a variety of useful information such as 1) seam depth and thickness; 2) in-situ analyses for sulfur, aluminum, silicon, and iron; 3) determination of ash content; and 4) determination of BTU content. We note, however, that other logging equipments presently exist that can provide most of this information faster and cheaper than the cryosonde. We speculate that if the germanium cryosonde spectrometer is to have a place in practical coal work, it will probably be in specialized applications involving in-situ determinations of specific environmentally undesirable minor elements such as sulfur and boron, which demand high-resolution spectroscopy, in situations that tolerate relatively lengthy measurement times.

SUMMARY AND RECOMMENDATIONS

In Phase I a germanium detector-based, gamma-ray spectroscopic borehole probe and support system were successfully designed and built.

The field studies of Phase II led to a number of inferences about the potential usefulness of the germanium borehole cryosonde in the mining industry. Uranium was successfully logged by means of natural gamma-ray spectroscopy. The use of the 1.001-MeV, Pa-234 gamma ray eliminated errors caused by lack of secular equilibrium among isotopic decay products. Copper and silver could in principle be logged at speeds in the range 1 to 5 minutes per measurement interval, (typically one to five feet), if a moderately active (about 100 microgram) Cf-252 neutron source were used with delayed-gamma spectroscopy. Although it was technically feasible to log for iron and the principal elements in coal with prompt gammas using a Cf-252 neutron source, such a tool is expected to be of little current interest in those applications. In-situ gold analysis suffered from insufficient sensitivity and uncertain calibration.

Throughout this study a californium-252 source has been used to produce the neutrons that excite the gamma rays for the assay mesurement. While it is simple to use, the radioactive californium source presents a number of limitations:

1) There is a reluctance in the mining industries to utilize radioactive sources if there is any possibility of such a source being dropped down a borehole. Although this is primarily a problem in education, not technical feasibility, it is a serious concern in making the technology industrially acceptable.

2) Since a californium source that is strong enough to be of practical value requires more than 1000 pounds of shielding, it is cumbersome to handle in the field.

3) Regulations governing the transportation of the californium source are complex and vary from state to state.

4) The californium source is active all the time. It cannot be switched off. This means that the analytical measurement must either be made in the presence of the primary source of neutrons or some significant amount of time must be allowed for the source to be removed and the detector to be placed. This time can perhaps be limited to a few seconds, but even a few seconds can be a long time compared with the half lives of some radioisotopes produced in the delayed gamma ray process. In the prompt gamma ray measurements the continuous neutron source causes a high background that limits the assay sensitivity.

There is an alternative to the use of radioactive source for generating neutrons in the borehole that might substantially improve the quality of logging for copper, silver, gold, impurities in coal, and other metals. It is the use of a miniature accelerator that produces 14.1-MeV neutrons during the bombardment of tritium by deuterons. Such accelerators are commercially available. Proprietary models have been used extensively in the oil industry for a number of years. There are several advantages in the use of accelerators as neutron sources:

1) The only time the accelerator needs to be turned on is when it is located in the borehole; so external shielding is not required. Accelerators presently can emit 10 neutrons per second. Some experimental models emit as many as 10 neutrons per second. Although californium is available in similar strengths, the shielding for a 10 n/s source would be prohibitively ponderous for field work.

2) Accelerators can be pulsed. In fact, this is the usual mode of operation. The thermal neutrons that are produced are captured within a millisecond, so that delayed activation of elements with half-lives greater than a few milliseconds could be investigated. Sources, such as californium, that must be physically moved away from the activated sample, can only be used to analyze elements with half-lives longer than a few seconds. The advantage of not requiring sudden gross motions of the system permits continuous measurement and reduces the logging time per hole. It also allows higher overall counting rates.

3) In the past, germanium detectors could not be used with accelerators because of the severe damage caused by the neutrons. Recent improvements in germanium technology have resulted in detectors that have at least an order of magnitude less sensitive to neutrons (22). Improved techniques for restoring neutron-damaged detectors offer the possibility of extending the useful life of a given detector even further (6).

We recommend that the design, development, and testing of a new integrated borehole system for logging of metals and minerals be the subject of future work. The suggested system ought to be based on high-resolution gamma-ray spectroscopy and neutron stimulation of the formation. It ought to combine an intense pulsed neutron source (accelerator) and a high-efficiency germanium detector with appropriate electronics in a hardened, fieldworthy package that could be field tested in boreholes. The main purpose would be to provide a speedier, less costly, and more reliable alternative to coring-and-assaying in the search for and mining of valuable and strategic metals.

REFERENCES

1. Block, C. and Dams, R., "Determination of the Ash Content of Coal on the Basis of its Chemical Composition," Bull. Soc. Chimique Belge 83 (1974) 457.

2. Brodzinski, R.L., and Wogman, N.A., "Californium-252 In Situ Activation and Photon Detection Techniques for Uranium Ore Deposit Evaluation". IAEA Conf., Vienna, Austria, IAEA-SM-208-50 (1976).

3. Semiconductor Nuclear-Particle Detectors and Circuits, edited by Brown, W.L., Higinbotham, W.A., Miller, G.L. and Chase, R.L., National Academy of Sciences, Washington, D.C. (1969) Publication 1593.

4. Coles, D.G., Meadows, J.W.T. and Lindekin, C.L., Lawrence Livermore Lab., University of California, Report UCRL-75619 (1974).

5. Cottini, C., Gatti, E. and Svelton, V., "A New Method for Analog to Digital Conversion," Nuclear Instr. & Methods 24 (1963) 241.

6. Darken, L.S., Trammell, R.C., Raudorf, T.W., and Pehl, R.H., "Neutron Damage in Ge (HP) Coaxial Detectors," IEEE Trans. Nucl. Sci. NS-28 (1981) 572.

7. Erdtmann, Gerhard, Neutron Activation Tables. Verlag Chemic, New York (1976).

8. Fanger, U., Heck, D., Martens, P., Pepelnik, R. and Schmidt, H., "Bestimmung des Wolframgehalts von Naturlichen Gesteinsproben aus Scheelitlagerstatten mit Hilfe der Prompten (N,)-Analyse,"Report KFK-1404, Inst. fur Amgewandte Kernfysik, Kernforschungszentrum, Karlsruhe, Germany (1971) 14 pp.

9. Given, P., "The Use of DAF and DMMF Ultimate Analyses of of Coal," Fuel 55 (1976) 256.

10. Heath, R.L., "Gamma-Ray Spectrum Catalogue" Vol. 2, Third Edition. Aeroject Neclear Company, Report ANCR-1000-2 (1974).

11. Hoyer, W.A. and Lock, G.A., "Logging for Copper by In Situ Neutron Activation Analysis," in Transactions, Society of Mining Engineering, Houston, Texas 252 (1972) 409.

12. Hoyte, A.F., Martinez, P., and Sentfle, F.E., "Neutron Activation Method for Silver Exploration," in Transactions, Society of Mining Engineers (March 1969) 94.

13. "Future Research in Borehole Assaying Technology" Volume 1: Technology Assessment of Borehole Logging Techniques. Final Report, U.S. Bureau of Mines Contract J0255018, IRT Corporation, March 18, 1976

14. Irving, James A. and Wahlgren, M.A., "Detection Sensitivities Nuclear Activation with an Isotopic Neutron Source (with a Collection of Gamma-Ray Spectra)". Argonne National Laboratory, Report ANL-7242 (1966).

15. Jensen, C.M., Overmeyer, R.F., Rogers, V.C. and Sandquist, G.M., "Borehole Logging with Neutron Activation: A Laboratory Assessment, "U.S. National Technical Information Service, Report PB-273454 (1977).

16. Kraner, H.W., Pehl, R.H. and Haller, E.E., IEEE Trans. Nucl. Sci. NS-22 (1975) 149.

17. Table of Isotopes, Seventh Edition, Edited by Lederer, C. Michael and Shirley, Virginia S. John Wiley & Sons, Inc., New York (1978).

18. Loska, L. and Gorski, L., "Radiometric Method for Determining Ash Content of Coal Using a Fast Nautron Generator, "Koks, Smola, Gaz 18, No.2 (1973) 52.

19. Mikesell, J.L., Dotson, D.W., Senftle, F.E., Zych, R.S., Koger, J. and Goldman, L., "In Situ Capture Gamma-Ray Analysis of Coal in an Oversize Borehole," in Cross, Aureal, editor, Economic Geology Volume, Congres International du Stratigraphie et de Geologie du Carbonifere, 9me, Urbana, Ill., (May 19-26, 1979), Comptes Rendus, V.2

20. Nargolwalla, S.S., Kung, A., Legvady, O.J., Strever, J. and Siegel, H.O., "Nuclear Metalog Grade Logging in Mineral Deposits," International Symposium on Nuclear Techniques in Exploration, Extraction, and Processing of Mineral Resources, March 7-10, Paper No. SM-216/8, International Atomic Energy Agency, Vienna, Austria (1977) 229.

21. Orphan, V.J., Rasmussen, N.C. and Harper, T.L., "Line and Continuum Gamma-Ray Yields from Thermal-Neutron Capture in 75 Elements." Defense Atomic Support Agency Report GA-10248 (1970).

22. Pehl, R.H., Madden, N.W., Elliott, J.H., Raudorf, T.W., Trammell, R.C., and Darken, L.S., "Radiation Damage Resistance of Reverse Electrode Ge Coaxial Detectors," IEEE Trans. Nucl. and Sci. NS-26 (1979) 321.

23. Senftle, F.E., Hoyte, A.F., Martinez, P., and Mitchell, C., "Neutron Activation Techniques for Mineral Exploration, USAEC Report TID-23668 (1966).

24. Senftle, F.E., Tanner, A.B., Philbin, P.W, Boynton, G.R. and Schram, C.W., "In Situ Analyses of Coal Using a 252Cf-Ge(Li) Borehole Sonde," Mining Engineering (AIME) 30 (1978) 666.

25. Senftle, Frank E., Moxham, Robert M., Tanner, Allan B., Boynton, George R., Philbin, Philip W. and Baicker, Joseph A., "Intrinsic Germanium Detector Used in Borehole Sonde for Uranium Exploration". Nuclear Instr. and Meth. 138 (1976) 371.

26. Senftle, F.E., Moxham, R.M., Tanner, A.B., Philbin, P.W., Boynton, G.R. and Wagner, R.E., "Importance of Neutron Energy Distribution in Borehole Activation Analysis in Relatively Dry, Low-Porasity Rocks". Geoexploration, 15 (1977) 121.

27. Senftle, Frank E., Macy, Robert J., Mikesell, Jon L., "Determination of the Optimum-Size Californium-252 Neutron Source for Borehole Capture Gamma-Ray Analysis". Nucl. Instr. and Meth. 158 (1979) 293.

28. Senftle, F.E., "Application of Gamma-Ray Spectral Analysis to Subsurface Mineral Exploration", in Short Course in Neutron Activation Analysis in the Geosciences, Meucke, G.K., editor Mineralogical Association of Canada, Halifax (May 1980) pp. 211-254.

29. Senftle, Frank E., "Field Studies of Borehole Gamma-Ray Spectrometer Methods for Mineral Exploration: A Selected Bibliography." U.S. Geological Survey Open-File Report 80-503 (1980).

30. Senftle, F.E., "Neutron Induced Radioactivity for Mineral Exploration," U.S. National Bureau of Standards, Special Publications, Washington, D.C.

31. Seyfarth, H., Hassan, A.M., Hrastnik, B., Gottel, P. and Delang, W., "Efficiency Determination for Some Standard Type Ge(Li) Detectors for Gamma Rays in the Energy Range from 0.04 to 11 MeV," Nucl. Instrum. & Methods 105 (1972) 301

32. Snow, William J., "The Response of Monoenergetic Gamma Rays in Finite Media". Argonne National Laboratory, Report ANL-7314 (1967).

33. Sohrabpour, M. and Bull, S.R., "Elemental Sensitivity Data Modeling for In Situ Neutron Capture Gamma Ray Experiments", Nucl. Instrum. and Methods 161 (1979) 281.

34. Spits, A.M.J. and Kopecky, J., "The Reaction 35Cl (n,)36Cl Studies with Non-Polarized and Polarized Thermal Neutrons," Nuclear Physics A264 (1976) 63.

35. Tanner, A.B., Moxham, R.M. and Senftle, F.E., "Assay for Uranium and Determination of Disequilibrium by Means of In Situ High Resolution Gamma Ray Spectrometry". U.S. Geological Survey Open File Report 77-571 (1977).

36. Tanner, Allan B. and Senftle, Frank E., "A Table of Photopeaks Useful in Nuclear Geophysics." U.S. Geological Survey Open-file Report 78-531 (1978, updated 1980).7

37. U.S. Atomic Energy Commission Report, "Californium 252 Its Use and Market Potential" (May 1969).

38. Wilson, Robert D., Colby, Michael S. and Stone, John M., "Field Evaluation of Direct Uranium Borehole Logging Methods". Proceedings of 20th Annual Logging Symposium, Society of Professional Well Log Analysts, (1980) Transactions.

39. Wormold, M.K., Clayton, C.G., Boyce, I.S. and Mortine, D. "A Method of measuring the Ash Content of Coal in Moving Wagons," in Nuclear Techniques in Exploration, Extraction, and Processing of Mineral Resources, International Atomic Energy Agency, Vienna (1976) Paper No. SM 216/48.

40. Zubovic, P., Oman, C., Coleman, S.L., Bragg, L., Kerr, P.T., Kozey, K.M., Simon, F.O., Rowe, J.J., Medlin, J.H. and Walker, F.E., "Chemical analysis of 617 coal samples from Eastern United States," U.S. Geological Survey Open-File Report 79-665, Washington, D.C. (1979)